SYNTHESIS OF POLY(LACTIC ACID)-NATURAL RUBBER COPOLYMER FOR TOUGHENING POLY(LACTIC ACID)

Sawitri Srisuwan

A Thesis Submitted in Partial Fulfillment of the Requirements for the Degree of Doctor of Philosophy in Polymer Engineering

Suranaree University of Technology

Academic Year 2018

การสังเคราะห์โคพอลิเมอร์ของพอลิแลคติกแอซิดและยางธรรมชาติเพื่อใช้ในการเสริมความเหนียวให้กับพอลิแลคติกแอซิด

นางสาวสาวิตรี ศรีสุวรรณ์

วิทยานิพนธ์นี้เป็นส่วนหนึ่งของการศึกษาตามหลักสูตรปริญญาวิศวกรรมศาสตรดุษฎีบัณฑิต
สาขาวิชาวิศวกรรมพอลิเมอร์
มหาวิทยาลัยเทคโนโลยีสุรนารี
ปีการศึกษา 2561

SYNTHESIS OF POLY(LACTIC ACID)-NATURAL RUBBER COPOLYMER FOR TOUGHENING POLY(LACTIC ACID)

Suranaree University of Technology has approved this thesis submitted in partial fulfillment of the requirements for the Degree of Doctor of Philosophy.

Thesis Examining Committee

(Assoc. Prof. Dr. Wimonlak Sutapun)
Chairperson

(Asst. Prof. Dr. Pranee Chumsamrong)
Member (Thesis Advisor)

(Assoc. Prof. Dr. Yupaporn Ruksakulpiwat)
Member

(Assoc. Prof. Dr. Sittipong Amnuaypanich)
Member

(Assoc. Prof. Dr. Chaiwat Ruksakulpiwat)
Member

(Asst. Prof. Dr. Nitinat Suppakarn)
Member

(Asst. Prof. Dr. Chantima Deeprasertkul)
Member

(Prof. Dr. Santi Maensiri)
Vice Rector for Academic Affairs
and Internationalization

(Assoc. Prof. Flt. Lt. Dr. Kontorn Chamniprasart)
Dean of Institute of Engineering

สาวิตรี ศรีสุวรรณ์ : การสังเคราะห์โคพอลิเมอร์ของพอลิแลคติกแอซิดและยางธรรมชาติเพื่อใช้ในการเสริมความเหนียวให้กับพอลิแลคติกแอซิด (SYNTHESIS OF POLY(LACTIC ACID)-NATURAL RUBBER COPOLYMER FOR TOUGHENING POLY(LACTIC ACID)) อาจารย์ที่ปรึกษา : ผู้ช่วยศาสตราจารย์ ดร.ปราณี ชุมสำโรง, 163 หน้า

จุดมุ่งหมายของงานวิจัยนี้ คือ การสังเคราะห์ไตรบล็อคโคพอลิเมอร์ของพอลิแลคติกแอซิดกับยางธรรมชาติ (PLA-NR-PLA) ผ่านปฏิกิริยาการควบแน่นระหว่างยางธรรมชาติเหลวที่มีหมู่ปลายเป็นหมู่ไฮดรอกซิล (hydroxyl terminated liquid natural rubber หรือ HTNR) กับพอลิแลคติกแอซิดน้ำหนักโมเลกุลต่ำ (pre-PLA) เปรียบเทียบผลการทำหน้าที่เป็นสารเสริมความเหนียวของ HTNR และ PLA-NR-PLA ให้กับ PLA และศึกษาผลการเป็นสารเสริมสภาพเข้ากันได้ของ PLA-NR-PLA ให้กับพอลิเมอร์ผสมระหว่าง PLA และ NR

HTNR ถูกเตรียมขึ้นโดยใช้กระบวนการแยกสลายด้วยแสงและเคมี (photochemical degradation) ของยางธรรมชาติบด pre-PLA ที่มีน้ำหนักโมเลกุลแตกต่างกัน 3 ขนาด เรียกว่า PLA1 PLA2 และ PLA3 ถูกเตรียมขึ้นโดยปฏิกิริยาพอลิเมอไรเซชันแบบควบแน่นของกรดแลคติก ไตร-บล็อกโคพอลิเมอร์สามชนิด ได้แก่ PLA1-NR-PLA1 PLA2-NR-PLA2 และ PLA3-NR-PLA3 ถูกเตรียมขึ้นจาก HTNR และ pre-PLA ที่อุณหภูมิ170 องศาเซลเซียส เป็นเวลา 24 ชั่วโมง โดยใช้สแตนเนียสออกโทเอท (stannous octoate, $Sn(Oct)_2$) เป็นตัวเร่งปฏิกิริยา โครงสร้างทางเคมีของ HTNR pre-PLA และไตรบล็อกโคพอลิเมอร์ถูกยืนยันด้วยเทคนิคโปรตอนและคาร์บอน-13 นิวเคลียร์แมกเนติกเรโซแนนสเปกโตรสโกปี (^{1}H and ^{13}C-nuclear magnetic resonance spectroscopy, ^{1}H-NMR and ^{13}C-NMR) และฟูเรียทรานสฟอร์มอินฟาเรดสเปกโตรสโกปี (Fourier transform infrared spectroscopy, FTIR) น้ำหนักโมเลกุลและสมบัติทางความร้อนของพอลิเมอร์ที่สังเคราะห์ได้ทุกชนิดถูกวิเคราะห์ด้วยเทคนิค GPC และ DSC ตามลำดับ

จากการทดสอบสมบัติทางกลของพอลิเมอร์ผสมระหว่าง PLA และ HTNR (PLA/HTNR) พบว่า พอลิเมอร์ผสมที่มีปริมาณ HTNR เท่ากับ 10 เปอร์เซ็นต์โดยน้ำหนัก มีค่าความทนแรงกระแทก (impact strength) สูงสุดเท่ากับ 67.78 ± 12.10 กิโลจูลต่อตารางเมตร และมีเปอร์เซ็นต์ความยืด ณ จุดขาด (% Elongation at break) เป็น 127.23 ± 6.00 เปอร์เซ็นต์ ซึ่งสูงกว่าของ PLA และพอลิเมอร์ผสมระหว่าง PLA และ NR (PLA/NR) ผลจากการตรวจสอบด้วย SEM แสดงให้เห็นว่าอนุภาค HTNR มีเส้นผ่านศูนย์กลางเฉลี่ยเท่ากับ 0.92 ± 0.71 ไมโครเมตร ผลการทดลองที่ได้จากเทคนิค DSC แสดงให้เห็นว่า T_g ของเฟส HTNR ในพอลิเมอร์ผสม PLA/HTNR มีค่าสูงกว่า T_g ของเฟส NR ในพอลิเมอร์ผสม PLA/NR

สำหรับพอลิเมอร์ผสมระหว่าง PLA และPLA-NR-PLA ค่าความทนแรงกระแทกมีค่าสูงสุดเมื่อปริมาณโคพอลิเมอร์เท่ากับ 10 เปอร์เซ็นต์โดยน้ำหนัก และมีค่าเพิ่มขึ้นเมื่อน้ำหนักโมเลกุลของโซ่ปลาย PLA เพิ่มขึ้น พอลิเมอร์ผสม PLA/PLA3-NR-PLA3 แสดงค่าความทนแรงกระแทกสูงสุดเท่ากับ 54.31 ± 3.87 กิโลจูลต่อตารางเมตร อย่างไรก็ตาม ยังคงต่ำกว่าค่าความทนแรงกระแทกของพอลิเมอร์ผสม PLA/NR และ PLA/HTNR ในขณะที่ค่าความต้านแรงดึงและมอดุลัสของพอลิเมอร์ผสม PLA/PLA3-NR-PLA3 มีแนวโน้มสูงกว่าของพอลิเมอร์ผสม PLA/HTNR(90/10) จากการตรวจสอบสัณฐานวิทยา อนุภาคของยางในพอลิเมอร์ผสม PLA/PLA-NR-PLA มีขนาดลดลงเมื่อหนักโมเลกุลของโซ่ปลาย PLA เพิ่มขึ้น จากผลการวิเคราะห์ด้วย DSC พบว่า T_g ของเฟส PLA ในพอลิเมอร์ผสมมีค่าลดลงอย่างต่อเนื่องเมื่อน้ำหนักโมเลกุลของโซ่ PLA ด้านปลายของไตรบล็อกโคพอลิเมอร์มีค่าเพิ่มขึ้น เมื่อปริมาณยางในพอลิเมอร์ผสมระหว่าง PLA/PLA-NR-PLA เป็น 10 เปอร์เซ็นต์โดยน้ำหนัก (R-10) ค่าความทนแรงกระแทกของพอลิเมอร์ผสม PLA/PLA-NR-PLA ทุกชนิดมีค่าสูงขึ้นอย่างมีนัยสำคัญ สมบัติทางกลของ PLA/PLA3-NR-PLA3 (R-10) สูงกว่าพอลิเมอร์ผสม PLA/HTNR และ PLA/NR การเติมไตรบล็อกโคพอลิเมอร์ลงในพอลิเมอร์ผสม PLA/NR ส่งผลให้ความทนแรงกระแทกและสมบัติการดึงมีค่าเพิ่มขึ้น โดย PLA/NR/PLA3-NR-PLA3 (90/7/3) แสดงสมบัติเชิงกลดีที่สุด

สาขาวิชา วิศวกรรมพอลิเมอร์
ปีการศึกษา 2561

ลายมือชื่อนักศึกษา ศิริพร ศิลาเกณ์
ลายมือชื่ออาจารย์ที่ปรึกษา ปราณี ชยางกูร
ลายมือชื่ออาจารย์ที่ปรึกษาร่วม

SAWITRI SRISUWAN : SYNTHESIS OF POLY(LACTIC ACID)-NATURAL RUBBER COPOLYMER FOR TOUGHENING POLY(LACTIC ACID). THESIS ADVISOR : ASST. PROF. PRANEE CHUMSAMRONG, Ph.D. 163 PP.

POLY(LACTIC ACID)/ NATURAL RUBBER/ TOUGHENING AGENTS/ BLOCK COPOLYMER

The aim of this research was to synthesize triblock copolymer of natural rubber (NR) and poly(lactic acid) (PLA) (PLA-NR-PLA) via condensation reaction of hydroxyl terminated liquid natural rubber (HTNR) and low molecular weight poly(lactic acid) (pre-PLA). The effect of HTNR and PLA-NR-PLA as a toughening agent for PLA was compared. The application of triblock copolymer as a compatibilizer for PLA/NR blend was also studied.

HTNR was prepared by photochemical degradation of masticated NR. Three different molecular weight pre-PLA which coded as PLA1, PLA2, and PLA3 were prepared by condensation polymerization of L-lactic acid. Three types of triblock copolymers which were PLA1-NR-PLA1, PLA2-NR-PLA2 and PLA3-NR-PLA3 were synthesized from HTNR and pre-PLA at 170 °C for 24 h using $Sn(Oct)_2$ as a catalyst. The chemical structure of HTNR, pre-PLA, and PLA-NR-PLA was confirmed by ^{1}H-NMR, ^{13}C-NMR and FTIR. Molecular weight and thermal properties of all synthesized polymers were characterized by GPC and DSC techniques respectively.

From the investigation of mechanical properties of PLA/HTNR blends, the blend containing 10 %wt. HTNR showed the highest impact strength of 67.78 ± 12.10 kJ/m^2 with the elongation at break of 127.23 ± 6.00% which was higher than PLA and

PLA/NR(90/10) blend. From SEM result, the particle size of HTNR in the blend was 0.92 ± 0.71 μm. The results obtained from DSC technique indicated that the T_g of HTNR phase in PLA/HTNR blend was higher than that of NR phase in PLA/NR blend.

For PLA/PLA-NR-PLA blends, the highest impact strength was found for the blend containing 10 %wt. copolymer and it was increased with an increase of the molecular weight of PLA end block. The highest impact strength of 54.31 ± 3.87 kJ/m^2 was belonged to PLA/PLA3-NR-PLA3 blend. However, it was lower than that of PLA/HTNR and PLA/NR blends. In contrast, tensile strength and modulus of the blend tended to be higher than those of PLA/HTNR(90/10) blend. From SEM observation, the rubber particle size in PLA/PLA-NR-PLA blends was reduced as molecular weight of PLA end block increased. From DSC analysis, T_g of PLA phase in the blends was steadily decreased as molecular weight of PLA end block increase. When the amount of rubber in PLA/PLA-NR-PLA blends was adjusted to 10 %wt. (R-10), the impact strength of all PLA/PLA-NR-PLA blends was significantly improved. PLA/PLA3-NR-PLA3(R-10) blend showed higher mechanical properties than PLA/HTNR and PLA/NR blends. The addition of triblock copolymers into PLA/NR blend resulted in an improvement of impact strength and tensile properties. The optimum mechanical properties were found for PLA/NR/PLA3-NR-PLA3 (90/7/3) blend.

School of Polymer Engineering

Academic Year 2018

Student's Signature Sanitsri Srisuwan

Advisor's Signature Pranee Chumsamrong

Co-Advisor's Signature Nyapapan

ACKNOWLEDGEMENTS

I would like to thank Suranaree University of Technology and Center of Excellence on Petrochemicals and Materials Technology for financial support.

I am very grateful and appreciation to my thesis advisor, Asst. Prof. Dr. Pranee Chumsamrong, for her supporting information, advice and encouragement throughout this study. I also special thank my thesis advisor for her tireless effort in encouraging me to complete my work. Moreover, I would like to thank Assoc. Prof. Dr. Yupaporn Ruksakulpiwat, my co-advisors for advices during my research work. I gratefully thank the chairperson, Assoc. Prof. Dr. Wimonlak Sutapun and the committee, Assoc. Prof. Dr. Sittipong Amnuaypanich, Assoc. Prof. Dr. Chaiwat Ruksakulpiwat, Asst. Prof. Dr. Nitinat Suppakarn, and Asst. Prof. Dr. Chantima Deeprasertkul for their valuable suggestion and encouragement.

I wish to thank all staff members, and all friends of the School of Polymer Engineering for their helps and supports throughout my work. Finally, I would like to express my honest gratefulness to my family and my parents, Mr. Somchai and Mrs. Sawai Srisuwan, who give my life, constant support, love, and encouragement throughout my life.

Sawitri Srisuwan

TABLE OF CONTENTS

Page

TABLE OF CONTENTS (Continued)

Page

TABLE OF CONTENTS (Continued)

Page

TABLE OF CONTENTS (Continued)

Page

TABLE OF CONTENTS (Continued)

Page

TABLE OF CONTENTS (Continued)

Page

TABLE OF CONTENTS (Continued)

Page

TABLE OF CONTENTS (Continued)

Page

LIST OF TABLES

Table **Page**

LIST OF TABLES (Continued)

Table **Page**

LIST OF TABLES (Continued)

Table **Page**

LIST OF FIGURES

Figure **Page**

LIST OF FIGURES (Continued)

Figure **Page**

LIST OF FIGURES (Continued)

Figure **Page**

LIST OF FIGURES (Continued)

Figure **Page**

LIST OF FIGURES (Continued)

Figure **Page**

LIST OF FIGURES (Continued)

Figure **Page**

LIST OF FIGURES (Continued)

Figure **Page**

SYMBOLS AND ABBREVIATIONS

°C	=	Degree Celsius
g	=	Gram
%	=	Percent
%wt	=	Percent by weight
wt/wt	=	Weight by weight
NR	=	Natural rubber
HTNR	=	Hydroxyl terminated natural rubber
PLA	=	Poly(lactic acid)
pre-PLA	=	Low molecular weight poly(lactic acid) prepared by condensation polymerization
FTIR	=	Furior transform infarred spectroscopy
GPC	=	Gel permeation chromatography
^{1}H-NMR	=	Proton nuclear magnetic resonance spectroscopy
^{13}C-NMR	=	13-Carbon nuclear magnetic resonance spectroscopy
SEM	=	Scanning electron microscope
DSC	=	Differential scanning calorimetry
$\bar{M}_w$	=	Weight average molecular weight
$\bar{M}_n$	=	Number average molecular weight
$\bar{M}_{n,\,cal}$	=	Calculated number average molecular weight

SYMBOLS AND ABBREVIATIONS (Continued)

PDI	=	Polydispersity index
phr	=	Parts per hundred resin
kJ	=	Kilojoule
J	=	Joule
μm	=	Micrometer
mm	=	Millimeter
min.	=	Minutes
MPa	=	Megapascal
GPa	=	Gigapascal
mbar	=	Millibar, a metric unit of pressure, bar pressure unit
NR-STR 5L	=	Standard Thai rubber 5L grad natural block rubber
PLA1	=	Example of nomenclature used to identify individual low molecular weight PLA. ‘1’ denotes as a condition was used for synthesis PLA.
HTNR54	=	Example of nomenclature used to identify individual HTNR produced from photochemical degradation of natural rubber. ‘54’ denotes degradation hours.
PLA1-NR-PLA1	=	Example of nomenclature used to identify individual .block copolymer that was synthesized from HTNR and Pre-PLA

SYMBOLS AND ABBREVIATIONS (Continued)

PLA1-NR-PLA1	=	Example of nomenclature used to identify individual block copolymer that was synthesized from HTNR and pre-PLA.

CHAPTER I

INTRODUCTION

1.1 General introduction

A large quantity of non-biodegraded, fossil-based plastics can cause environmental problems. For example, harmful chemicals leach from plastic products, and plastic debris can injure or poison wildlife. Therefore, solutions for such problems need to be developed. Many researchers have focused on the improvement of technical properties of bioplastic materials to create a potential replacement for non-degradable plastics. The uses of bio-based plastic materials are growing rapidly; the estimated worldwide production capacity of bio-based plastic's will be about 3.45 million metric tons in 2020 (Shen, Haufe, and Patel, 2009). Poly (lactic acid) (PLA) is one of the most promising bio-based polymers because it is not only produced from lactic acid that is derived from renewable resources such as corn and tapioca, but also it is fully biodegradable (Kulkarni, Moore, Hegyeli, and Leonard, 1971). In addition, PLA has attracted attention because of its interesting mechanical properties such as high strength, high stiffness and biocompatibility. PLA is mainly used in medical and food packaging applications (Datta, Tsai, Bonsignore, Moon, and Frank, 1995). However, the poor thermal resistance, limited gas barrier, and inherent brittleness properties of PLA have been major limitations for its large-scale commercial applications (Singh, Pandey, Rutot, Degee, and Dubois, 2003).

In recent years, numerous approaches have been used to improve the toughness

of brittle PLA, including copolymerization of PLA with other ductile synthetic polymers; such as polycaprolactone (Chavalitpanya, and Phattanarudee, 2013), polybutylenesuccinate, (Berthé, Ferry, Bénézet, and Bergeret, 2010), and poly(butylene adipated-co-terephthalate) (Jiao, Huang, Zeng, Wang, and Wang, 2012), blending with plasticizer (Shi, Li, Zheng, 2014), and a variety of elastomers (Zhao, Ding, Yang, Ning, and Fu, 2013); (Yuan, Chen, Xu, Chen, and Chen, 2014).

Natural rubber (NR) is one of the most interesting elastomers due to its renewable resource, biodegradability, and low cost (Bitinis, Verdejo, Cassagnau, and Lopez-Manchado, 2011). The main interesting points of NR is the high production yield of NR in Thailand which was about 4,000,000 metric tons in 2012-2014 (Thailand Board of Investment, 2016). Many researches have shown that toughness of PLA was achieved by the addition of NR (Pongtanayut, Thongpin, Santawitee, 2013); (Xu, Yuan, Fu, Chen, 2014). Nevertheless, the compatibility between PLA and NR is poor because of different polarity and the high molecular weight of NR, resulting in large NR particles and low interfacial adhesion. Therefore, in order to achieve higher mechanical properties, compatibility improvement for PLA/NR blends has been studied by many researchers. For example, Juntuek, Ruksakulpiwat, Chumsamrong, and Ruksakulpiwat (2012) studied the effect of NR grafted with glycidyl methacrylate (NR-g-GMA) on the compatibility and mechanical properties of PLA/NR blends. They found that elongation at break and impact strength of the PLA/NR blends was increased with the addition of NR-g-GMA. Chumeka, Tanrattanakul, Plilard, and Pasetto (2013) used NR grafted with vinyl acetate (NR-g-PVAc) as a toughening agent for PLA and as a compatibilizer for the PLA/NR blends. It was generally found that PVAc decreased the particle size of NR. PLA/NR-g-PVAc blends showed higher impact strength and elongation at break

than the PLA/NR blend. Zhang et al. (2011) modified NR molecules by grafting with butyl acrylate (NR-g-PBA) and added into PLA. They reported that the NR-g-PBA showed higher compatibility with PLA than NR. In addition, Jaratrotkamjorn, Khaokong, and Tanrattanakul (2012) found the Charpy impact strength of PLA/NR blends increased with increasing rubber mastication from 20 to 180 passes. They explained that it was due to the decrease in molecular weight and Mooney viscosity of NR, leading to a reduction of NR particle size in the blends. Therefore, it is of interest to study the influence of low molecular weight NR that contains hydroxyl functional groups and its copolymer with PLA as toughening agents for PLA. Moreover, the use of PLA-NR copolymer as a compatibilizer for PLA/NR blends is also conducted. Low molecular weight and more polar NR and copolymers of PLA and NR are expected to improve the compatibility of PLA and NR, leading to smaller NR particles and better interfacial adhesion. Consequently, the mechanical properties, especially the impact strength and elongation at the break-point of PLA, will be increased.

1.2 Research objectives

The objectives of this study are:

(i) To study the preparation of HTNR and PLA-NR-PLA triblock copolymer from HTNR.

(ii) To characterize the chemical structure and molecular weight of HTNR and PLA-NR-PLA triblock copolymer.

(iii) To study the effect of HTNR and PLA-NR-PLA triblock copolymer on the mechanical and morphological properties of PLA.

(iv) To study the effect of PLA-NR-PLA triblock copolymer on the

mechanical and morphological properties of PLA/NR blends.

1.3 Scope and limitation of the study

In this study, hydroxyl terminated natural rubber (HTNR) was prepared by means of a photochemical reaction. The PLA-NR-PLA triblock copolymer was synthesized by solution polymerization. Tin(II) 2-ethylhexanoate $Sn(Oct)_2$ was used as an initiator. The hydroxyl number of HTNR was estimated according to ASTM D4274-11. The Molecular weight and molecular weight distribution of HTNR and PLA-NR-PLA triblock copolymer were measured by gel permeation chromatography (GPC). The chemical structure of HTNR and PLA-NR-PLA triblock copolymer were characterized using an ^{1}H-NMR, ^{13}C-NMR spectrophotometer and a Fourier transform infrared microspectrometer (FTIR). PLA/HTNR and PLA/NR/PLA-NR-PLA triblock copolymer blends were prepared using an internal mixer. The effects of HTNR and triblock copolymer contents on the physical properties of the blends were investigated. The compatibilizing effect of PLA-NR-PLA triblock copolymer on mechanical, morphological properties of PLA/NR blend was also studied.

CHAPTER II

LITERATURE REVIEW

2.1 Poly (lactic acid)

Poly (lactic acid) (PLA) is thermoplastic aliphatic polyester, commonly made from lactic acid, that can be obtained from annually renewable resources. The chemical structure of PLA is shown in Figure 2.1.

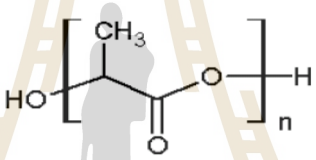

Figure 2.1 Chemical structure of PLA (Mahapatro and Singh, 2011).

PLA is considered to be a biodegradable and compostable material. The biodegradability of PLA occurs in six months to two years, when disposed of properly (Tokiwa et al., 2009). PLA is increasingly being used as an alternative to conventional plastics for short shelf-life products, disposable bags, packaging, and in agriculture. In addition, PLA has excellent biocompatibility. PLA is also found in drug delivery systems and tissue engineering. Moreover, the fossil fuel energy and gas requirement for the production of PLA is about 50% of the energy requirement for the production of conventional plastics, by petrochemical industries that use up more than two hundred and seventy million tons of oil and gas every year worldwide (Vink et al., 2003; Vaidya et al., 2005). This indicates that PLA not only comes from renewable resources, but

that it also has economic advantages over a number of alternative petroleum-based polymers. The fossil energy requirement for a variety of petroleum-based polymers and PLA is shown in Figure 2.2.

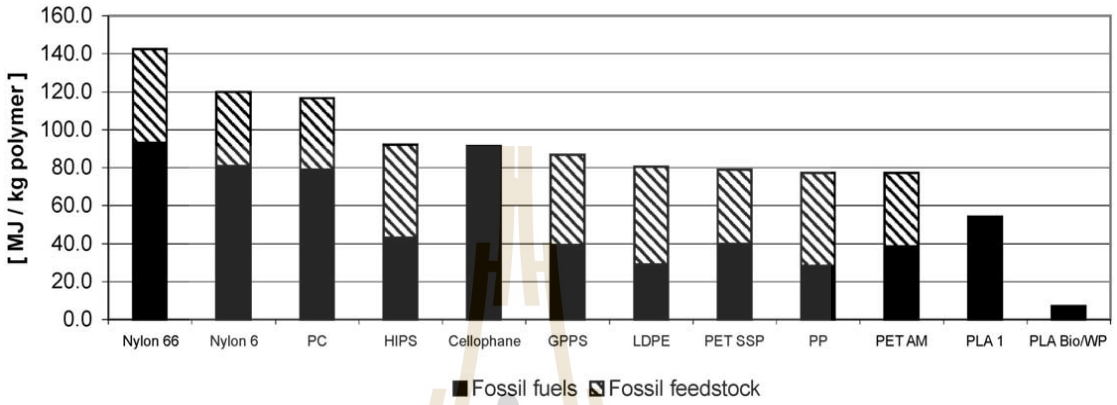

Figure 2.2 Fossil energy requirement for some petroleum-based polymers and PLA. The cross-hashed part of the bars represents the fossil energy used as chemical feedstock (the fossil resource to build the polymer chain). The solid part of each bar represents the gross fossil energy used for the fuels and operating supplies used to drive the production processes (Vink, Rábago, Glassner, and Gruber, 2003).

PLA is produced from lactic acid monomer. Lactic acid (2-hydroxypropionic acid) is a hydroxy acid with an asymmetric carbon atom and exists in two optically active configurations. The D-(-)-lactic and L-(+)-lactic acid are produced by the bacterial fermentation process of carbohydrates received from renewable resources such as starch and corn. The stereoisomers of L-(+)-lactic acid and D-(-)-lactic acid are shown in Figure 2.3.

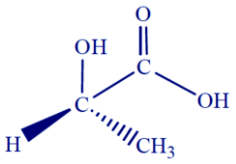

L-(+)-lactic acid

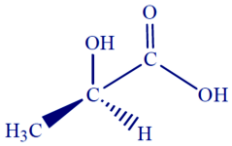

D-(-)-lactic acid

Figure 2.3 The stereoisomers of lactic acid (Xiao, Wang, Yang, and Gauthier, 2012).

2.1.1 Synthesis of poly (lactic acid)

Synthesis of high-molecular weight PLA from lactic acid can be carried out using three different polymerization methods including a condensation and coupling reaction, azeotropic dehydrative condensation, and ring- opening polymerization (ROP) of lactide as depicted in Figure 2.4.

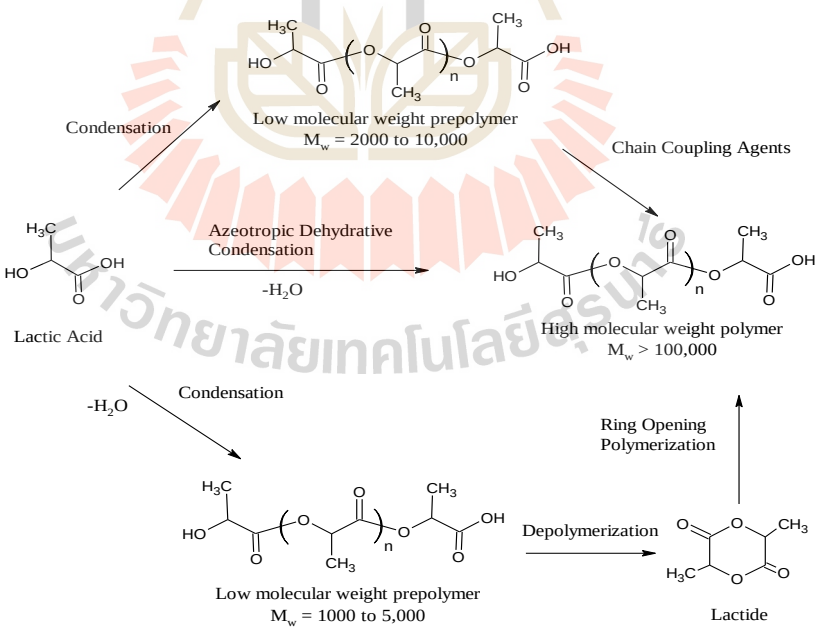

Figure 2.4 Schematic of synthesis methods for high-molecular-weight PLA (Garlotta, 2001).

2.1.1.1 Condensation polymerization and coupling reaction

Lactic acid is condensation polymerized to yield a low-molecular-weight, brittle, glassy polymer, which, for the most part, is unusable for any application, unless external coupling agents are used to increase the molecular weight of the polymer. Therefore, the use of coupling agents is required, or esterification-promotion with a variety of diisocyanates e.g. 1,6-hexamethylene diisocyanate, or 1,4-butanediisocyanate. An example of a coupling agent used to obtain high molecular weight PLA is shown in Figure 2.5.

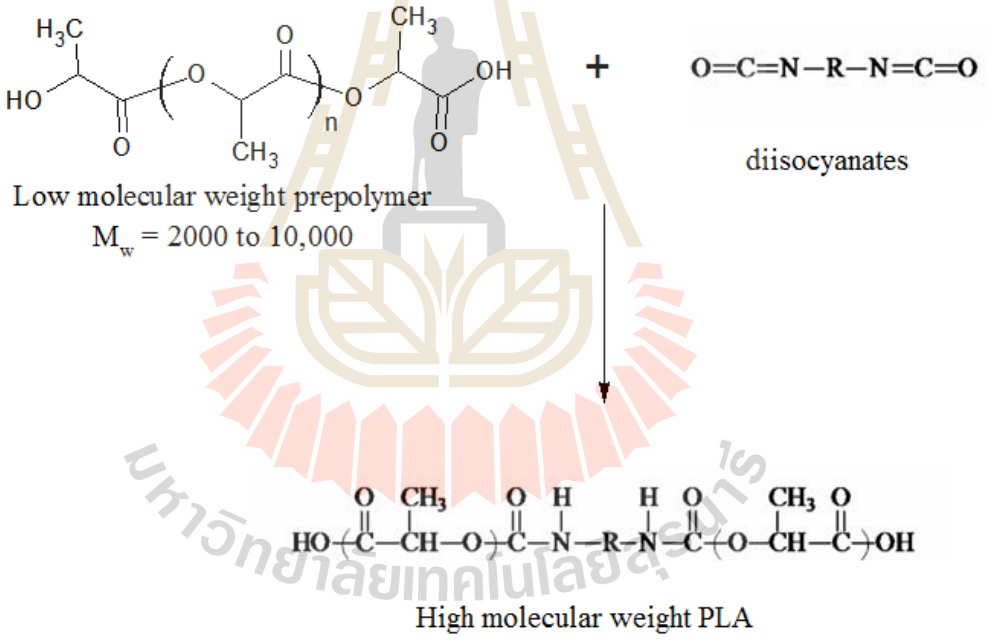

Figure 2.5 Coupling reactions in the preparation of high molecular weight PLA using diisocyanates (Auras et al., 2010)

The self-condensation of lactic acid results in a low-molecular-weight PLA with hydroxyl and carboxyl for each end-chain. Chain-coupling agents are added and react with either the hydroxyl or carboxyl group for an increase of the molecular weight. The

condensed PLA can be modified to produce all hydroxyl by the addition of a small amount of a multifunctional hydroxyl compound, such as cis-2-butene-1, 4-diol, or the post-condensation reaction of a mono-functional epoxide, which leads to hydroxyl end-groups. An example of hydroxyl terminated PLA end-groups is modified by cis-2-butene-1, 4-diol, as shown in Figure 2.6. In addition, all-carboxyl-terminated PLA can be synthesized by the condensation reaction in the presence of multifunctional carboxylic acids such as maleic and succinic acid. The presence of multifunctional carboxylic acids can convert the hydroxyl to carboxylic end-group (Bonsignore, 1995). However, the addition of coupling agents causes an increase of PLA's synthesis cost and complexity.

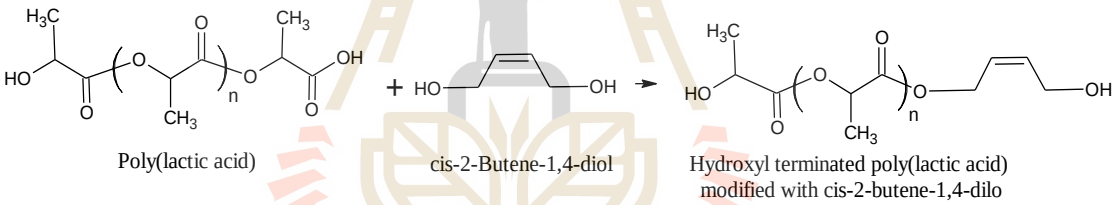

Figure 2.6 Hydroxyl terminated PLA was modified by multifunctional hydroxyl compounds.

2.1.1.2 Azeotropic dehydration condensation polymerization

Azeotropic dehydration condensation polymerization is used to obtain high-molecular weight PLA without the use of coupling agents or chain extenders. This method includes the reduction of pressure, distillation of lactic acid to remove the majority of the water, and the addition of a catalyst. The main drawback of this polymerization technique is the remaining catalyst impurities due to the high level of catalyst needed for reaction rates. This residual catalyst can cause degradation,

uncontrolled or unreproducible hydrolysis rates, catalyst toxicity and differing slow-release properties. However, the catalyst can be deactivated by the addition of phosphoric or pyrophosphoric acid. The catalyst can also be precipitated and filtered out by the addition of strong acids such as sulfuric acid (Kaplan, 1998).

2.1.1.3 Ring-opening polymerization

The ring opening polymerization technique for high molecular weight PLA (M_w > 100,000) was developed by DuPont in 1954. Lactide is obtained by the depolymerization of low molecular weight PLA under reduced pressure to give a mixture of L- lactide, D- lactide, and meso- lactide (D,L- lactide) . The different percentages of the lactide isomers formed depends on the lactic acid isomer feedstock, temperature, and catalyst. The schematic of different lactide ring formation is shown in Figure 2.7.

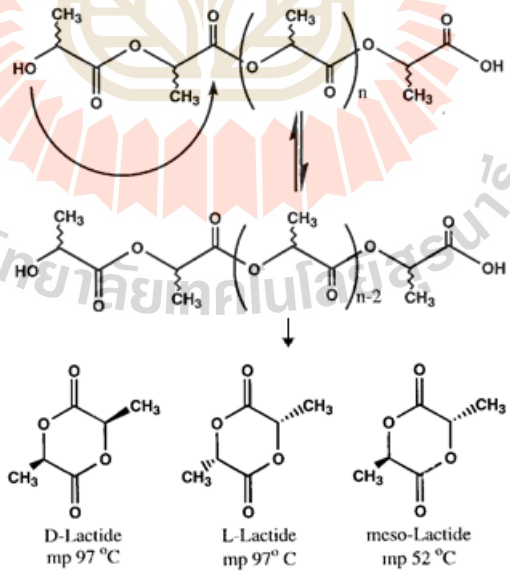

Figure 2.7 Lactide ring formation (Kaplan, 1998).

Anionic and cationic initiations are usually applied in ring opening polymerization due to their high reactivities, susceptibility to racemization, transesterification, and low impurity levels.

2.1.1.3.1 Cationic ring-opening polymerization

PLA can be synthesized by cationic ring-opening polymerization. Successful cationic initiators to polymerize lactide are trifluoromethane sulfonic acid (triflic acid) and methyl trifluoromethanesulfonic acid (methyl triflate) (Kricheldorf, and Kreiser, 1987; Kricheldorf, and Sumbél, 1989). The polymerization proceeds via triflate ester endgroups instead of free carbenium ions, which yields, at low temperatures (<100˚C), an optically active polymer without racemization. The chain growth proceeds by cleavage of the alkyl-oxygen bond as shown in Figure 2.8. The propagation mechanism begins with the positively charged lactide ring being cleaved at the alkyl-oxygen bond by the triflate anion. The triflate end group reacts with a second molecule of lactide to yield a positively charged lactide which is opened. Then the triflate anion again opens the charged lactide, and polymerization proceeds (Kaplan, 1998).

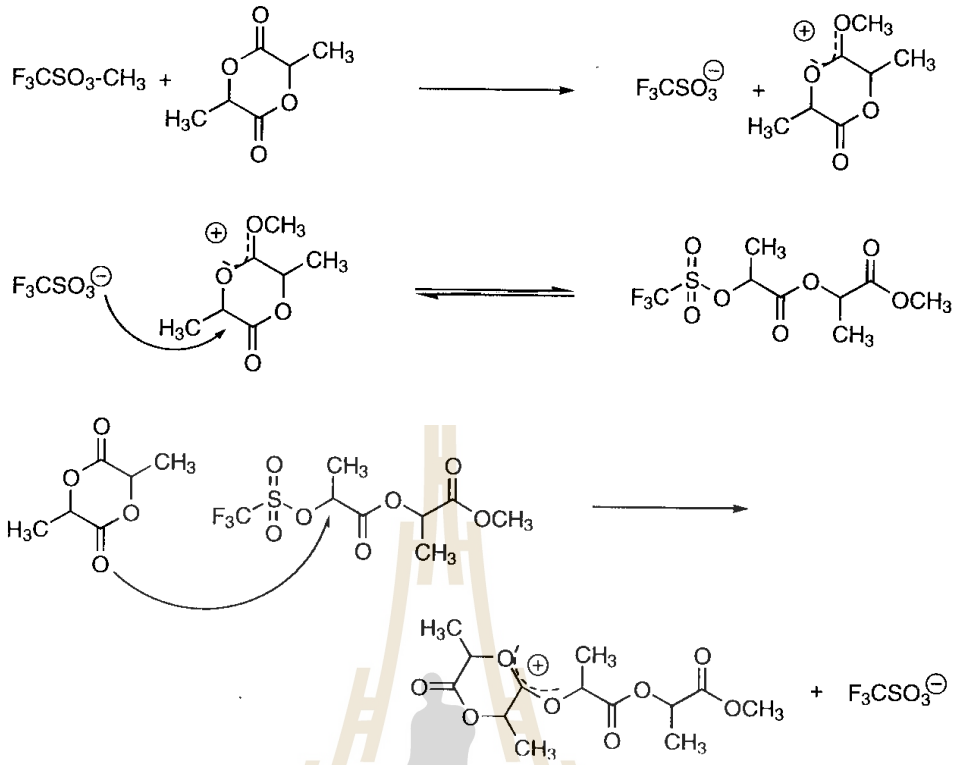

Figure 2.8 Schematic of cationic polymerization mechanism (Kaplan, 1998).

2.1.1.3.2 Anionic ring-opening polymerization

Anionic lactide polymerization proceeds by the nucleophilic reaction of the anion with the carbonyl and the subsequent acyl-oxygen cleavage and results in production of an alkoxide end-group, which continues to propagate. The schematic of the anionic polymerization mechanism is shown in Figure 2.9. The use of primary alkoxides such as potassium methoxide can yield well-defined polymers with negligible racemization, termination, or transesterification. Racemization of less than 5% was seen, starting with 99.9% pure L-lactide (Jedlinski et al., 1995). On the other hand, high nucleophilicity initiators are needed to initiate the lactide. Weaker bases, such as potassium benzoate, potassium phenoxide, or zinc

stearate, do not initiate at low temperatures, but will initiate at higher temperatures (120˚C). The high-temperature

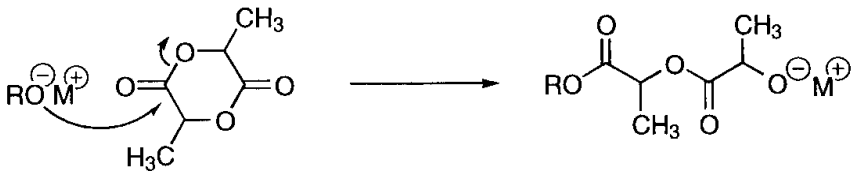

Figure 2.9 Schematic of anionic polymerization mechanism (Kaplan, 1998).

initiations occur in bulk but with considerable racemization and other side reactions, which hinder propagation (Kricheldorf et al., 1989). Initiators such as *n*-, *sec*-, or *tert*-butyl lithium and potassium tert-butoxide rapidly initiate the polymerization at low temperatures, but are plagued by side reactions, such as deprotonation of the lactide monomer. This deprotonation causes inconsistent polymerization, racemization, and, when done by the active chain end, termination, which thereby limits the molecular weights. The use of 18-crown-6 ether complexes will yield higher molecular weights with narrow distributions, (PDI of 1.1-1.2), but they slow the rate and give lower overall conversions (Sipos, Zsuga, and Kelen, 1992).

2.1.1.3.3 Coordination polymerization

The anionic and cationic initiations described above are usually done in solvent systems and, due to their high reactivities, are susceptible to racemization, transesterification, and especially to impurity-level problems. For large-scale production of high molecular weight PLA, it is preferable to do bulk melt polymerizations that use lower levels of nontoxic catalysts and are not plagued by these problems. The use of less reactive metal carboxylates, oxides, and

alkoxides has been extensively studied to correct these problems. It has been found that high molecular weight PLA is easily polymerized in the presence of tin, zinc, aluminum, and other heavy metal catalysts, with tin(II) and zinc yielding the purest polymers. These catalysts are favored because of their covalent metal oxygen bonds and free *p*- or *d*- orbitals. Kricheldorf, and Serra (1985) report that, tin(II) oxide or octoate, lead(II) oxide, antimony octoate, and bismuth octoate were the most effective catalysts with respect to yield, molecular weight, and racemization. The best results were obtained with tin oxide and octoate at 120-150˚C with conversions > 90% and less than 1% racemization. Few carbonates gave acceptable polymerizations, and all had considerable racemization. The alkali metal carboxylates, such as sodium and calcium, were similar to the carbonates (Kricheldorf, and Serra 1985). Early research has been conducted to test the wide use of tin (II) bis-2-ethylhexanoic acid (tin or stannous octoate) as a catalyst for synthesis of high molecular weight PLA. This was because of its solubility in many lactones, low toxicity, high catalytic activity, and low racemization. The mechanism and polymerization variables of the tin octoate polymerization have been studied by various groups, but considerable debate about the true mechanism still remains. The effect of certain variables on the tin octoate- and zinc- catalyzed polymerization was studied. It was found that the yield and transesterification was affected, in the following order; by polymerization temperature > monomer to catalyst ratio > polymerization time > type of catalyst (Sn or Zn) > and monomer degassing time. The interaction of time and temperature, as would be expected, was very significant, since this led to degradation reactions that would limit molecular weight and affect the reaction rate. However, the molecular weight was

directly controlled by the amount of hydroxyl impurities and is independent of carboxylic acid impurities and catalyst concentration (Kaplan, 1998).

2.1.2 Chemical and physical properties of PLA

PLA is a chiral polymer containing asymmetric carbon atoms with a helical conformation. Two optical isomers, L-(+)-lactic acid and D-(-)-lactic acid, are used to synthesize PLA. Chemical reactions that form the cyclic dimer lactic acid to the production of PLA could result in macromolecular chains with LLA and DLA monomer units (Endo et al., 2005). The properties of PLA, such as molecular weight, melting point, extent of crystallization and mechanical properties were controlled by adjusting the ratios and the sequence of L-(+)-lactic acid and D-(-)-lactic acid units (Rasal, R.M., Amol V. Janorkar, A.V., and Hirta, D.E., 2010). The polymerization of optically pure L- and D-lactid give isotactic homopolymers of PLLA and PDLA, respectively. Pure PLLA and PDLA were semi-crystalline and crystalline, respectively with a melting transition temperature (T_m) near 207˚C but typical T_m were the 170˚C-180˚C. Crystallinity and T_m of PLLA and PDLA usually decrease with decreasing optical purity (OP) of the lactate unit in PLA. Optically inactive poly (DL-lactide) (PDLLA), prepared from meso-lactides, was an amorphous polymer, having an atactic sequence of D and L units. However, crystalline polymers can be obtained when the sequence of both D and L units are stereo-regularly controlled. The mixing of isotactic PLLA and PDLA in 1: 1 ratio afforded stereo-complex crystals (sc-PLA) whose T_m was 230 ˚C higher than that of PLLA or PDLA. Stereo-block copolymers, sb-PLA consisting of isotactic PLLA and PDLA sequences were also synthesized by stereo-regular polymerization techniques involving block copolymerization. The sc-PLA structural diversities of PLA polymers provided a broad range of physicochemical

properties for PLA materials (Masutani, and Kimura, 2014) . The effects of stereochemistry and crystallinity on mechanical properties of PLA are shown in Table 2.1.

Table 2.1 Effects of stereochemistry and crystallinity on mechanical properties of PLA (Garlotta, 2001).

Mechanical properties	Poly(lactic acid)		
	Annealed L-PLA	L-PLA	D,L-PLA
Yield strength (MPa)	70	70	53
Tensile strength (MPa)	66	59	44
Flexural strength (MPa)	119	106	88
Notch Izod impact (J/m)	66	26	18
Vicat Penetration (˚C)	165	59	52

The chemical structure of PLA can be characterized by Fourier Transform Infrared (FT-IR) spectroscopy, proton nuclear magnetic resonance spectroscopy (^{1}H-NMR) and Carbon-13 nuclear magnetic resonance spectroscopy (^{13}C-NMR). FT-IR is sensitive to the conformation and local molecular environment, this technique has also been used to elucidate the structure of the crystalline polymers. Peak band assignments for semi-crystalline and amorphous PLLA in the infrared range are summarized in Table 2.2.

Table 2.2 The peak assignment of semi-crystalline and amorphous PLLA Infrared spectra (Auras, Lim, Selke, and Tsuji, 2010).

Semi-crystalline PLA		Amorphous PLA		Peak assignment
Peak position (cm^{-1})	Intensity of each band	Peak position (cm^{-1})	Intensity of each band	
3,571	weak	-	-	υOH (free)
2,997	medium	2,997	medium	$\upsilon_{as}CH_3$
2,947	medium	2,947	medium	$\upsilon_{s}CH_3$
2,882	weak	2,882	weak	υCH
1,760	very strong	1,760	very strong	υ(C=O)
1,452	strong	1,452	strong	$\delta_{as}CH_3$
1,348, 1,388	strong	1,385	strong	$\delta_{s}CH_3$
1,368	strong	1,365	shoulder	$\delta_{l}CH$ + $\delta_{s}CH_3$
1,360	strong	1,360	strong	$\delta_{l}CH$ + $\delta_{s}CH_3$
1,300, 1,313	medium	1,300, 1,315	medium	$\delta_{2}CH$
1,270	strong	1,270	strong	δCH + υCOC
1,215	very strong	1,211	very strong	$\upsilon_{as}COC$
1,185	very strong	1,185	very strong	υasCOC
1,130	strong	1,130	strong	rasCH3
1,090	very strong	1,090	very strong	υsCOC
1,045	strong	1,045	strong	υC-CH3
960	weak	960	shoulder	rCH3 + υCC
925	weak	-	-	rCH3 + υCC

Table 2.2 The peak assignment of semi-crystalline and amorphous PLLA Infrared spectra (Auras, Lim, Selke, and Tsuji, 2010). (Continued)

Semi-crystalline PLA		Amorphous PLA		Peak assignment
Peak position (cm^{-1})	Intensity of each band	Peak position (cm^{-1})	Intensity of each band	
875	medium	873	medium	υC-COO
760	strong	760	strong	δC=O
740	shoulder	740	shoulder	δC=O
715	medium	710	medium	γC=O
695	medium	690	medium	γC=O
515	weak	-	-	δ1C-CH3 + δCCO
415	shoulder	415	shoulder	δCCO
400	medium	395	medium	δCCO
350	medium	345	medium	δ2C-CH3 + δCOC
300	medium	300	medium	δσC-CH3 + δCOC
295	shoulder	295	shoulder	COC deformation
245	medium	240	medium	τCC

Band is classified as υ = stretching, δ = bending, γ = out of plane vibration, r = rocking, τ = torsion, s (symmetrical), and as (asymmetric)

Auras, Lim, Selke, and Tsuji (2010) reported that the peaks at 2,997, 2,946 and 2,877 cm^{-1} are assigned to the -CH stretching region, $\upsilon_{as}CH_3$, υ_sCH_3, and υCH modes. The peak at 1,748 cm^{-1} is corresponding to C=O stretching region. The region between 1,500 and 1,360 cm^{-1} are characterized by the 1,456 cm^{-1} CH_3 band. The CH deformation and asymmetric bands appear at 1,382 cm^{-1} and 1,365 cm^{-1}, respectively.

The peaks at 1,315 cm^{-1} and 1,300 cm^{-1} are the CH bending modes. In the region of 1,300 cm^{-1} to 1,000 cm^{-1}, it is possible to observe the C-O stretching of the ester groups at 1,225 cm^{-1} and the C-O-C asymmetric mode appears at 1,090 cm^{-1}. For the peaks between 1,000 cm^{-1} and 800 cm^{-1}, peaks can be observed at 956 cm^{-1} and 921 cm^{-1} which can be attributed to the characteristic vibrations of the helical backbone with CH_3 rocking modes. Similar findings have been reported by Garlotta (2001). Finally, the peaks below 300 cm^{-1} correspond mainly to CH_3 torsion modes and to the skeletal C-C torsions.

The appearance of high molecular weight PLA is a colorless, glossy, and rigid thermoplastic material. The properties range of PLA depends on the ratio of isomer used, variable molecular weight, and crystallinity as shown in Table 2.3. Compared to other conventional polymers, PLA is one of the most promising polymers in packaging applications, due to its physical properties being nearly the same as polyethylene terephthalate (PET) and oriented polystyrene (PS) as shown in Table 2.4.

Table 2.3. Material properties of selected PLA (Chen et al., 2003; Xiao, Wang, Guang, and Gauthier, 2012; Omay, and Guvenilir, 2013).

Material properties	PDLA	PLLA	PDLLA
Crystalline structure	Crystalline	Semicrystalline	Amorphous
Melting temperature (T_m)/ °C	~180	~180	-
Decomposition temperature/°C	303-386	~330	~309
Elongation at break/ (%)	20-30	20-30	Variable
Breaking strength/ (g/d)	4.0-5.0	5.0-6.0	Variable
Glass transition temperature (T_g)/ °C	-	55-60	Variable

Table 2.4. PLA properties compared to those of most common polymers used in commodity applications (Kfoury et al., 2013).

Material properties	Poly(lactic acid) (PLA)	Polyethylene terephthalate (PET)	Polystyrene (PS)	High Impact Polystyrene (HIPS)	Polypropylene (PP)
Tg (˚C)	55-60	75	105	~90	10
Tensile modulus (GPa)	0.36	2.8	2.9	2.1	0.9
Elongation at break (%)	6	130	7	45	120
Tensile strength at break (MPa)	53	54	45	23	31
Notched impact strength (J/m)	13	59	27	123	27 (i-PP)
Gardner impact(J)	0.06	0.32	0.51	11.3	0.79
Cost(€/kg)	1.91-2.08	0.94	1.35	1.46	1.25-1.36

* Ingeo biopolymer 4043D grade PLA, 3D Printing Monofilament–General PurposeGrade; NatureWorks LLC

In general, PLA polymers are soluble in dioxane, acetonitrile, chloroform, methylene chloride, 1,1,2-trichloroethane and dichloroacetic acid. In addition, ethyl benzene, toluene, acetone and tetrahydrofuran only partly dissolve PLA when cold, nevertheless PLA polymers are readily soluble in these solvents when heated to boiling temperatures. However, crystalline PLA is not soluble in acetone, ethyl acetate or tetrahydrofuran (Auras, Harte, and Selke, 2004). Moreover, PLA is one of the

promising polymers used in packaging applications because of its more promising physical and chemical properties than other biopolymers as shown in Table 2.5.

Table 2.5 Overview of various additional physical and chemical properties of biopolymer materials (Endres and Siebert-Raths, 2011).

Biopolymer	Transparency	Light-fastness	Oil and fat resistance	Aroma barrier	Antistatic
Polycaprolactone	-	+	+	+/-	+/-
Bio-polyester	-	+/-	+	+/-	+/-
Polyhydroxyal-kanoates	-	+/-	+	+	-
PLA	+	+	+	+/-	+/-

+ referred to good in each properties, - referred to poor in each properties, and +/- referred to properties depending on chemical structure and composition.

2.1.3 The advantages and limitations of PLA

2.1.3.1 The advantages of PLA

2.1.3.1.1 An eco-friendly polymer

Raw materials for synthesized PLA are derived from short-term renewable resources such as wheat, starch, and corn. Moreover, PLA is a biodegradable and compostable polymer (Imre, Renner, and Pukánszky, 2014). Additionally, compared to conventional polymer production, the energy required and carbon dioxide (CO_2) emissions of PLA were less than 50% (Gironi and Piemonte, 2011). These are eco-friendly characteristics of PLA, and make PLA more attractive biopolymer materials.

2.1.3.1.2 Biocompatibility

Nowadays, PLA plays an effective role in medical applications because of its biocompatibility. In addition, PLA works very well and provides excellent properties at a low cost compared to other traditional biodegradable polymers used in medical applications. Examples of medical devices produced from PLA and its copolymer are degradable sutures, drug releasing micro- particles, nanoparticles, and porous scaffolds for cellular applications (Sachlos and Czernuszka, 2003, Langer and Tirrell, 2004).

2.1.3.1.3 Processability

Biopolymers are directly comparable to conventional polymers regarding their injection molding, blow molding, and thermoforming capability in term of melting temperature, heat storage capacity, and shrinkage (Endres and Siebert-Raths, 2011). Compared to PLA, other biopolymers such as poly (hydroxyl alkanoates) (PHAs), and poly (ε-caprolactone) (PCL) have poorer thermal processability. From Figure 2. 10, PLA shows a higher melting temperature than PCL and PHAs, and exhibits a melt temperature comparable to polystyrene (PS), polypropylene (PP) and acrylonitrile butadiene styrene (ABS).

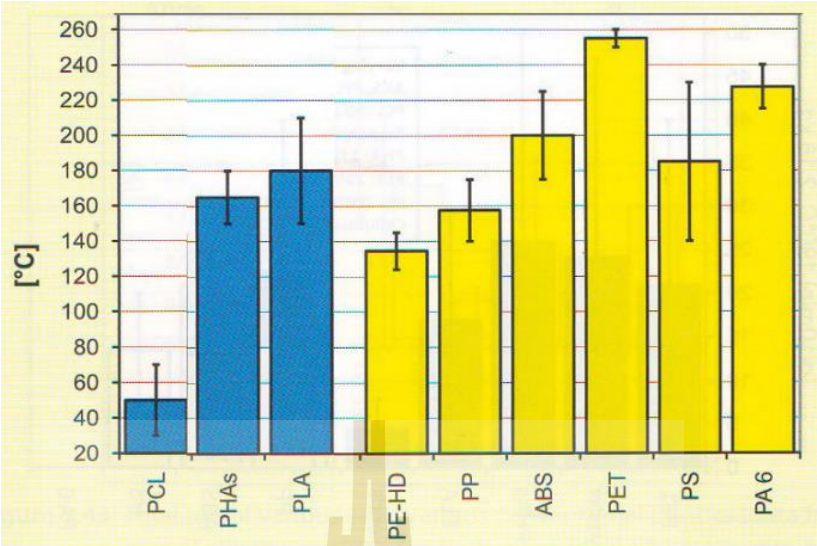

Figure 2.10 Melting temperature for various biopolymers compared with various conventional polymers (Endres and Siebert-Raths, 2011).

Figures 2.11 and 2.12 show shrinkage versus melting temperature and shrinkage versus heat resistance for various biopolymers compared with various conventional polymers. Shrinkage is an important processing parameter that is the sum of processing shrinkage and post-shrinkage. It is taken into account during product design in order to obtain the required final dimension. Shrinkage is strongly dependent on the degree of crystallinity. During the crystallization process, the molecular chain becomes more ordered, the density increases, and their volume is reduced. Figure 2.11 shows the average shrinkage value and deviation for each material. The lowest shrinkage values belong to the amorphous structures of PLA. The low shrinkage value of PLA is advantageous for precision design. On considering shrinkage as a function of heat resistance, for manufacturing parts with high dimensional stability, PLA exhibits lower heat resistance, but lower shrinkage than other biopolymers and conventional polymers.

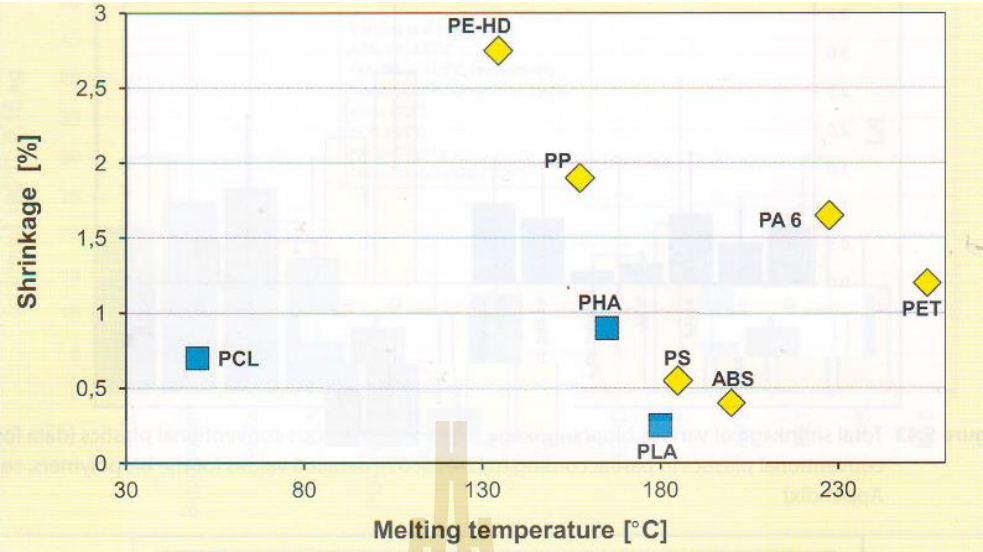

Figure 2.11 Shrinkage versus melting temperature for various biopolymers compared with various conventional polymers (Endres and Siebert-Raths, 2011).

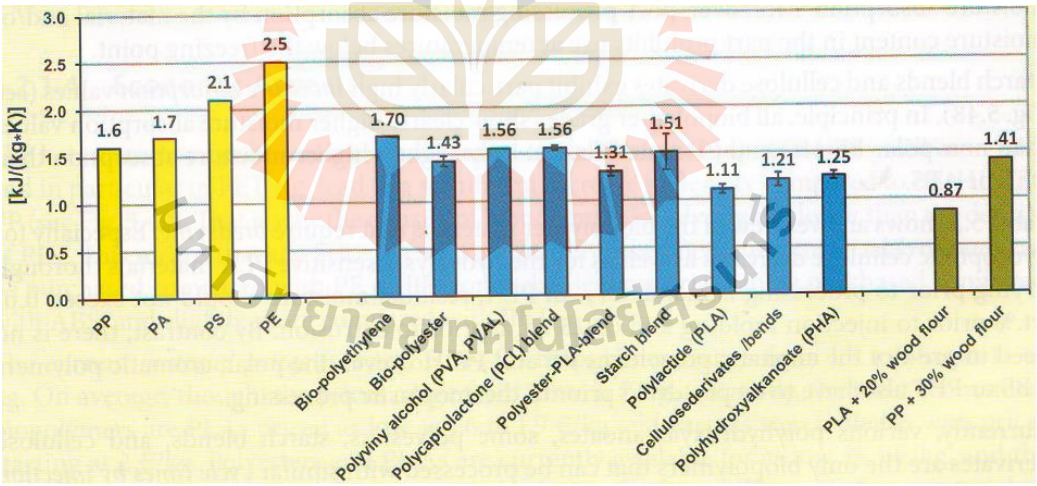

Figure 2.12 Shrinkage versus heat resistance for various biopolymers compared with various conventional polymers (Endres and Siebert-Raths, 2011).

2.1.3.2 The limitation of PLA

Even though PLA shows some physical properties that are nearly the same as PET and oriented PS, some properties of PLA are disadvantages and limit its applications. Examples of PLA drawbacks are as follows.

2.1.3.2.1 Hydrophobicity

PLA is a hydrophobic polymer and its static water contact angle is approximately 65° (Zhu, Zhang, Wu, and Shen, 2002). This results in low cell affinity, and can elicit an inflammatory response from the living host upon direct contact with biological fluids.

2.1.3.2.2 Low water barrier

Besides approval for contact with food and composability. The permeation of gases, aromas, or water vapor through the packing must not change food composition or organoleptic properties. For example, chip packages have to exhibit zero permeability to water vapor, because otherwise the product would lose its crispness. On the other hand, packing for fresh fruit or vegetables has to be permeable for gas and water vapor in order to prevent decay. Water vapor transmission rates below 100g/ m^2d are considered satisfactory and represent sufficiently high water vapor barrier properties (Endres and Siebert-Raths, 2011). Water vapor permeation was measured in some Nature Works™ PLA polymers from Cargill Dow LLC (Whiteman, 2000). A water vapor transmission rate of 340 g mL/m^2d was reported.

2.1.3.2.3 Low toughness

Although, PLA has tensile strength and a tensile modulus comparable to poly(ethylene terephthalate) (PET) (Endres and Siebert-Raths,

2011), it is a very brittle material with lower than 10% elongation at break (Yu at el., 2016; Yang, 2016). Its brittleness is the limitation for applications that need plastic deformation at higher stress levels, such as products used in orthopaedic applications (Raghoebar et al., 2006) and also in packaging applications. Consequently, toughness improvement of PLA should be applied.

2.2 Toughness improvement of PLA through polymer blending

Toughness is the ability of a material to absorb energy and plastically deform before fracture. Mostly, toughness of PLA has been improved by blending it with tough or rubbery polymers.

2.2.1 Polymer blends

A polymer blend is mixture of at least two macromolecular substances, polymers, or copolymers blended together, in which the ingredient content is more than 2 %wt. (Utracki, 2002). The goals of making a polymer blend include: (i) to get materials with properties profile combinations of the blended polymers at reduced cost, (ii) to improve specific properties and to extend the performance of engineering resins, (iii) to reduce scrap from the polymer shaping process, as blending technology makes it possible to produce high performance articles via recycling of industrial and/ or municipal plastic waste, and (iv) to increases the rate of production, as blending ascertains quick formulation changes and improves product uniformity (Robeson, 2007). Polymer blends can be categorized into three groups due to miscibility of the blend, such as; miscible, partially miscible, and immiscible, depending on the change in value of the free energy of mixing (ΔG_m). ΔG_m is the thermodynamic potential, which can predict the direction of the reaction under constant temperature and constant pressure conditions. The change in free energy of mixing is given by:

$$\Delta G_m = \Delta H_m - T\Delta S_m \quad (2.1)$$

Where ΔG_m is the change of Gibbs free energy.

ΔH_m is the change in enthalpy that is either consumed (endothermic) or generated (exothermic) during mixing.

ΔS_m is the change in entropy that is a measure of disorder or randomness of polymer molecules.

2.2.1.1 Miscible polymer blend

The polymer blend indicates a homogeneity down to the molecular level. The thermodynamic nature of miscibility is $\Delta G_m \approx \Delta H_m - T\Delta S_m \leq 0$ and the second derivative is positive value; $d^2\Delta Gmd\varphi^2 > 0$. Properties of the blend have average values between the properties of its components with one glass transition temperature (T_g).

2.2.1.2 Partially miscible polymer blend

A part of one blend component is dissolved in the other, exhibits normally good compatibility and fine phase dispersion morphologies.

2.2.1.3 Immiscible polymer blend

Immiscible blends exhibit a coarse phase morphology having a sharp interface and a poor adhesion between both blend phases. This is the reason for often observed poor properties of immiscible blends, which strongly depend on the size and distribution of the phases. The change in free energy of mixing exhibits positive value; $\Delta G_m > 0$. Usually, an immiscible polymer blend has two T_g and the two components are phase separated.

The relation between the change in free energy of mixing and molar fraction (φ) of miscible, partially miscible, and immiscible polymer blends is shown in Figure 2.13.

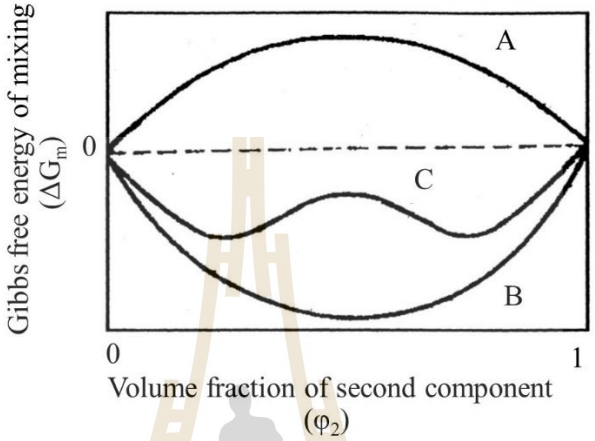

Figure 2.13 The change in free energy of mixing versus volume fraction of second component (A) immiscible blend system (B) miscible blend system, and (C) partially miscible blend system (Braihi, 2016).

Flory-Huggins theory provides an expression for the change in Gibbs free energy upon mixing two dissimilar polymers. Flory–Huggins theory was expressed as;

$$\Delta G_m/RT = (\varphi_1/ M_1) \ln \varphi_1 + (\varphi_2/ M_2) \ln \varphi_2 + \chi_{12} \varphi_1 \varphi_2 \quad (2.2)$$

Where φ_1 is the volume fractions of polymer 1.

φ_2 is the volume fractions of polymer 2.

M_1 is degrees of polymerization of polymers 1.

M_2 is degrees of polymerization of polymers 2.

χ_{12} is the Flory interaction parameter.

The values of configurational entropy of mixing two long chain molecules in the first two terms on the right-hand side of this equation are negative, but very small due to the large numerical values of M_1 and M_2. In addition, dispersion forces between the mixed polymers are relatively weak, then the value of χ_{12} is usually positive. Therefore, the summation of the right hand side of this equation is positive, as a value of $\Delta G_m > 0$. Thus, most polymer blends are immiscible. With non-homogeneity down to the molecular level of the polymer blends, very few entanglements exist at the interface between the two polymers, resulting in poor energy transfer between the two phases of polymer blends, limiting the ability to create a useful material from polymer blends. The illustration of the interface between two polymers that do not dissolve down to molecular level as shown in Figure 2.14.

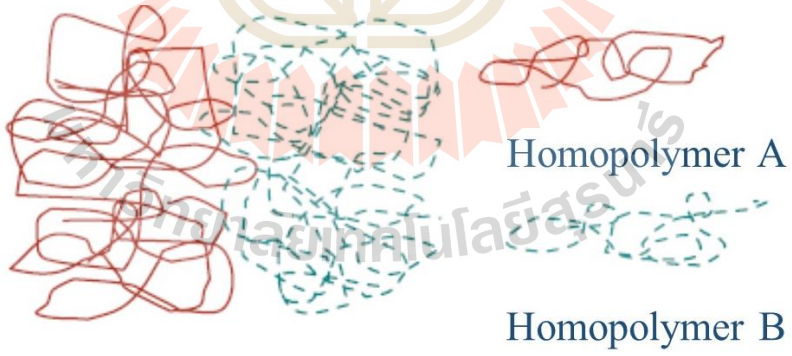

Figure 2.14 Diagram of the interface between two immiscible polymers. The lack of entanglement between the two polymers at the interface results in a material with poor macroscopic properties (Eastwood et al., 2005).

In order to achieve better target properties from polymer mixtures, the modification of polymer molecules or compatibilization should be applied to polymer blends**.**

2.2.2 Blending PLA with tough polymers

Gui et al. (2013) synthesized a poly(polyethylene glycol-co-citric acid) (PEGCA) copolymer by condensation polymerization of polyethylene glycol and citric acid. PEGCA copolymer was blended with PLA as a toughening modifier. PLA and PEGCA copolymer were partially miscible, as evidenced by the shift of T_g of both components. Maximum elongation at break and impact strength took place for the blends containing 15 wt% PEGCA.

Jăso, Cvetinov, Rakic´, and Petrović (2014) prepared the blends of PLA and thermoplastic polyester-urethane (TPU) with 0-40%wt TPU content. The effect of the blend ratio on blend morphology and properties was examined. The results showed that, an increasing TPU concentration in the blends resulted in reduction of the glass transition and melting temperature of PLA. They suggested that the blends were compatible and partially miscible. The PLA blends with 10-40 wt % TPU were tough plastics. Impact strength increases from 3.4 to 8.9 kJ/m^2 by increasing polyurethane content from zero to 40 %wt.

Ma et al. (2014) prepared in situ compatibilization of a PLA/ Polybutylene adipate terephthalate (PBAT) (80/20) blend by addition of dicumyl peroxide (DCP) as a free radical initiator. They proposed that, an addition of DCP in to PLA/PBT blends could improve compatibility of the blend by an induced branching or grafting reaction between PLA and PBAT. The results showed an improvement of elongation at break and impact strength of the PLA/PBAT blend.

Eyiler et al. (2014) enhanced flexibility and ductility of PLA film by blending it with poly(trimethylene malonate) (PTM). PTM was miscible with PLA and synthesized from 1,3-propane diol and malonic acid via melt polycondensation. They found that PTM not only improves toughness but also enhances mechanical strength and modulus.

Deng, and Thomas (2015) studied the synergistic effects of blending two bio-based, bio-degradable polymers, poly(butylene succinate) (PBS) and PLA. A series of melt-blended compounds were prepared at PLA/PBS weight ratios of 100/0, 90/10, 80/20, and 60/40. The tensile testing results showed that both Young's modulus and tensile strength decreased with increasing concentration of PBS, as expected on adding a flexible, ductile polymer to a rigid, brittle polymer. Elongation at break dramatically rose within the composition range 10-40 %wt. of PBS. Phase morphology results showed co-continuous phase morphologies. The reason for the continuous phase of PBS is explained by the relative melt viscosities of PBS and PLA. At a temperature of 175 ˚C and a shear strain rate of 47 s^{-1}, the shear viscosities of PBS and PLA were measured to be 162 and 1759 Pa s respectively. The ratio of the volume fractions at which a co-continuous phase can be formed is equal to the ratio of the viscosities of the polymers. The threshold volume fraction ratio for formation of a co-continuous phase structure in this system was calculated to be 0.092, which is a PBS concentration of 8.4 wt%. This result explains why when blended with as little as 10 wt% of PBS, the ductility of PLA can be transformed.

Xu et al. (2015) used an ethylene-glycidyl methacrylate−methyl acrylate terpolymer (PEGMMA) as a reactive compatibilizer for PLA with polypropylene (PP) or a polypropylene based elastomer (PBE) blend. They found that epoxide of

PEGMMA and PLA end groups formed graft copolymers at the interface during melt processing. The formation of graft copolymers enhanced the adhesion between PLA and polyolefin phases and decreased the interfacial tension. The results exhibited substantial improvement in elongation at break and tensile toughness as compared to the corresponding binary blends.

2.2.3 Blending PLA with natural rubber and its derivatives

2.2.3.1 Natural rubber

Natural rubber (NR) is made from latex, which is a milky colloid usually obtained from the Hevea Brusiliensis tree. The rubber component from Hevea Brusiliensis tree contains 93-95% of cis-1,4-polyisoprene (Nakason, 2002). Typical compositions of NR latex included 36% total solid content (dry rubber content ≈ 30%), 1.5% proteins, l-1.5% resins, lower than 1% ashes, 1% sugars l%, and about 60% water (Nor and Ebdon, 1998). NR particles varied in size from 0.15 μm to 3 μm (Kroschwitz and Jacqueline, 1990). Molecular weight and molecular weight distribution of NR was about 10^4 to 10^7 g/mol and between 2 and 11, respectively depending on age, clone, weather, tapping frequency and other factors (Westall, 1968; Bhowmick and Stephens, 2001; Kovuttikulrangsie and Sakdapipanich, 2005). Chemical structure of cis-1, 4- polyisoprene is shown in Figure 2.15.

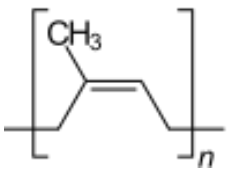

Figure 2.15 Chemical structure of cis-1, 4-polyisoprene from natural rubber (Herculano et al. 2011).

Natural rubber is considered a renewable resource and an environmentally friendly material. NR has been used as a versatile material in engineering applications for many years. It has excellent flexibility, outstanding resilience, and high elongation at break.

The fresh NR latex can be processed into primary rubber products that can be widely used in many industrial applications. The important forms in which NR is processed are:

2.2.3.1.1 Concentrated latex

NR latex comes directly from tapping Hevea Brusiliensis trees, it typically has a solid rubber content of about 30% by weight, which makes it unsuitable for use directly in downstream production. Therefore, NR latex is converted into concentrated latex by high-speed centrifuging to separate out water, dissolved chemicals and other impurities (Chuasuwan, 2018). Ammonia is then added to prevent coagulation before packing for storage or shipment. The concentrated latex is at least 60 wt% of rubber and can be used as a raw material in further processing such as latex examination gloves, surgical gloves, condoms, elastic threads and adhesives. Figure 2.16 shows the latex concentrate production process.

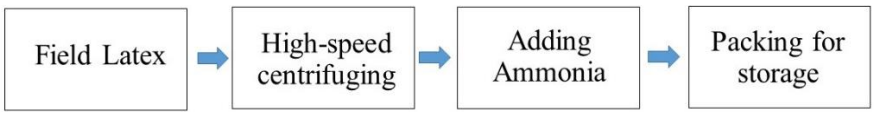

Figure 2.16 Diagram of the latex concentrate production process (Chanchaichujit and Saavedra-Rosas, 2018).

2.2.3.1.2. Block rubber

Block rubber can be produced from field latex, a mixture of cup- lump, and unsmoked rubber sheet. A high- grade of block rubber depends on the amount of field latex, the more field latex in the product, the higher the grade of the block rubber. The block rubber production process is shown in Fig. 2.17.

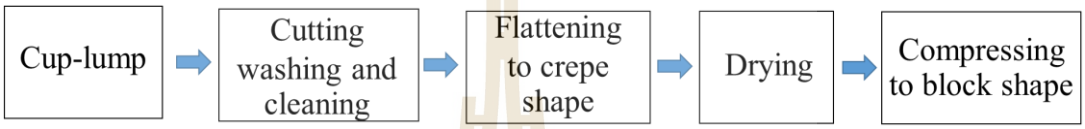

Figure 2.17 Diagram of the block rubber concentrate production process (Chanchaichujit and Saavedra-Rosas, 2018).

In Thailand, the standard Thai rubber (STR) comprises five main groups these are: TSR CV, TSR L, TSR 5, TSR 10, and TSR20. Comparison of each type of standard block rubber is shown in Table 2.6.

Table 2.6 Natural Rubber Comparison Chart (Astlett Rubber Inc., 2012).

		TSR	TSR L		TSR5	TSR10		TSR20	
Parameter	Unit	STR 5 CV	STR XL	STR 5L	STR 5	STR 10	STR 10CV	STR 20	STR 20CV
Dirt (max)	% wt	0.04	0.02	0.04	0.04	0.08	0.08	0.16	0.16
Ash (max)	% wt	0.6	0.4	0.4	0.6	0.6	0.6	0.8	0.8
Nitrogen	% wt	0.6	0.5	0.6	0.6	0.6	0.6	0.6	0.6
Volatile	% wt	0.8	0.8	0.8	0.8	0.8	0.8	0.8	0.8
Initial		NA	35	35	30	30	NA	30	NA
PRI Index		60	60	60	60	50	50	40	40

Table 2.6 Natural Rubber Comparison Chart (Astlett Rubber Inc., 2012). (Continued)

		TSR	TSR L		TSR5	TSR10		TSR20	
Parameter	Unit	STR 5 CV	STR XL	STR 5L	STR 5	STR 10	STR 10CV	STR 20	STR 20CV
Colour Lovibond Scale		NA	4	6	NA	NA	NA	NA	NA
Mooney		60	NA	NA	NA	NA	60 +7	NA	65 +7

*Not specification status, but are controlled at the producer end. ** Note: Mooney Viscosity limits are at the time of production. Values will drift higher over time. These figures are limits, not typical values. Typical values will vary by producer.

2.2.3.2 Modified of NR

NR is non-polar polymer with high molecular weight**.** The blending of NR with a more polar polymer exhibits an immiscible blend and results in missing some desirable target properties**.** Therefore, in order to achieve desirable target properties, the modification of NR blend molecules has been studied by many researchers**.** Modified NR is considered useful as a toughening agent or an impact modifier for brittle polymers. The modification of NR molecules is as follows:

2.2.3.2.1 Epoxidized natural rubber (ENR)

ENR is prepared by epoxidation reaction from NR latex usually using peracid, where the peracid can either be prepared separately, or formed in situ from a precursor using acid and hydrogen peroxide. Figure 2.18 shows the epoxidation of NR with peracid prepared (a) separately and (b) in situ.

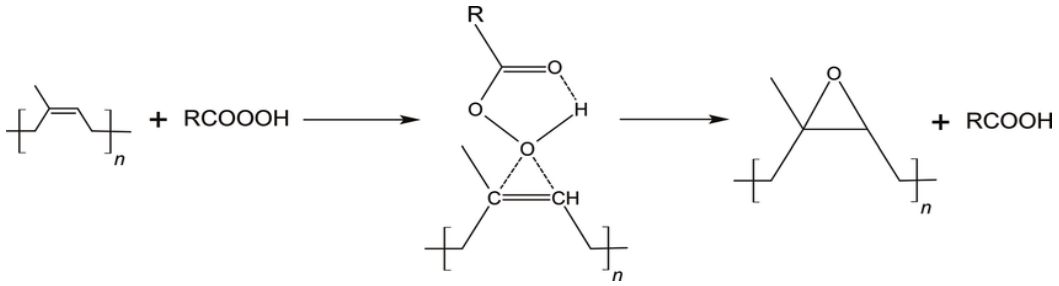

(a) Epoxidation of NR with peracid

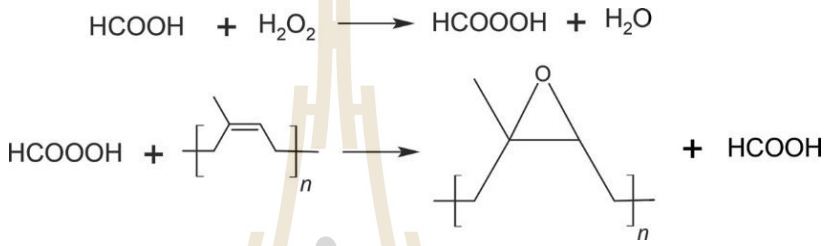

(b) In situ epoxidation of NR

Figure 2.18 Epoxidation of NR (Hashim and Ong, 2017).

ENR can be varied from 10 - 50% mol of epoxidation. Compared to NR, ENR has a higher T_g, higher damping, better air permeability, higher hysteresis, and higher polarity.

2.2.3.2.2 Graft copolymerization of NR

Graft copolymers of NR are usually prepared by grafting another polar functional monomer branch on to the NR main chain. Monomer grafting of NR can be carried out in solid phase, solution or emulsion phase. Emulsion phase graft copolymerization is favored for economic reasons, and it is also more practical than in the other phases. Several studies have been carried out on the grafting of NR, with various monomers used for improvement of blend properties; for example, methyl methacrylate (MMA) (Jaratrotkamjorn *et al.*, 2012), vinyl acetate (Chumeka,

2014), butyl acrylate (Zhang *et al.*, 2011), glycidyl methacrylate (Juntuek *et al*., 2012), and maleic anhydride (Nakason *et al.*, 2006; Kalkornsurapranee *et al.*, 2012). The examples of grafted NR molecules with two monomers are shown in Figure 2.19

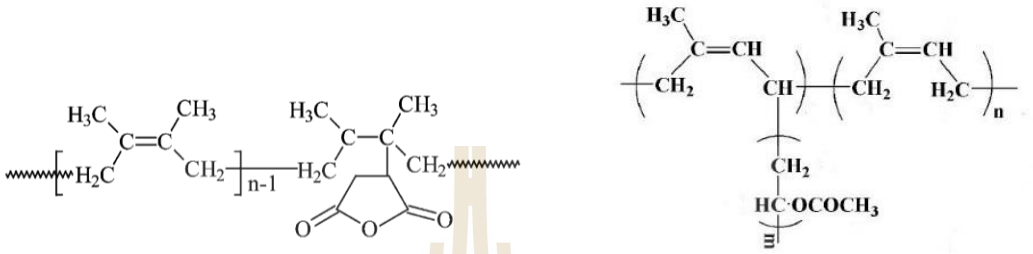

Figure 2.19 Grafted NR molecules (Nakason et al., 2006; Chumeka, 2014).

2.2.3.2.3 Liquid natural rubber (LNR)

LNR is a modified form of natural rubber (NR) with a shorter polymeric chain. LNR can either be obtained from mastication, photochemical degradation, or chemical decomposition of NR.

Shashidhara and Pradeepa (2014) prepared LNR of desired molecular weight by mastication of pale latex crepe in the presence of 0.5 phr peptizing agent, Peptizol 7. They found that 27 minutes of mastication time yielded LNR of molecular weight from about 9,60,000 to 12,275 g/mol.

Dahlan *et al.* (2000) prepared LNR through photochemical oxidation of NR with variation of the irradiation time. They found that an increase of irradiation time up to 60 hours resulted in reduction of LNR molecular weight from 107.00 x10^4 to 7.59 x 10^4 g/mol.

Ravindran *et al.*, (1988) used a photochemical degradation process of NR in the presence of hydrogen peroxide to yield hydroxyl terminated NR. They found that after 50 hour of irradiation time, the molecular weight of NR was about 5000 g/mol which gave a functionality of 1.97. The suggested mechanism for depolymerization and hydroxylation of NR is shown in Figure 2.20

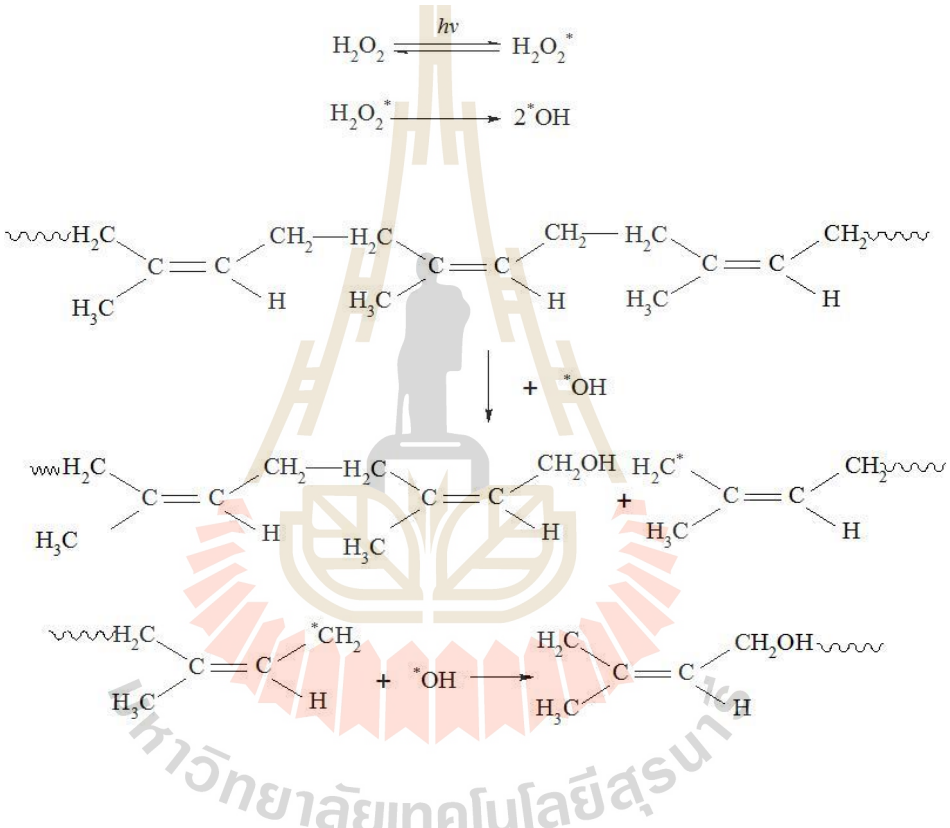

Figure 2.20 Mechanism for depolymerization and hydroxylation of NR (Ravindran et al., 1988).

2.2.3.3 PLA/NR/modified NR blends

Bitinis, Verdejo, Cassagnau, and Lopez-Manchado (2011) developed new formulations based on PLA/NR blends. They optimized processing parameters which included temperature of blending (160-180˚C), blending time (10 and 15 min), and rotor speed (30, 60, and 90 rpm) in order to obtain a blend with useful

properties such as blend morphology, crystallization rate, and mechanical properties. The SEM micrographs of the fracture surfaces of PLA/NR blends with 10%wt. NR showed that in all the blends the rubber formed small dispersed droplets with low interfacial adhesion with the PLA matrix. They observed an increase of the NR average droplet size with increasing temperature, rotor speed, and blending time and the dispersion of the droplet size became broader. The optimum processing condition for PLA/ NR was blending at 160˚C for 10 min with a rotor speed of 60 rpm. The morphology received from the optimum processing condition were uniformly dispersed with droplet size 1.15 ± 0.40 μm. They explained that decreasing the matrix viscosity by increasing the temperature resulted in an increase of the average droplet size of rubber domains in the blend. Moreover, a decrease of the viscosity of the matrix facilitated the coalescence of the droplets of the dispersed phase as the contact time required for drop coalescence is lower. The ductility of PLA has been significantly improved by blending with NR. The elongation at break improved, from 5% for neat PLA to 200%, by adding 10 wt% NR. Moreover, the incorporation of NR not only increased the crystallisation rate but also enhanced the crystallisation ability of PLA. These materials are, therefore, very promising for industrial applications.

Pongtanayut, Thongpin, and Santawitee (2013) investigated the effect of rubber on morphology, thermal properties and mechanical properties of PLA/NR and PLA/ epoxidized natural rubber (ENR) blends. PLA/NR and PLA/ENR were prepared at various compositions from 0-30 %wt. They found that the rubber phase of NR was dispersed in the continuous PLA matrix with small droplets. With increasing content of NR, larger droplet sizes of dispersed particles were observed. Incorporation of NR would enhance the crystallization ability of PLA better than ENR,

but thermal stability was decreased with both rubbers. The ductility of PLA was significantly improved by blending with NR. The amount of NR at 10 %wt. seems to give optimum properties. In the case of the addition of ENR, crystallization ability, thermal resistance, and tensile properties of the blend were decreased.

Zhang et al (2011) prepared NR grafted with poly(butyl acrylate) (NR-g-PBA) by emulsion polymerization and used it as a toughening agent for PLA. The successful preparation of NR-g-PBA was confirmed by Fourier transform infrared spectroscopy and nuclear magnetic resonance spectroscopy. PLA/NR-g-PBA blend and PLA/NR blend were prepared using an internal melt mixer. The morphology and mechanical properties of the blends were investigated as a function of rubber content. SEM showed that the spherical-particle-dispersed phase appearing in the NR/PLA blend was not found in the NR-g-PBA/PLA blend, which showed that NR-g-PBA was compatible with PLA. The elongation at break and the impact strength were significantly improved with an increase in NR-g-PBA content. The thermal stability of PLA decreased after blending with NR but it was retained when NR-g-PBA was blended with PLA.

Bijarimi, Ahmad, and Rasid (2014) prepared PLA/NR blends using melt blending. Liquid epoxidised natural rubber (LENR) was used as a compatibilizer for the blends. The stress-strain behavior of various blend compositions were investigated. It was found that, the stress-strain properties were gradually changed with increasing rubber composition in the blend. The addition of LENR compatibilizer improved the stress at break and Young's modulus of 40/60 PLA/rubber blend. The researchers proposed that an improvement in the mechanical properties of the blend was associated with the compatibilizing effect of LENR.

Jaratrotkamjorn, Khaokong, and Tanrattanakul (2012) prepared PLA/NR blends with the addition of 10 %wt. of NR-based polymer using a twin-screw extruder. They focused on the effect of polarity and molecular weight of rubber on mechanical properties of the blends. NR, masticated NR, epoxidized natural rubber, and natural rubber grafted with poly(methyl methacrylate) (NR-g- PMMA) were used. They found that all blends showed higher impact strength than PLA. Impact strength of PLA/ NR blends increased after applying masticated NR due to an achievement of appropriate NR particle size. They suggested that molecular weight, viscosity, and appropriate particle diameter of rubber played a major role in the mechanical properties and morphology of the blends.

Juntuek et al. (2012) investigated the effects of NR and NR grafted with glycidyl methacrylate (NR-g-GMA) ratios on physical properties of PLA/NR blends. They found that the impact strength and elongation at break of PLA/NR blend increased with increasing NR content up to 10 wt%. The addition of NR-g-GMA as a compatibilizer for PLA/NR blend showed significant improvement in impact strength and elongation at break of the blend compared with that of the neat PLA and PLA/NR blend without NR-g-GMA. The impact strength and elongation at break of PLA/NR blend were increased with an increase of NR-g-GMA content up to 1 wt%. In addition, by increasing the grafting percentage of NR-g-GMA in the blend from 0.76 up to 4.35, the impact strength and elongation at break of the blend also increased.

Chumeka, Pasetto, Pilard, and Tanrattanakul (2014) synthesized PLA-NR diblock copolymers with variation of PLA and HTNR molar ratio. They obtained hydroxyl telechelic natural rubber oligomers (HTNR) by

modification of NR molecules. They found an appearance of new ester linkage in the diblock copolymers from ^{1}H-NMR spectrum. PLA-NR diblock copolymers were used as a toughening agent of PLA and as a compatibilizer of the PLA/NR blend. PLA/PLA-NR blend showed higher impact strength than PLA/NR blend. SEM micrographs showed smaller dispersed particles, indicating the increase in compatibility of the blend. The compatibilization was effective in the blends containing ≈ 10 %wt. of rubber. At a higher rubber content (>10 wt %), coalescence of NR and diblock copolymer was responsible for the larger rubber diameter in the blends, which caused a decrease of impact strength.

Yuan, Xu, Chen, and Chen (2014) designed a novel super toughened PLA/NR blend by peroxide-induced dynamic vulcanization, in which the crosslinked NR phase had a specific continuous structure. They found that sharp brittle to ductile transition occurred in the blend with 35 wt% NR, showing impact strength of 58.3 kJ/m^2, approximately 21 times that of the neat PLA. They suggested that peroxide initiated reactive compatibilization at the interface between PLA and NR. SEM micrograph of the cryo-fracture surface showed a continuous "net-like" NR located in the PLA matrix with good interfacial adhesion that enhanced the impact properties and elongation at break of the blend. Moreover, FTIR analysis suggested that the PLA-NR grafts occurred by adding peroxide and increasing NR content, indicating the reactive compatibilization at the PLA/NR interfaces. They proposed that when the dynamically vulcanized blend is under load, PLA phase dissipates the fracture energy effectively to the deformed continuous NR phase through the strong interface, resulting in significantly increased toughness and elongation.

2.3 Rubber toughening mechanisms

All of the toughening mechanisms proposed for rubber-toughen glassy matrix rely on a dispersion of rubber particles, these include energy absorption, matrix crazing, shear yielding, combination of shear yielding and matrix crazing, and cavitation.

2.3.1 Energy absorption by rubber particles

The idea of rubber particles absorbing energy in order to toughen polymers was first proposed by Merz, Claver, and Bear (1956). They observed that in high impact polystyrene (HIPS) an increase in volume and stress-whitening accompanied elongation of the material and concluded that these phenomena were associated with the formation of many micro-cracks. They suggested that the fibrils of stryrene-butadiene compolymer bridged across the fracture surface of a developing crack and in so doing prevented the crack growing to a catastrophic size. This resulted in more energy being absorbed than an equivalent volume of the polystyrene matrix. The amount of energy absorbed in the impact was attributed to the sum of the energy to fracture the glassy matrix and the work to break the rubber particles. A similar mechanism was proposed by Kunz-Douglass, Beaumont, and Ashby (1980). They proposed that a mechanism for rubber modified epoxies in which the elastic energy, stored in the rubber particles during stretching, is dissipated irreversibly when particles rupture. However, the main disadvantage of these proposals is that they are concerned primarily with the rubber rather than matrix. The total amount of energy associated with the deformation of the rubbery phase accounts for no more than a small fraction of the observed enhanced impact energies. Therefore, this mechanism plays only a minor role in the toughening of multiphase polymers (Collyer, 1994). At that time,

toughening theories concentrated on the deformation mechanisms associated with the matrix, which were enhanced by presence of the rubber phase.

2.3.2 Matrix crazing

Rubber particles have been shown both to initiate and to control craze growth. When the stress is applied, crazes are initiated at points of maximum principal strain, typically near the equator of rubber particles (maximum concentration of triaxial stresses), and propagate outwards normal to the maximum applied stress, although interactions between the particles' stress fields can introduce derivations. Craze growth is terminated when a further rubber particle is encountered, preventing the growth of very large crazes. The dense crazing that occurs throughout a comparatively large volume of the multiphase material accounts for the high energy absorption observed in tensile test, impact test, and the extensive stress whitening which accompanies deformation and failure.

Craze actually contains fibrils of polymer drawn across, normal to the craze surfaces, in an interconnecting void network. The void network is established at the craze tip. The craze tip growth is produced by the meniscus instability mechanism. The fibrils are formed at the polymer webs between voids and contain highly oriented polymer with the chain axis parallel to the fibril axis. As the craze tip advances the craze thickens by drawing in more polymer from the craze surfaces. It is the presence of the relatively strong craze fibrils that makes the craze load bearing. In addition, cracks can be formed by the breakdown of craze fibrils to form voids. These voids expand slowly by the rupture of surrounding craze fibrils until the void becomes a crack of critical size that can propagate catastrophically (Collyer, 1994).

2.3.3 Shear yielding

Shear yielding in the matrix phase also played a major role in the mechanism of rubber toughening in a polymer matrix. Shear yielding is a localized shear band, or more generalized and diffuse regions of shear yielding, which usually occur in addition to elastic deformation. Not only did this phenomenon act as an energy absorbing process, but the shear bands also presented a barrier to the propagation of crazes and hence crack growth, thereby delaying failure of the materials. The function of rubber particles was to produce enough triaxial tension in the matrix so as to increase the local free volume and initiate extensive shear yielding and drawing of the matrix. However, shear yielding alone did not account for the stress whitening characteristic of rubber whitening, and the fact that triaxial tension promotes crazing and brittle fracture rather than shear yielding. It is now generally accepted that the shear yielding mechanism constitutes cavitation of the rubber particles followed by extensive shear yielding throughout the matrix. The cavitation of the rubber particles explains the observed stress whitening as light scattering occurs which is enhanced by the holes enlarging. Cavitation is followed by the onset of shear yielding, because on cavitation of the rubber particles the buildup of hydrostatic tension is locally relieved, lowering the yield stress. After cavitation the constrained conditions, triaxial stresses, disappear and the matrix behaves as if it were under plane stress conditions. Shear yielding deformations occur more readily under a biaxial stress state rather than the craze-favouring triaxial state. The voids created by the cavitated rubber particles act further as stress concentrators (Collyer, 1994).

2.3.4 Crazing and shear yielding

Crazing and shear yielding may occur simultaneously in many rubber toughened plastics. The contribution of each mechanism to toughening of the system depends on a number of variables such as the rubber particle size and dispersion, the concentration of the rubber particles, and the rate and temperature of the test. The contribution of each mechanism to the toughening process can be assessed to some extent by using tensile dilatometry. It is assumed that deformations such as voiding and crazing are dilatational processes, which manifest themselves by an increase in volume strain. Unfortunately, if both voiding and crazing occur simultaneously, it is impossible to separate their contributions to volume strain. However, when shear occurs, a decrease in the volume strain rate occurs since shear yielding is a non-dilatational or constant volume process.

2.3.5 Cavitation

The occurrence of cavitation in the presence of shear yielding has been observed in rubber toughened polymer, whereas it is absent in the untoughened matrix (Collyer, 1994). In the rubber toughened blends, the presence of the rubber gives rise to volume increase if the strain rate is sufficiently high. The expansion is caused by the cavitation of the rubber particles. Rubber particles dissipate the bulk strain energy by cavitation, leading to a reduction in local hydrostatic stress and a reduction in the yield stress of the blend. Therefore, shear band formation is enhanced by the voids in the matrix caused by the cavitated rubber particles. In the presence of a sharp crack, a triaxial stress exists ahead of the crack tip. This gives rise to rapid cavitation and growth of the resulting voids. A zone of voids and shear bands is formed ahead of the crack tip and further tension causes an even larger plastic zone to form. The increasing size of

the large plastic zone acts as the principal toughening mechanism. The rubber particles toughen by acting as stress concentrators, enhance shear yielding, and then cavitate, dissipating energy, and giving rise to more shear yielding (Collyer, 1994).

2.4 Compatibilization for PLA blends

Physical blending of PLA with other polymers provides the most promising way to modify the properties of PLA. PLA-based materials with a wide range of properties are theoretically obtainable by blending, since a great number of polymers with various properties can be selected to blend with PLA. However, acceptable properties of PLA blends are not easily obtainable by simple blending. To accomplish the required properties for each application, compatibilization must be applied to the blends. Compatibilization is a technique to improve compatibility and enhance properties of immiscible polymer blends. The most important roles of compatibilization are to reduce the size of the dispersed phase through the reduction of interfacial tension, and to prevent the dispersed phase from coalescing, and thus stabilizing the formed fine phase morphology. The achievement of compatibility has played an important role in the development of polymer blends. Several methods of compatibilization are (1) addition of block and graft copolymer; (2) addition of functional/reactive polymer; or (3) In situ grafting/polymerization (reactive blending) (Folkes and Hope, 1993).

2.4.1 Addition of copolymers

Copolymers are occasionally used to compatibilize immiscible polymer blends. The most widely used copolymers are those which have blocky structures with one constituent block miscible with one component and a second block miscible with

the other component. If a copolymer is located at the interface of two phases, then the segments of copolymer dissolve in each bulk phase of the same identity. A copolymer should act as an emulsifying agent for the blend, resulting in improved interfacial adhesion. Numerous researches have been focused on the addition of various copolymers as compatibilizers for PLA blends. Figure 2. 21 illustrates possible conformations of different types of copolymers at the interface.

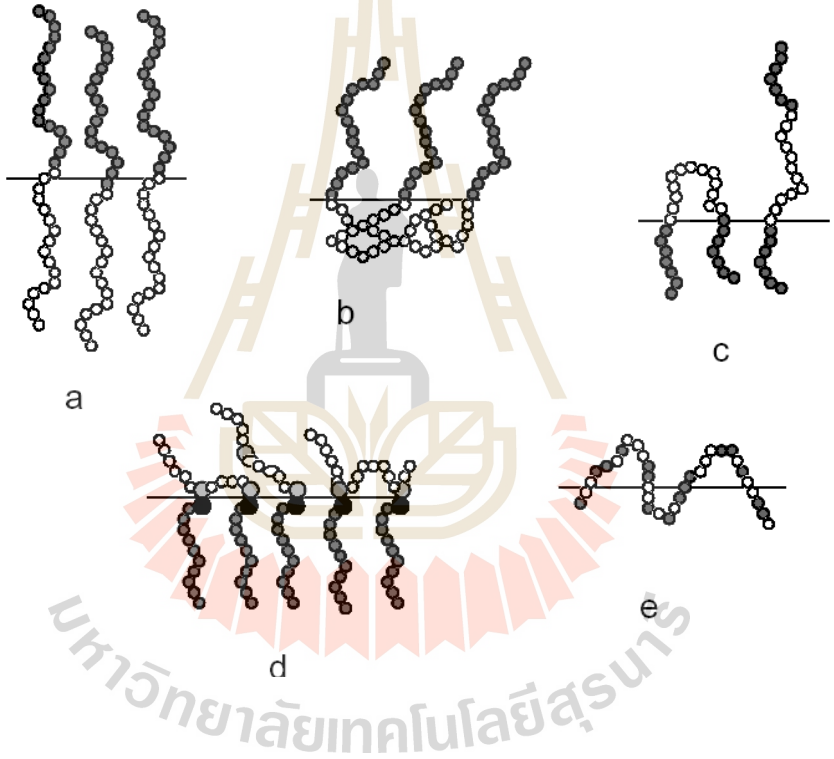

Figure 2.21 Conformations of different types of copolymers at the interface (a) diblock copolymers (b) end grafted chains (c) triblock copolymers (d) multiple grafted chains (e) random copolymer (Horák, et al., 2005).

2.4.1.1 Addition of random copolymers

Random copolymers usually have sequential comonomer units although they are distributed randomly as seen in Figure 2.21 (e). The sequential comonomer units can be regarded as short blocks which are miscible with each polymer component. Thus, the addition of random copolymers can improve the compatibility of immiscible blends.

Biodegradable PLA/PCL blends can offer a wide variety of physical properties; the glassy PLA with a relatively high degradation rate showed better tensile strength, while the rubbery PCL with a much slower degradation rate shows better toughness. However, a PCL/PLA blend is a typical immiscible blend. Peponi, Marcos-Fernández, and Kenny (2012) synthesized a random architecture of poly (DL-lactic acid) and poly(ε-caprolactone), poly(DL-lactide-*co*-caprolactone). The chemical structure was characterized by ^{1}H-NMR. The result showed that spherical nanodomains detection in the thin films of PLA/PCL/copolymer blend were obtained after solvent evaporation. Nanodomains were studied by atomic force microscopy and transmission electron microscopy, progressively grown under annealing until they collapsed and formed a homogenous disordered structure.

2.4.1.2 Addition of graft copolymers

Graft copolymerization is one of a number of convenient methods to impart a polymer with unique properties, and is generally performed in a separate reaction step (Utracki, 2002). Compatibilization of immiscible PLA blends has also been attempted by the addition of graft copolymers.

Wootthikanokkhan et al. (2012) prepared polylactic acid grafted with maleated thermoplastic starch (PLA-g-MTPS) and studied the

compatibilizing efficacy of PLA-g-MTPS in PLA/thermoplastic starch (TPS) blends. They found that PLA-g- MTPS was capable of acting as a compatibilizer by reducing coalescence and surface tension of the TPS phase during blending.

Chen et al. (2006) investigated the compatibilizing efficiency of poly(L-lactide) (PLLA) grafting starch (PLLA-g-St) copolymers in PLLA/starch blends. The results showed that PLLA-g-St could improve the performance of the blend without changing their whole biodegradability. PLLA-g-St was also a good compatibilizer for the blend of hydrophobic PLLA and hydrophilic granular corn starch. It could effectively improve the interfacial adhesion and the mechanical properties of the composites. The 50/50 composite of PLLA/starch compatibilized by 10% PLLA-g-St gave a tensile strength of 24.7 MPa and an elongation at break of 8.7%, whereas the value was 11.3 MPa and 1.5%, for the simple 50/50 blend of PLLA/starch.

2.4.1.3 Addition of block copolymers

Many researchers have focused on toughness improvement of PLA blends after the addition of block copolymers as compatibilizing agents.

Hillmyer and Wang (2001) synthesized polyethylene-poly(L-lactide) diblock copolymer (PE-b-PLLA) using hydroxyl-terminated PE (PE-OH) as a macroinitiator for ring- opening polymerization of L- lactide. Ternary blends, PLLA/ LDPE/ PE- b- PLLA, were prepared by solution blending followed by precipitation and compression molding. From particle size analysis and scanning electron microscopy, results showed that the particle size and size distribution of the LDPE dispersed in the PLLA matrix was sharply decreased upon the addition of PE-b-PLLA. The tensile and Izod impact testing results from the ternary blends showed

significantly improved toughness as compared to the PLLA homopolymer or the corresponding PLLA/LDPE binary blends.

For immiscible PLA/ PCL blends, PLA- PCL diblock or triblock copolymers have been widely used as a compatibilizing agent. Choi, Kim, Cho, and Park (2002) studied the effect of PLA-PCL diblock copolymer on the morphology of PLA/ PCL blend. They found that the size of PCL domains in PLA matrix reduced upon addition of PLA- PCL diblock copolymer. However, the extent of reduction was less than caused by the addition of PLA-PCL random copolymer.

Maglio, Malinconico, Migliozzi, and Groeninckx (2004) and Wu (2010) studied the effect of PLLA-PCL-PLLA copolymer on morphology of poly (L- lactide) (PLLA) / poly(ε- caprolactone) (PCL) blend. The ternary blend of PLLA/PCL/PLLA-PCL-PLLA triblock copolymer was 70:30:2 by weight. The good emulsifying effect was evidenced by the strong reduction in particle size of dispersed PCL phase upon addition of the triblock copolymer. The dimension of dispersed PCL domains in PLA/PCL (70/30, w/w) radically decreases from about 10 -15 μm to about 3-4 μm after adding 2 wt% of the triblock copolymer.

Wu, Zhang, Yuan, and Zhang (2010) studied phase morphologies and interfacial properties of PCL/ PLA blends after using PLA/ PCL diblock and PLA- PCL- PLA triblock copolymers as compatibilizers. They found that droplet size of dispersed phase in PLA/PCL/PLA-PCL-PLA triblock copolymer blend was lower than that of PLA/PCL/PLA-PCL diblock copolymer blend. They suggested that the triblock copolymers are more efficient as a compatibilizer than diblock copolymers. In addition, the presence of copolymers reduces the interfacial tension, and emulsified the phase interface, leading to stabilization of the interface and retarding

both the shape relaxation and the elastic interface relaxation. In contrast to that of the diblock copolymers, the triblock copolymers showed a higher emulsifying level.

To improve the compatibility of PLA with natural rubber, Chumeka, Pasetto, Pilard, and Tanrattanakul (2015) synthesized a diblock copolymer from hydroxyl telechelic natural rubber (NR) oligomers and PLA. The diblock copolymers were used as compatibilizers for the PLA/NR blend. They found that the particle size of the disperse phase was reduced by the addition of the diblock copolymer. The maximum impact strength of the blends appeared in the PLA/NR/PLA-NR diblock copolymer (90/7.5/2.5) blend and was higher than that of the PLA/NR blend. The compatibilization effect became less effective when the diblock copolymer content was further increased.

Chumeka, Pasetto, Pilard, and Tanrattanakul (2014) developed a synthetic method to produce a novel bio-based triblock copolymer (PLA-NR-PLA) that consisted of poly(lactic acid) and natural rubber. Carbonyl telechelic natural rubber (CTNR) was prepared and transformed to hydroxyl telechelic natural rubber (HTNR). HTNR was use to synthesize PLA-NR-PLA triblock copolymer. ^{1}H NMR analysis confirmed the PLA-NR-PLA was successfully synthesized by the presence of ester linkages between the carboxyl end-groups of the PLA and the hydroxyl end-groups of the HTNR. PLA-NR-PLA triblock copolymer acted as a toughening agent for PLA and as compatibilizer for the PLA/NR blend. The PLA-NR-PLA was as good a toughening agent as NR although the PLA-NR-PLA had a much lower molecular weight than NR. The compatibilization effect was more dominant in the blend containing 10% rubber than in the blend that contained >10% rubber. The compatibilization effect was also observed in the morphology of the blend as a

reduction in the rubber particle diameter. PLA-NR-PLA triblock copolymer not only increased the impact strength of the blends, but also increased the elongation at break.

2.5 Synthesis of PLA block copolymer

In general, PLA block copolymer can be synthesized through ring-opening copolymerization. For example, Zhang et al. (2005) synthesized a hydroxyl-terminated diblock copolymer of monomethoxy-poly(ethylene glycol)-b-poly(lactide) (MPEG-PLA) by ring-opening polymerization of lactide with monomethoxy-terminated PEG as a macroinitiator and stannous octoate ($Sn(Oct)_2$) as a catalyst in toluene solution. The schematic diagram showing the preparation route of MPEG-PLA is shown in Figure. 2.22.

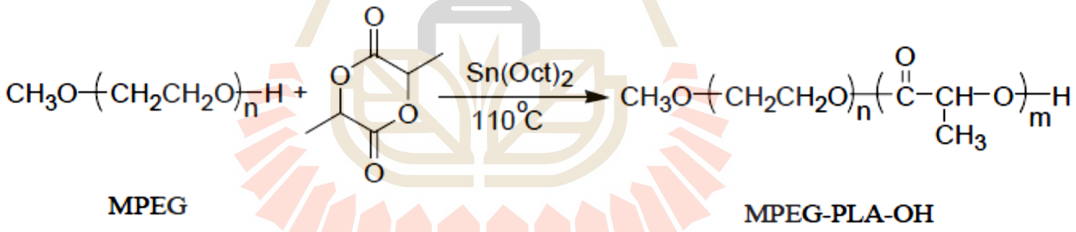

Figure 2.22 Synthesis route of MPEG-PLA-OH diblock copolymer (Zang et al., 2005).

PLA triblock copolymer can also be prepared via ring opening polymerization. For example, Aluthge et al. (2013) synthesized poly(lactic acid)-b-poly(hydroxybutyrate)-b-poly(lactic acid), (PLA-PHB-PLA) triblock copolymers by sequential addition of living ring-opening polymerization of cyclic esters lactide (LA) and β-butyrolactone (BBL) with $((NNO)InCl)_2(\mu\text{-}OEt)(\mu\text{-}Cl)$ catalyst. A schematic diagram representing the synthesis of PLLA-PHB-PLLA triblock copolymer is shown in Figure 2.23.

The preparation of poly(d- lactide) - PluronicF68- poly(d- lactide) (PDLA- PluronicF68- PDLA) multiblock copolymer via ring opening polymerization of D-lactide was proposed by Qi et al. (2015). PluronicF68 with a molecular weight of 8400 g/ mol containing about 80% polyethylene oxide (PEO) segment and 20% poly(phenylene oxide) (PPO) segment which behaved as a macroinitiator and $Sn(Oct)_2$ was used as a catalyst. The synthesis scheme of the PLDA- PluronicF68- PDLA multiblock copolymer is shown in Figure. 2.24.

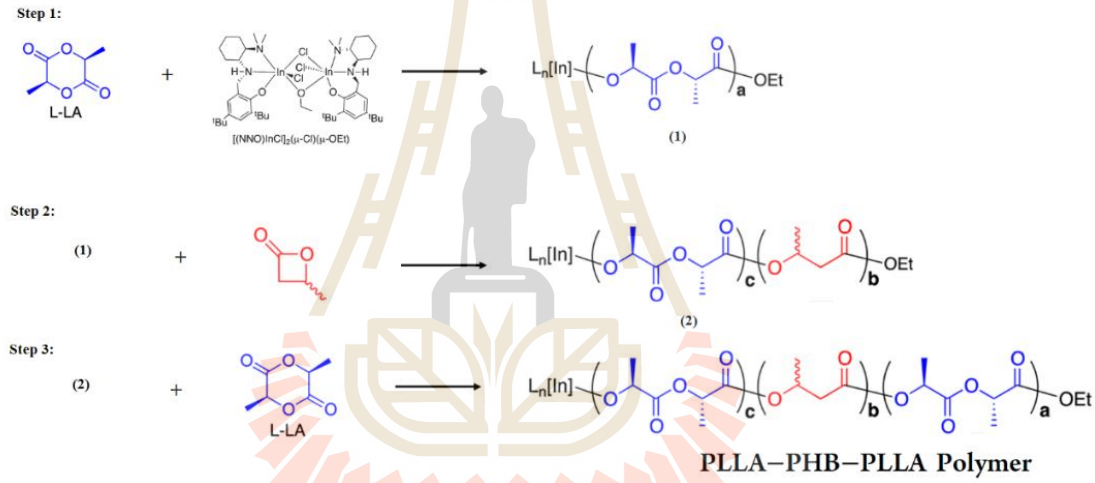

Figure 2.23 Schematic diagram of synthesis of PLLA−PHB−PLLA Polymer (Aluthge et al., 2013).

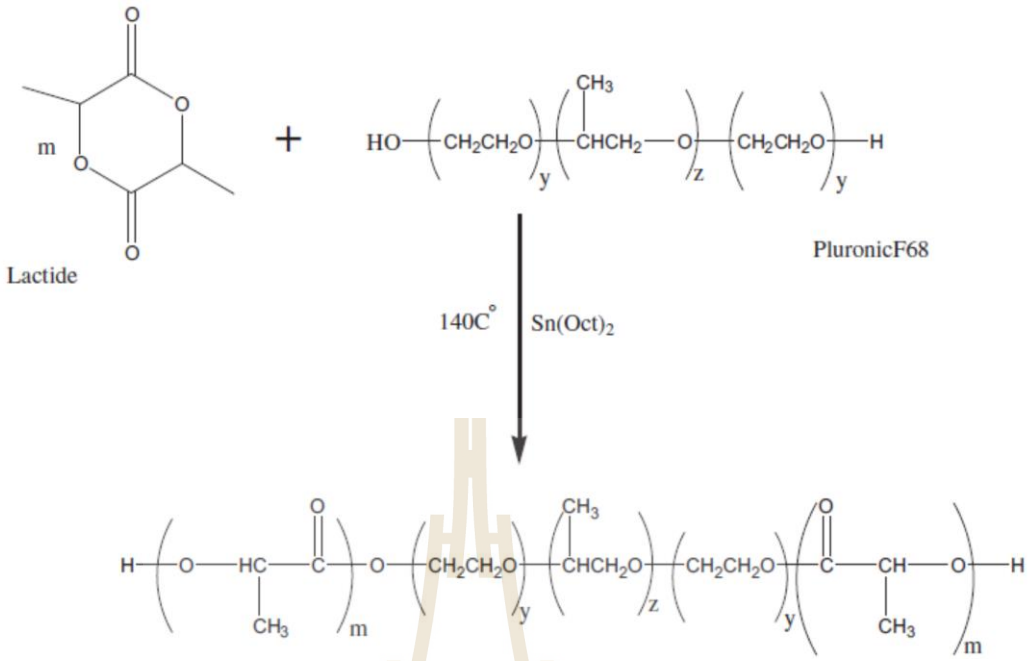

Figure 2. 24 Synthesis scheme for the PDLA- PluronicF68- PDLA multiblock copolymer (Qi et al., 2015).

For the synthesis of PLA block copolymers with nonspecific functional group hydrocarbon polymer e. g. polybutadiene, polyisoprene, polyisobutylene, and poly (dimethylsiloxane), functional groups have to be added onto a hydrocarbon polymer before further synthesis via ring opening polymerization.

For examples, Hillmyer and Schmidt (1999) synthesized model polyisoprene-polylactide (PI- PLA) diblock copolymers by a combination of living anionic polymerization and controlled coordination- insertion polymerization. Living anionic polymerization of isoprene followed by end- capping with ethylene oxide yielded hydroxyl terminated polyisoprenes (PI- OH) with narrow molecular weight distributions. In a second step, an aluminum alkoxide macroinitiator was formed from the equimolar reaction of triethylaluminum with the PI- OH prepolymer and

subsequently utilized for the ring-opening polymerization of lactide to produce the desired PI-PLA diblock copolymer. The synthesis route of polyisoprene-poly(lactic acid) diblock copolymer is schematically presented in Figure 2.25.

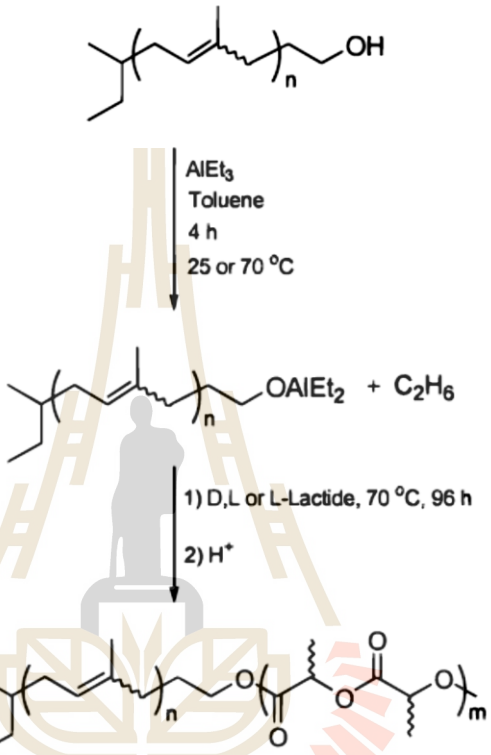

Figure 2.25 Schematic diagram for the synthesis of polyisoprene-poly(lactic acid) diblock copolymers (Hillmyer, and Schmidt, 1999).

Apart from ring opening polymerization, sometimes PLA block copolymer of PLA is prepared by condensation polymerization reaction of PLA prepolymer. For example, Chumeka et al. (2014) synthesized PLA-NR diblock copolymer by condensation reaction using PLA prepolymer and hydroxyl terminated liquid rubber which was obtained by modifying carbonyl telechelic NR. The synthesis PLA-NR diblock copolymer is schematically presented in Figure 2.26.

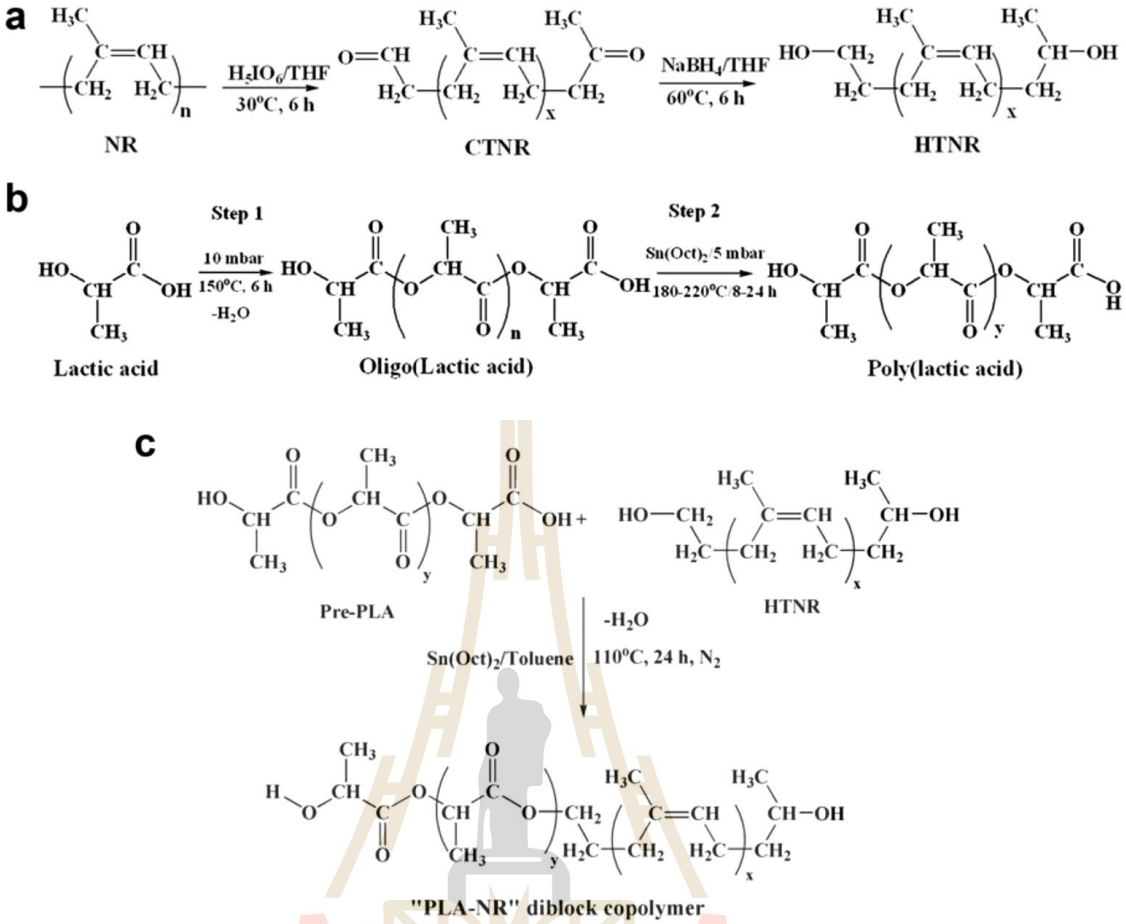

Figure 2.26 Schematic diagram of the synthesis methods: (a) HTNR; (b) PLA; and (c) PLA-NR diblock copolymer (Chumeka et al., 2014).

2.6 Molecular characterization of block copolymer

Analytical techniques that can be used to determine the molecular structure of block copolymer and its average chemical composition are explained in the following section.

2.6.1 Nuclear magnetic resonance spectroscopy (NMR)

NMR can provide both qualitative and quantitative information with respect to comonomer composition and sterochemical configuration of polymer molecules. This is because a proportional relation exists between the observed peak

intensity in NMR spectrum and the number of nuclei that produce signal. NMR can be used in the characterization of block copolymers. The most frequently used for polymers are proton (^{1}H) NMR and carbon-13 (^{13}C) NMR.

Proton NMR has been widely used in order to provide information on the monomeric species used in the preparation of polymers, the average composition, tacticity, and configuration of polymeric chains. Proton NMR studies are usually done in solution. The disadvantage of this technique is polymer spectra are frequently poorly resolved with broad overlapping lines but it has been improved by the used of high magnetic field equipment.

Carbon-13 NMR is more revealing than ^{1}H-NMR in polymer work because of the inherently wider spectral separation of carbon chemical shifts that make ^{13}C-NMR spectra more readily interpretable. In addition, the development of special decoupling techniques and pulse sequences have enhanced the utility of NMR spectroscopy in the field of polymers (Hadjichristidis, Pispas, and Floudas, 2003).

2.6.2 Fourier transform infrared spectroscopy (FTIR)

In infrared absorption spectroscopy, absorption of energies corresponding to transitions between vibrational or rotational energy states gives rise to characterized patterns. IR and Raman spectroscopy are complementary techniques. IR spectroscopy is used for measurement of the asymmetric vibrations of polar groups, whereas Raman spectroscopy is suitable for the symmetric vibrations of non-polar groups. These patterns can be translated into qualitative and quantitative information regarding the presence of functional groups, which can lead to the identification of the monomer types and their concentration in a block copolymer. The technique provides information on chemical, structural, and conformational aspects of polymeric chains.

Advances in instrumentation and data analysis techniques such as difference spectroscopy (spectral substraction), factor analysis, spectral deconvolution, and least square curve fitting of calibration plots for quantitative analysis, together with its ability for studying solid polymer samples, make IR a method of choice in the molecular characterization of complex block copolymers (Hadjichristidis, Pispas, and Floudas, 2003).

2.6.3 UV spectroscopy

This technique is often utilized for the identification and quantitative determination of comonomers in block copolymers. The coupling of UV detectors with size- exclusion chromatography (SEC) enhances the detection capabilities and applicability of both techniques.

2.6.4 Gel permeable chromatography (GPC)

GPC, a type of size exclusion chromatography (SEC) is an analytical technique that separates dissolved macromolecules by size based on their elution from columns filled with a porous non- ionic gel. Porous non- ionic materials, usually polystyrene/ divinyl benzene or silica gel containing pores of various sizes and distributions are packed into a column in GPC. A GPC/ SEC instrument consists of a pump to push the solvent through the instrument, and an injection port to introduce the macromolecules that are being analyzed into the column. Fractionation of the polymer sample results as different-sized molecules that are eluted at different times. The largest polymers in the solution cannot penetrate the pores, so they will elute first as they are excluded, and their retention volume is smaller. The smaller polymer molecules in the solution are retained in the interstices (or the voids) within the pores, and so require more time to elute and their retention volume is bigger. A chromatogram is a plot of

the retention volume or retention time. In order to obtain a molecular weight distribution, the column must be calibrated by using fractions of known molecular weight to relate molecular weight to the eluted volume (usually PS with narrow molecular weight distributions). A calibration curve used to determine the molecular weight of a polymer from its retention time as illustrated in Figure 2.27.

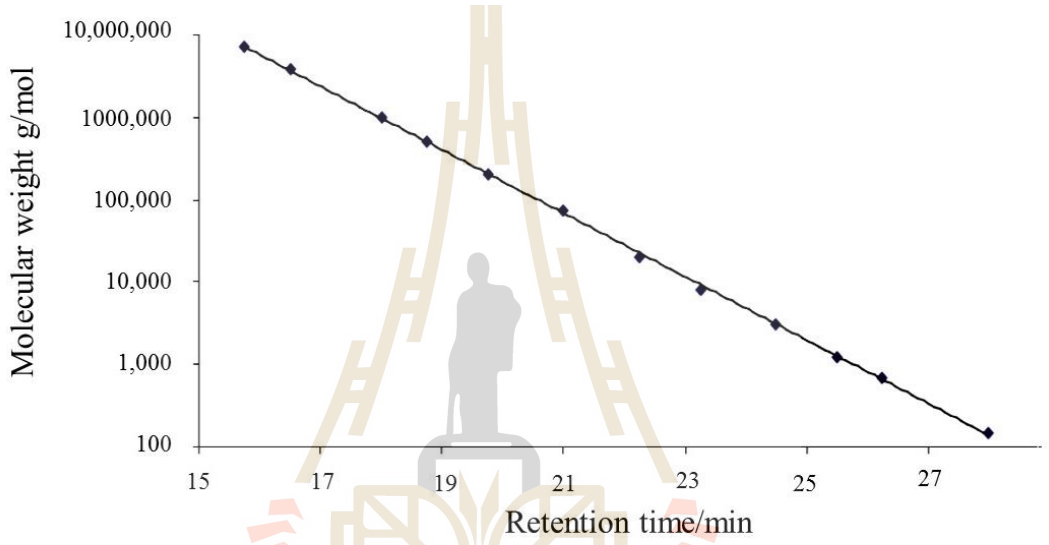

Figure 2.27 calibration graph used to determine the molecular weight of a polymer from its retention time.

CHAPTER III

EXPERIMENTAL

3.1 Preparation and characterization of hydroxyl terminated natural rubber (HTNR)

3.1.1 Materials

Natural crumb rubber (STR 5L) was purchased from Pee Jae rubber Co., Ltd. Hydrogen peroxide, methanol, hydroquinone, and toluene reagents grade were purchased from Carlo Erba Reagents.

3.1.2 HTNR preparation method

HTNR was prepared using depolymerization and hydroxylation methods proposed by Ravindaran et al. (1998). Natural crumb rubber was cut into small pieces and masticated for 30 min using a two-roll mill mixer. Masticated natural rubber was dissolved in toluene with a ratio of 1 gram per 10 ml. After that, the masticated natural rubber solution was charged into the photochemical reactor, a glass vessel of 2.5 liter capacity fitted with a water condenser and mechanical stirrer as shown in Figure 3.1. Next, hydrogen peroxide was added into the rubber solution with a ratio of 0.5 ml of hydrogen peroxide per 1 gram of rubber. The solution mixture was homogenized by the addition of 1.5 ml methanol per 1 gram of rubber. A 500 watt medium pressure mercury lamp was placed next to the photochemical reactor. Depolymerization reaction time was varied as tabulated in Table 3.1.

Figure 3.1 Photograph of a reactor setting for preparation of hydroxyl terminated natural rubber.

When designed time was reached, hydroquinone (0.002 grams of hydroquinone per 1 ml of natural rubber) was added into the solution mixture. Toluene and water in an obtained product were removed by precipitation in methanol to separate most of toluene from HTNR product. Finally, the hydroxyl terminated natural rubber (HTNR) was dried in a vacuum oven at 40˚C until the weight of HTNR was constant.

Table 3.1 Depolymerization reaction time for preparation of HTNR.

HTNR code	Depolymerization reaction time (h)
HTNR18	18
HTNR36	36
HTNR54	54

3.1.3 Characterization of HTNR

The molecular weight of HTNR was characterized by gel permeable chromatography (GPC, Agilent1200) using chloroform as a solvent with a flow rate of 0.5 ml/min. Polystyrene standard (polyscience) was used to establish a caribration curve.

Hydroxyl number of HTNR was estimated according to ASTM D4274-11. Firstly, HTNR was esterified with a solution of phthalic anhydride in pyridine under reflux conditions at 115 ± 2°C, for 1 hour. After that, the excess reagent is titrated with standard sodium hydroxide solution to a pink end point that persists for at least 15 s. The hydroxyl number, mg KOH/g, and functionality of sample was calculated as follows:

$$\text{Hydroxyl number} = [(B - A)N \times 56.1]/W \quad (3.1)$$

where: A = NaOH required for titration of the sample, ml,

B = NaOH required for titration of the blank, ml,

N = normality of the NaOH, and

W = sample used, g.

The functionality of HTNR was calculated from hydroxyl number using the following formula:

$$F = (\overline{M}_n \times \text{Hydroxyl number})/56100 \quad (3.2)$$

Where: $\overline{M}_n$ = number average molecular weight (g/mol) of sample

F = functionality, the number of OH group/mol and

56100 = equivalent weight of KOH, in milligrams.

The chemical structure of HTNR was studied using proton nuclear magnetic resonance spectroscopy (^{1}H-NMR) and Carbon-13 nuclear magnetic resonance spectroscopy (^{13}C-NMR) (Varian model Inova 300 NMR spectrometer) at 25˚C, 500 MHz. Deuterated chloroform ($CDCl_3$) and tetramethylsilane (TMS) were used as a solvent and an internal standard, respectively. A Fourier transform infrared microspectrometer (FT-IR) was employed. The FT-IR spectra was collected over the 4000 to 400 cm^{-1} wave number range, at resolution of 4 cm^{-1}.

3.2 Synthesis and characterization of poly(lactic acid) (PLA) prepolymers

3.2.1 Materials

L-(+)-Lactic acid as a 80% solution in water and Tin(II) 2-ethylhexanoate ($Sn(Oct)_2$) were purchased from Sigma-Aldrich, USA. Toluene, dichloromethane and methanol were purchased from Acros Organics, USA.

3.2.2 Preparation of PLA prepolymers

The pre-PLA was prepared following the work of Songprateepkul et. al. (2011). It was synthesized using condensation polymerization of lactic acid. A 80% aqueous solution of lactic acid was added into a round bottom flask equipped with a mechanical stirrer, and condenser, and this was connected to a vacuum line with a pressure sensor. The experimental set up is shown in Figure 3.2. Lactic acid was dehydrated for 2 hours at 130˚C. Next, the reaction temperature was raised to 170˚C. After that, $Sn(Oct)_2$ was added into the reactor. The reaction time and the amounts of reagents shown in Table 3.2 were used. The obtained PLA was precipitated by pouring

the polymer solution into an excess of methanol, filtered and dried in a vacuum oven at 40˚C to a constant weight.

Figure 3.2 Photograph showing experimental set up for synthesis of PLA pre-polymer.

Table 3.2 The amount of lactic acid (LA), and reaction time used in the synthesis of poly(lactic acid) prepolymer.

Prepolymer	LA (ml)	1st step		2nd step	
		$Sn(Oct)_2$ (v/v%)	Reaction time (h)	$Sn(Oct)_2$ (v/v%)	Reaction time (h)
PLA1	150	0.2	24	-	-
PLA2	150	0.2	24	0.1	18
PLA3	150	0.2	24	0.1	24

3.2.3 Characterization of PLA prepolymer

The molecular weight of PLA prepolymer was characterized by gel permeable chromatography (GPC, Agilent1200) as discussed in section 3.1.3.

The chemical structure of PLA prepolymer was examined using ^{1}H-NMR, and ^{13}C-NMR (Varian model Inova 300 NMR spectrometer) at 25˚C, 500 MHz using $CDCl_3$ as a solvent and TMS as an internal standard, respectively. A Fourier

transform infrared microspectrometer (FT-IR) was also employed. The FT-IR spectra was collected over the 4000 to 400 cm-1 wave number range, at resolution of 4 cm^{-1}.

3.3 Synthesis and characterization of PLA- NR- PLA block copolymer

3.3.1 Materials

HTNR54 produced according to photochemical reaction in section 3.1 was used. Three different molecular weights of PLA prepolymers (PLA1, PLA2, and PLA3) produced according to condensation polymerization in section 3.2 were employed. Tin (II) 2-ethylhexanoate ($Sn(Oct)_2$ was purchased from Sigma Aldrich, USA. Toluene, dichloromethane, chloroform, and methanol were purchased from Acros Organics, USA.

3.3.2 Preparation method

HTNR was dissolved in toluene with 0.0025mol of HTNR per 1 liter of toluene. After that, PLA prepolymer was added into the HTNR solution. The molar ratio of PLA prepolymer and HTNR was 2:1. The reaction temperature was 170˚C. After that, 0.5 %wt. $Sn(Oct)_2$ was added into the solution mixture. The reaction time was 24 h. Toluene was removed by the evaporation technique at 40˚C after finishing the reaction. The obtained products were dissolved in dichloromethane (CH_2Cl_2) and precipitated in an excess of distilled ethanol. Finally, the obtained products were dried in a vacuum oven at 40˚C to a constant weight. The synthetic block copolymers from PLA1, PLA2, and PLA3 were coded as PLA1-NR-PLA1, PLA2-NR-PLA2, and PLA3-NR-PLA3, respectively.

3.3.3 Characterization of PLA-NR-PLA triblock copolymer

The molecular weight and chemical structure of PLA-NR-PLA triblock copolymers were determined using GPC, NMR and FTIR. The characterization method was the same as mentioned in section 3.2.3.

3.4 Preparation and characterization of PLA/HTNR, PLA/PLA-NR-PLA, and PLA/NR/PLA-NR-PLA blends

3.4.1 Preparation of PLA/HTNR blends

PLA/HTNR blends were prepared from a commercial grade of poly(lactic acid) (PLA 4043D) which was purchased from NatureWorks LLC and HTNR master batch. HTNR master batch was prepared form HTNR and PLA at 50/50 %wt. Firstly, HTNR was dissolved in chloroform with a ratio of 1 gram per 10 ml of chloroform. After HTNR was completely dissolved, PLA was added into HTNR solution. Next, the solution mixture was stirred by mechanical stirrer until PLA was already dissolved and shown homogenous phase. Then, the solution mixture was poured into a smooth and clean tray. The layer thickness of solution mixture in a tray was about 3 mm. After that, solution mixture was dried at 40˚C to a constant weight. Finally, the film of HTNR master batch was trimmed into small pieces and was named as HTNR master batch. HTNR master batch was blended with PLA via melt blending process in a Haake Rheomix, 3000p internal mixer at 170°C with a rotor speed of 60 rpm for 10 minutes. The blend compositions in weight percentage ratio (%wt.) of PLA and HTNR as shown in Table 3.3 were used. All test specimens were prepared by compression molding (LabTech, LP20-B) at 170°C for 10 minutes. In order to estimation an efficiency of toughening agents in PLA blending with modified NR. The

blend of PLA and NR (STR 5L) at 10%wt. NR was also prepared via melt blending process in an internal mixer as same method as PLA/HTNR blends.

Table 3.3 PLA/HTNR blend compositions.

Designation	PLA (%wt.)	HTNR (%wt.)	NR (%wt.)
Neat PLA	100	-	-
PLA/NR(90/10)	90	-	10
PLA/HTNR(97/3)	97	3	-
PLA/HTNR(95/5)	95	5	-
PLA/HTNR(90/10)	90	10	-
PLA/HTNR(85/15)	85	15	-

3.4.2 Preparation of PLA/PLA-NR-PLA and PLA/NR/PLA-NR-PLA blends

PLA/PLA-NR-PLA and PLA/NR/PLA-NR-PLA blends were prepared by by melt blending in a Haake Rheomix, 3000p internal mixer at 170˚C with a rotor speed of 60 rpm for 10 minutes. The blend compositions of PLA/PLA-NR-PLA were divided into two cases. In case 1, the amount of PLA-NR-PLA triblock copolymer was fixed at 10 weight percentage (%wt.) as shown in Table 3.4. For case 2, the amount of triblock copolymer was adjusted to make the actual rubber content in the blends to be 10 %wt. as tabulated in Table 3.5. The blend compositions for PLA/NR/PLA-NR-PLA blends in weight percentage (%wt.) were shown in Table 3.6

. **Table 3.4** PLA/PLA-NR-PLA blend compositions (Case 1).

Designation	PLA (%wt.)	PLA-NR-PLA (%wt.)
PLA/PLA1-NR-PLA1(90/10)	90	10
PLA/PLA2-NR-PLA2(90/10)	90	10
PLA/PLA3-NR-PLA3(90/10)	90	10

Table 3.5 PLA/PLA-NR-PLA blend compositions (Case 2).

Designation	PLA (%wt.)	PLA-NR-PLA (%wt.)
PLA/PLA1-NR-PLA1(R-10)	87.6	12.4
PLA/PLA2-NR-PLA2(R-10)	85.3	14.7
PLA/PLA3-NR-PLA3(R-10)	82.7	17.3

Table 3.6 PLA/NR/PLA-NR-PLA blend compositions.

Designation	PLA (%wt.)	NR (%wt.)	PLA-NR-PLA (%wt.)
PLA/NR/PLA1-NR-PLA1 (90/9/1)	90	9	1
PLA/NR/PLA1-NR-PLA1 (90/8/2)	90	8	2
PLA/NR/PLA1-NR-PLA1 (90/7/3)	90	7	3
PLA/NR/PLA2-NR-PLA2 (90/9/1)	90	9	1
PLA/NR/PLA2-NR-PLA2 (90/8/2)	90	8	2
PLA/NR/PLA2-NR-PLA2 (90/7/3)	90	7	3
PLA/NR/PLA3-NR-PLA3 (90/9/1)	90	9	1
PLA/NR/PLA3-NR-PLA3 (90/8/2)	90	8	2
PLA/NR/PLA3-NR-PLA3 (90/7/3)	90	7	3

3.4.3 Characterization of PLA/HTNR, PLA/PLA-NR-PLA, and PLA/NR/PLA-NR-PLA blends

3.4.3.1 Mechanical properties

3.4.3.1.1 Tensile properties

Tensile properties of PLA/NR, PLA/HTNR, PLA/PLA-NR-PLA and PLA/NR/PLA-NR-PLA blends were evaluated following ASTMD 638 using a tensile testing machine (Instron model 5565) with a load cell of 5 kN, a cross head speed of 10 mm/min, and a gauge length of 7.62 ± 0.02 mm. The number of test specimens was at least 5 specimens. The shape of the tensile test specimens is shown in Figure 3.3 and the dimension of the standard test specimen is shown in Table 3.7.

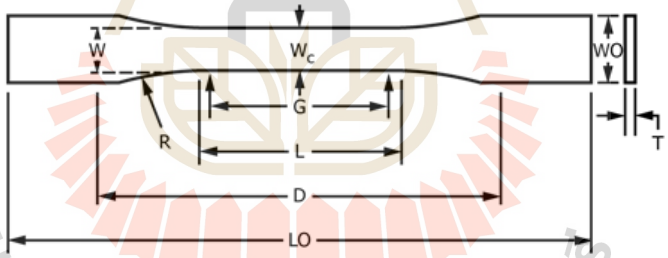

Figure 3.3 The dimensions of tensile test specimens (Type V).

Table 3.7 The dimensions of standard test specimens.

Dimensions (as shown in Figure 3.3)	Size (mm)
W-Width of narrow section	3.18 ± 0.03
L-Length of narrow section	9.53 ± 0.08
WO-Width overall	9.53 ± 0.08
LO-Length overall	63.5
G-Gage length	7.62 ± 0.02

Table 3.7 The dimensions of standard test specimens. (Continued).

Dimensions (as shown in Figure 3.3)	Size (mm)
D-Distance between grips	25.4 ± 0.2
R-Radius of fillet	12.7 ± 0.08

3.4.3.1.2 Impact properties

The Izod impact strength of the all blends were tested according to the ASTM D 256, method A, using a basic pendulum impact tester (Atlas model BPI). The total striking impact energy of 2.7 J was assigned at room temperature. The geometry of specimens was 5 mm in thickness, 63.5 ± 2.0 mm in length and 12.7 ± 0.2 mm in width. The shape of impact test specimens is shown in Figure 3.4. Ten specimens were tested on each blend. The impact strength (kJ/m^2) was calculated and reported.

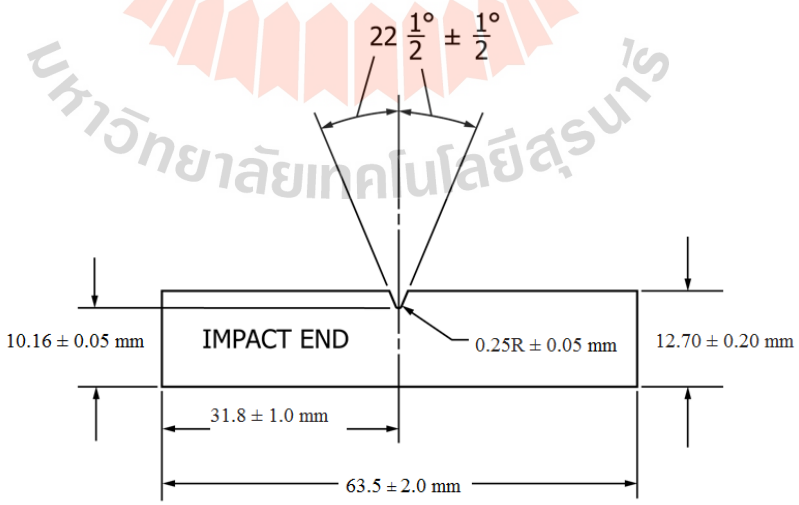

Figure 3.4 Dimensions of notch Izod-Type Test Specimen.

3.4.3.2 Morphological properties

The freeze fracture surfaces, tensile and impact fractured morphologies of neat PLA and all blends were examined by a scanning electron microscope (SEM) (JEOL, model JSM6400) at 10 kV. The sample surfaces were coated with gold before SEM analysis.

3.4.3.3 Thermal properties

Thermal properties of PLA, and PLA/ NR, PLA/ HTNR, PLA/ PLA-NR-PLA, and PLA/ NR/ PLA-NR-PLA blends was characterized using a differential scanning calorimeter (DSC204F1). 5-10 mg of each sample was putted in an aluminum pan and sealed with an aluminum cover. Each sample was heated from -100°C to 200°C at the rate of 5°C/min (the first heating) and kept for 2 min at 200°C to remove the previous thermal history. Subsequently, the sample was cooled to 120°C at the rate of 5°C/min (cooling) and heated again to 200°C at the rate of 5°C/min (the second heating).

CHAPTER IV

RESULTS AND DISSCUSTION

4.1 Characteristics of HTNR

In this part, hydroxyl terminated liquid natural rubber (HTNR) was obtained from photochemical degradation of natural rubber as reported by Ravindran et al. (1988). This procedure was not complicated to prepare large scale production of HTNR. The production yield of HTNR in the current work was 91.04 ± 3.92%. The production yield of HTNR was calculated from weight of obtained product compared with the weight of starting masticated NR used. The appearance of obtained HTNR was honey yellow colour, viscous and sticky liquid. It is thoroughly soluble in chloroform. The appearance of obtained HTNR is shown in Figure 4.1.

Figure 4.1 The photograph of HTNR obtained from photochemical degradation of masticated NR.

Molecular weight and chemical structure HTNR were reported and discussed in following part.

4.1.1 Molecular weight of HTNR

Molecular weight of HTNR and masticated NR with masticated time of 30 min was examined using GPC. The number average molecular weight ($\bar{M}_n$), weight average molecular weight ($\bar{M}_w$), and polydispersity index (PDI), of masticated NR and HTNR are tabulated in Table 4.1.

Table 4.1 Molecular weight and PDI of HTNR and masticated NR.

Code	$\bar{M}_n$ (g/mol)	$\bar{M}_w$ (g/mol)	PDI
masticated NR	202,982	477,028	2.35
HTNR18	100,324	247,386	2.46
HTNR36	48,840	105,826	3.37
HTNR54	28,003	98,030	3.12

From the results obtained, $\bar{M}_w$ and $\bar{M}_n$ of HTNR were highly decreased after photochemical degradation reaction. PDI of HTNR was slightly board.

4.1.2 Hydroxyl number and functionality of HTNR

For an estimation of hydroxyl number and functionality of HTNR, each HTNR sample was dissolved and esterified with a solution of phthalic anhydride in pyridine under reflux conditions. After that, HTNR solution was titrated with standard sodium hydroxide solution to a pink end point as explained in section 3.1.3. An example of an appearance of pink end point for each HTNR sample is shown in Figure 4.2. It

was very difficult to investigate the true pink end point due to light yellow color of HTNR, pH indicator strips were also used to confirm the end point.

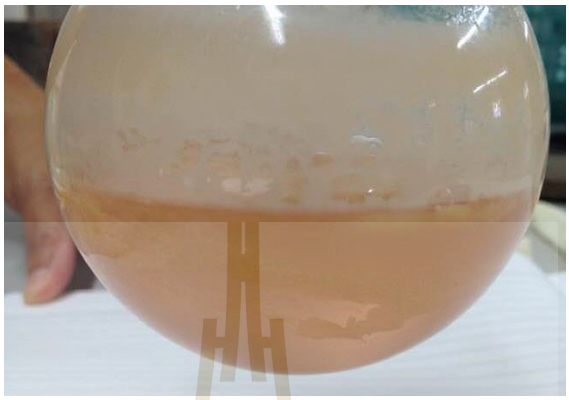

Figure 4.2 The photograph showing pink end point of HTNR titration.

Hydroxyl values and functionality estimated from equation 3.1-3.2 for HTNR18, HTNR36, and HTNR54 are summarized in Table 4.2.

Table 4.2 Hydroxyl number and functionality of HTNR**.**

HTNR code	Average hydroxyl number (mg KOH/g)	Average functionality
HTNR18	0.92 ± 0.19	1.65 ± 0.36
HTNR36	2.01 ± 0.36	1.75 ± 0.38
HTNR54	3.55 ± 0.42	1.77 ± 0.21

So far, a study on the effect of molecular weight and reactive groups of natural rubber on the properties of the blends had been reported, Dahlanc, Zaman, and Ibrahim, (2000) found that low molecular weight of NR in some range played a very important role in determining mechanical properties in NR/polyolefin blends. Utara and Boochathumtara, (2011) reported that the mechanical properties including the

elongation at break and the impact strength of the blend were found to be enhanced by adding low molecular weight NR without using a compatibilizer by reducing the crystallinity and the change of a-relaxation temperature of polymer matrix. Therefore, the obtained HTNR54 ($\bar{M}_n$ = 28,000 g/mol) was further study on chemical structure, blending with PLA and preparation of triblock copolymer.

4.1.3 Chemical structure of HTNR

The ^{1}H-NMR spectrum of HTNR, masticated NR, and NR are compared in Figure 4.3. With an exception of a small peak at 2.68 ppm (H8), NR and masticated NR showed the same signal. The peak at 2.68 ppm was corresponding to epoxide group (Auras, 2010). The presence of slight amount of epoxide group in natural occurring NR was reported (Hwee, 2015). After mastication, molecular weight of NR was decreased, and the epoxide signal was evident. The signal of unsaturated methine proton (-C=C<u>H</u>-) of HTNR appeared at 5.12 ppm (H3). The peak at 2.04 ppm (H1, H4) and 1.68 ppm (H5) were corresponding to methylene proton (-C<u>H</u>$_2$-), and methyl proton (-C<u>H</u>$_3$-), respectively. New peak signals at 3.2 ppm (H12) and 3.4 ppm (H11) belonged to methylene proton (-C<u>H</u>$_2$-) adjacent to hydroxyl group which related to the presence of the hydroxyl end groups in HTNR. Moreover, HTNR product also had epoxide group which is a peak appeared at 2.68 ppm (H8). The signal was more obvious than in masticated NR. This could be attributed to the generation of epoxide group during the preparation of HTNR under the presence of hydrogen peroxide (Ibrahim et al., 2014). ^{13}C-NMR spectrum of HTNR, masticated NR, and NR are shown in Figure 4.4. The signal at 23.6 ppm (C5) was related to methyl carbon (-C<u>H</u>$_3$-). The peak signal at 26.0 ppm (C4) and 33.0 ppm (C1) belonged to methylene carbon (-<u>C</u>H2-). Carbon adjacent to methyl group (-<u>C</u>(CH$_3$)=) appeared at 135 ppm (C2). The peak signal at about 60

ppm (C8) and 65 ppm (C7) which corresponded to carbon of epoxide ring was also appeared. The peak signal about 60 ppm (C12) and 62 ppm (C11) indicated the attachment of hydroxyl group at to -$\underline{C}H_2$- of HTNR (Saetung, 2010).

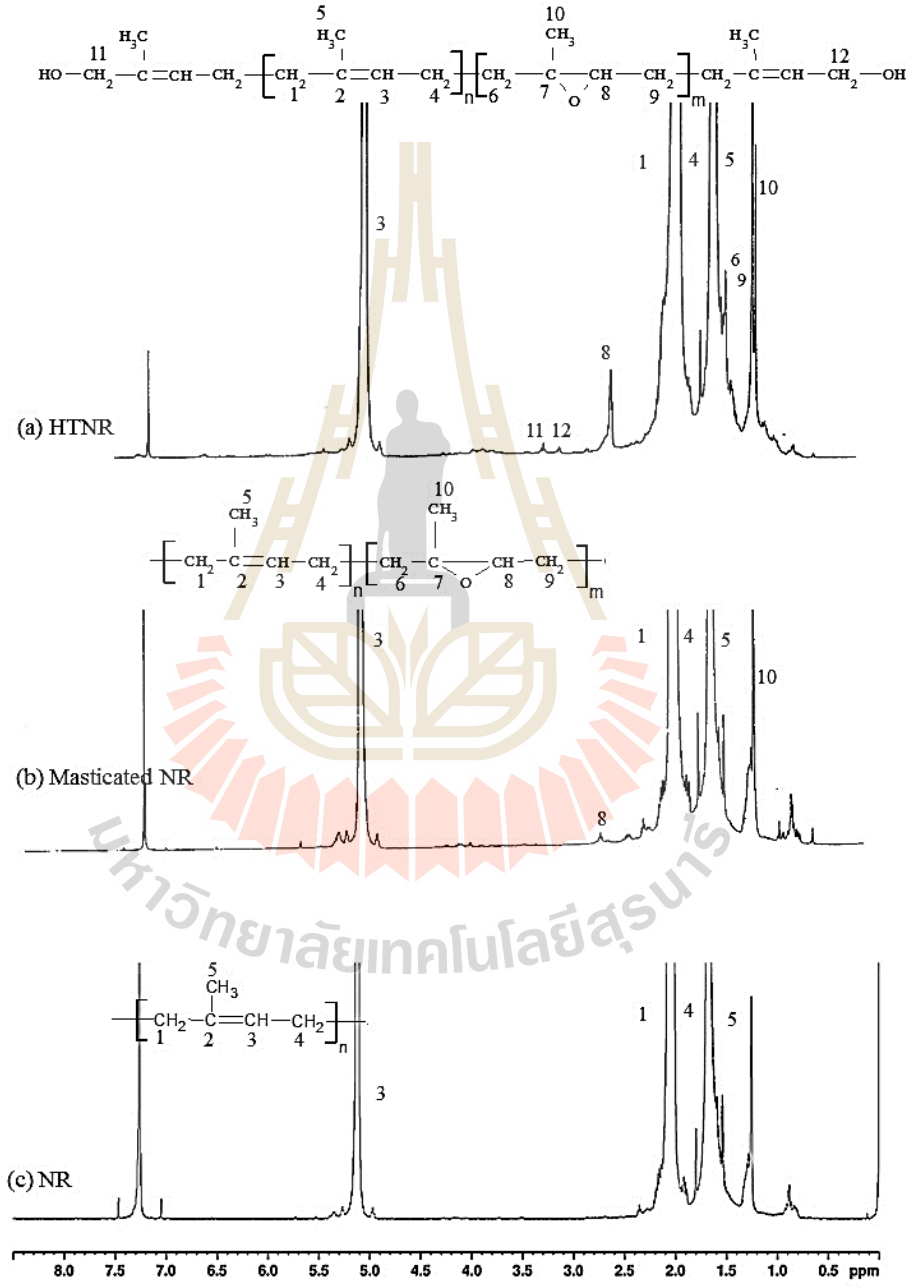

Figure 4.3 ^{1}H-NMR spectrum of (a) HTNR, (b) masticated NR and (c) NR.

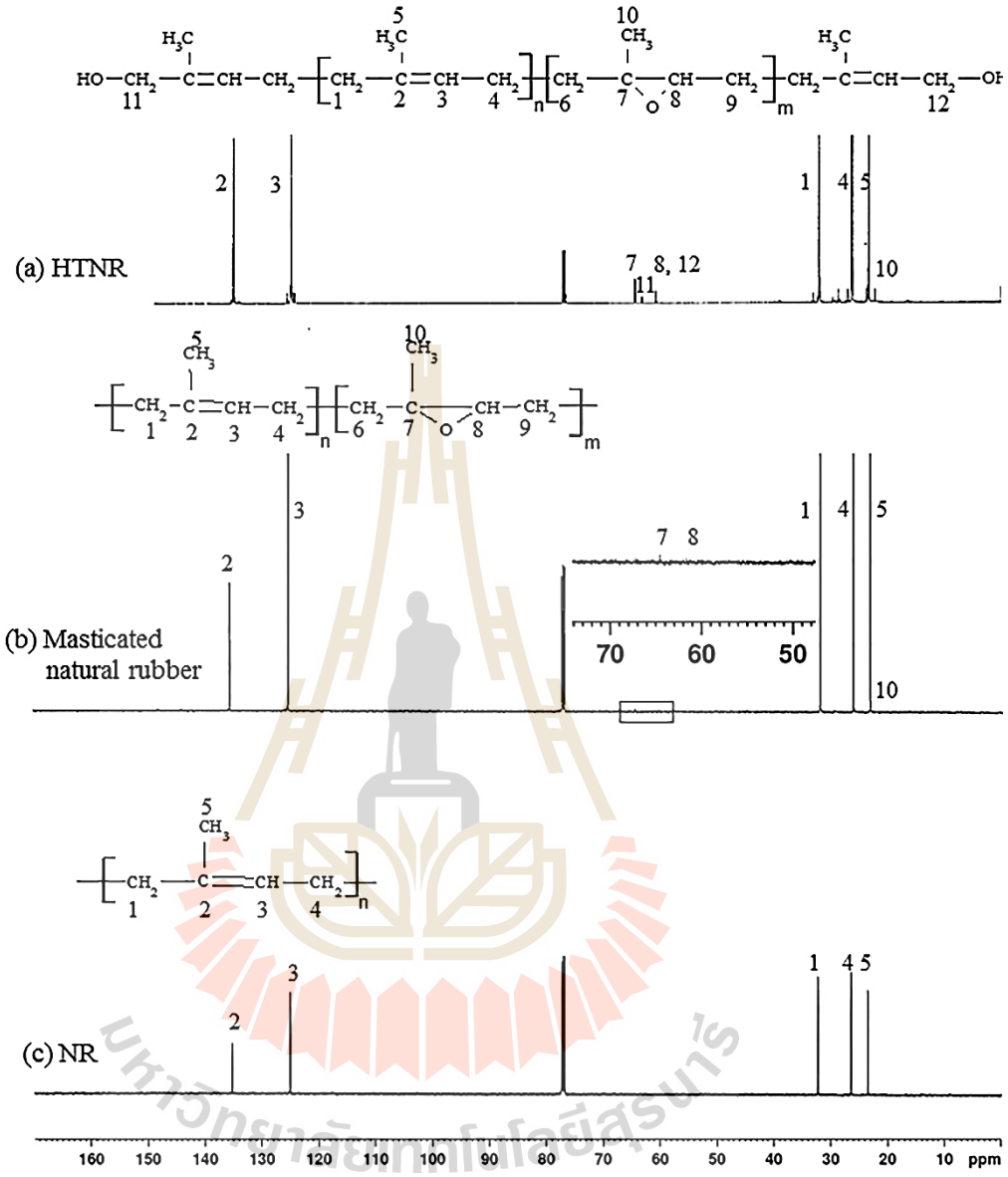

Figure 4.4 ^{13}C-NMR spectrum of (a) HTNR, (b) masticated NR and (c) NR.

From NMR characterization, the possible chemical reaction occurred during HTNR preparation are presented in Figure 4.5.

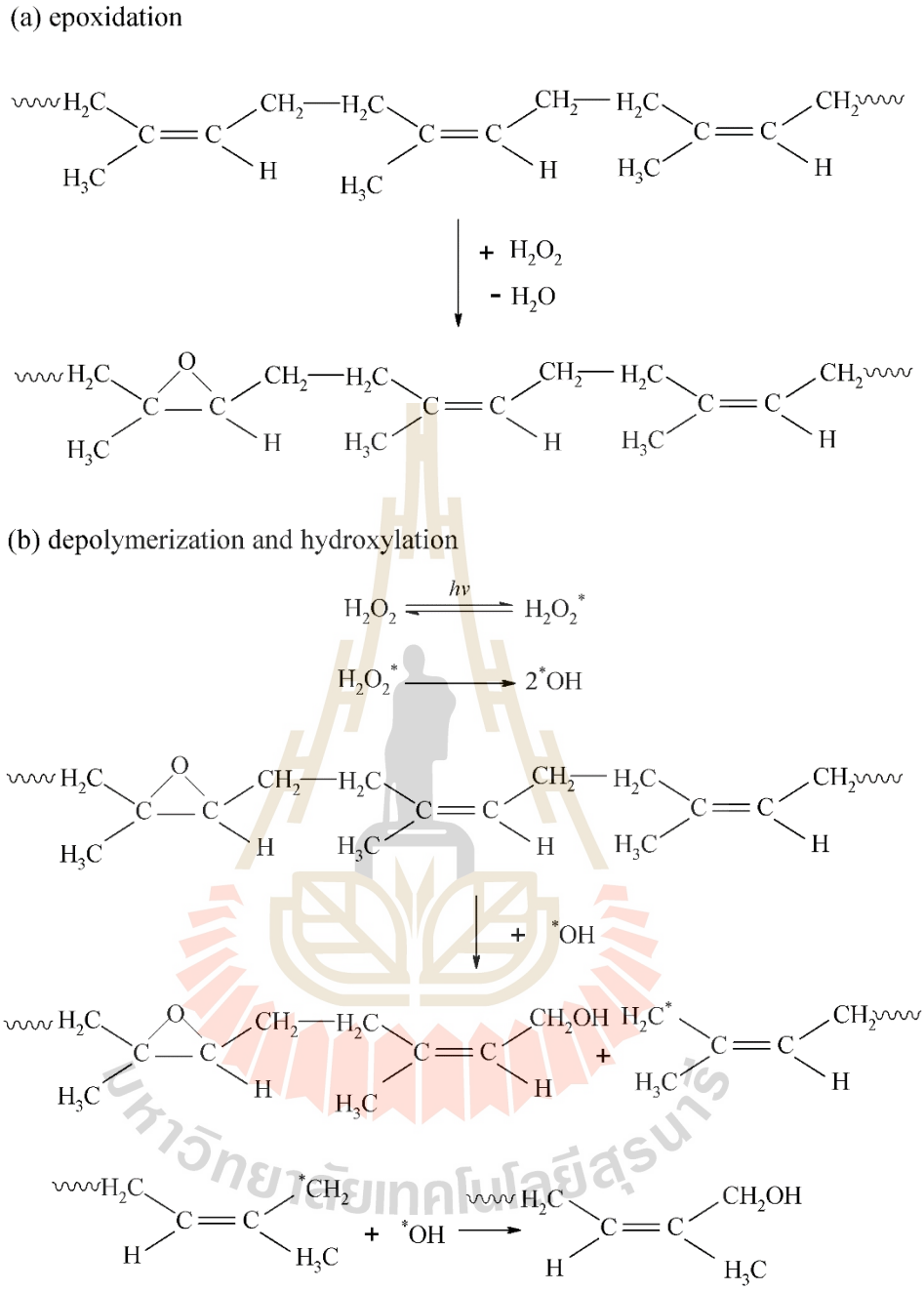

Figure 4.5 The possible chemical reaction occurred during HTNR preparation, (a) epoxidation, (b) depolymerization and hydroxylation.

FTIR in ATR mode was a useful technique for quantifying chemical functional groups of NR and its derivative. The FTIR spectra of HTNR, masticated NR,

and NR are shown in Figure 4.6. From the result obtained, the main characteristic peaks of NR, masticated NR and HTNR were indicated at 3030 cm^{-1}, 2965 cm^{-1}, 2923 cm^{-1}, and 2850 cm^{-1} corresponding to asymmetric =CH stretching, asymmetric CH_3 stretching, asymmetric CH_2 stretching, and symmetric CH_3 stretching, respectively. The peak at 1664 cm^{-1} belonged to C=C stretching. The peak assignment at 1450 and 1378 cm^{-1} was a deformation of $-CH_3$ and $-CH_2$. The peak at 835 cm^{-1} was =C-H. In addition, HTNR has some epoxide group that appear at 870 cm^{-1} responding to symmetric C-O-C stretching (Saramalee et al., 2014; Rolere et al.,2015). The spectrum of HTNR showed the OH stretching band at about 2845-3400 cm^{-1}. The confirmation of an attachment of OH group onto HTNR molecule showed the OH stretching band at about 2845-3400 cm^{-1}.

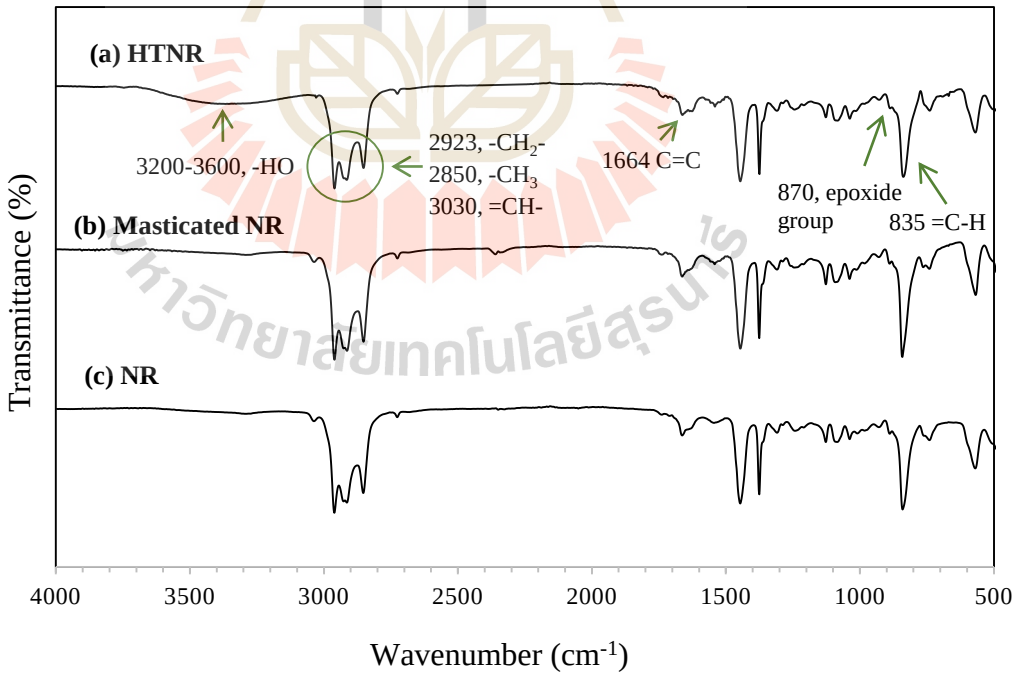

Figure 4.6 FTIR spectra of HTNR (a), masticated NR (b) and NR (c).

From the analysis of chemical structure and functionality of HTNR, the chemical structure of HTNR that was synthesized in this research should be as shown in Figure 4.7.

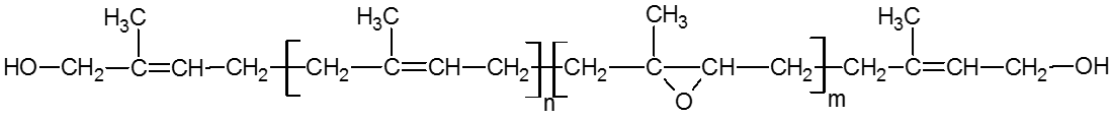

Figure 4.7 The possible chemical structure of obtained HTNR.

4.2 Mechanical, morphological and thermal properties of PLA/HTNR blends

4.2.1 Mechanical properties of PLA/HTNR

4.2.1.1 Tensile properties of PLA/HTNR

PLA/HTNR blends were prepared by melt blending in an internal mixer. The amount of HTNR ($\overline{M}_n$=28000 g/mol) in the blend were 3, 5, 10, and 15 wt%, respectively. All test specimens were prepared by compression molding. Impact and tensile test were applied to obtain the mechanical properties of the blends. The impact strength, tensile strength, modulus, and elongation at break of PLA, PLA/NR, and PLA/HTNR are summarized in Table 4.3 The tensile stress-strain curves of PLA, PLA/NR and PLA/HTNR blends are plotted in Figure 4.8. It was found that neat PLA showed brittle fracture behavior. Tensile strength and tensile modulus of PLA were 61.47 ± 3.69 MPa, and 0.60 ± 0.03 GPa respectively, whereas elongation at break of PLA was only 12.91 ± 1.00 %. Tensile stress-strain curves of PLA/HTNR blends exhibited higher elongation before failure with an increase of HTNR content. This

indicated that PLA/HTNR blends were ductile behavior. Tensile strength of PLA/HTNR blends

Table 4.3 Mechanical properties of neat PLA, PLA/NR and PLA/HTNR blends

Designation	Impact strength (kJ/m^2)	Tensile modulus (GPa)	Tensile strength (MPa)	Elongation at break (%)
Neat PLA	18.41 ± 1.49	0.68 ± 0.03	61.47 ± 3.69	12.91 ± 1.00
PLA/NR(90/10)	65.35± 2.85	0.55 ± 0.02	42.60 ± 0.64	60.54±13.00
PLA/HTNR(97/3)	45.50 ± 2.52	0.63 ± 0.02	55.71 ± 1.81	45.42 ± 3.81
PLA/HTNR(95/5)	60.44 ± 5.99	0.60 ± 0.02	51.60 ± 1.87	84.05 ± 3.14
PLA/HTNR(90/10)	67.78 ± 12.10	0.54 ± 0.02	44.46 ± 1.08	127.23 ± 6.00
PLA/HTNR(85/15)	58.21 ± 3.32	0.52 ± 0.03	37.33 ± 1.29	140.29 ± 9.77

was gradually decreased with an increase of HTNR concentration. The elongation at break were obviously improved upon incorporation of HTNR. It was also very interesting to observe that PLA/HTNR blends upon incorporation of 10 %wt. of HTNR showed a highly increase in tensile elongation at break of 127.23 ± 6.00%. As the content of HTNR increased to 15 wt%, the elongation at break is further increased to 144.66%, which was about 11 times higher than neat PLA.

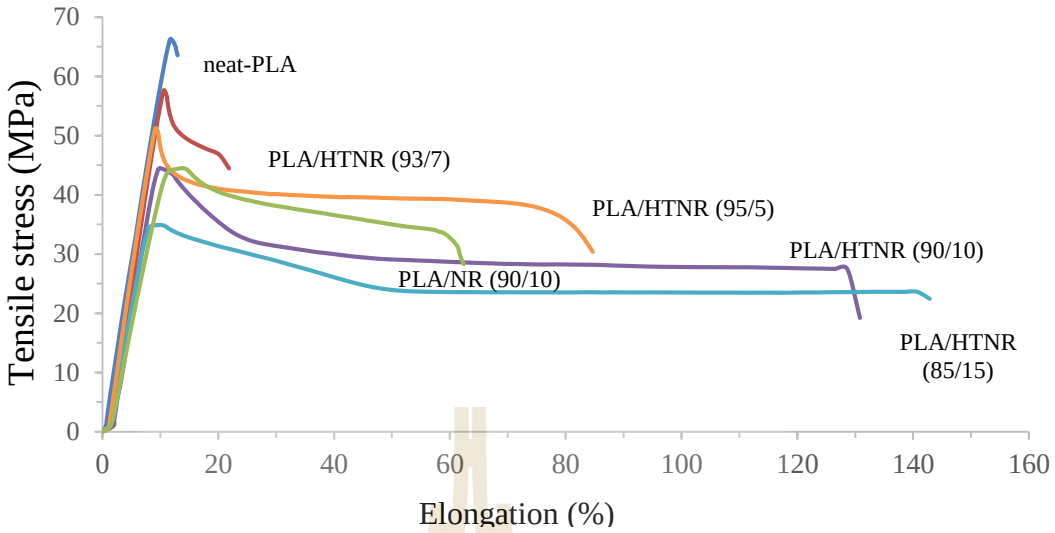

Figure 4.8 Stress-strain curves of PLA, PLA/NR, and PLA/HTNR blends.

PLA/NR (90/10) blend at 10 %wt. of NR, the optimum NR content that gave the optimum mechanical properties for PLA (Juntuek et al., 2012; Pongtanayut et al., 2013; Sawitri et al, 2015) was used to compare with 10 %wt of HTNR. PLA/HTNR exhibited slightly higher in tensile strength and significantly higher in elongation at break. The compatibility of PLA and HTNR might be better than that of PLA and unmodified NR.

4.2.1.2 Impact properties of PLA/HTNR

Figure 4.9 shows the impact strength of PLA, PLA/NR and PLA/HTNR blends. It was shown that impact strength of neat PLA was 18.41 ± 0.49 kJ/m^2. The impact strength of PLA/HTNR blends was increased with an increase of HTNR content. The highest impact strength of 67.78 ± 12.10 kJ/m^2 belonged to PLA/HTNR blend with 10 %wt. of HTNR. Comparing PLA/HTNR with PLA/NR blend at 10%wt of rubber content, PLA/HTNR also showed a slightly higher impact strength than PLA/NR (90/10) blend. A lower molecular weight of HTNR with OH functional groups was probably more compatible with PLA. This indicated that an

incorporation of 10 %wt. HTNR not only significantly increased elongation at break but also tended to improve an impact strength of the blends.

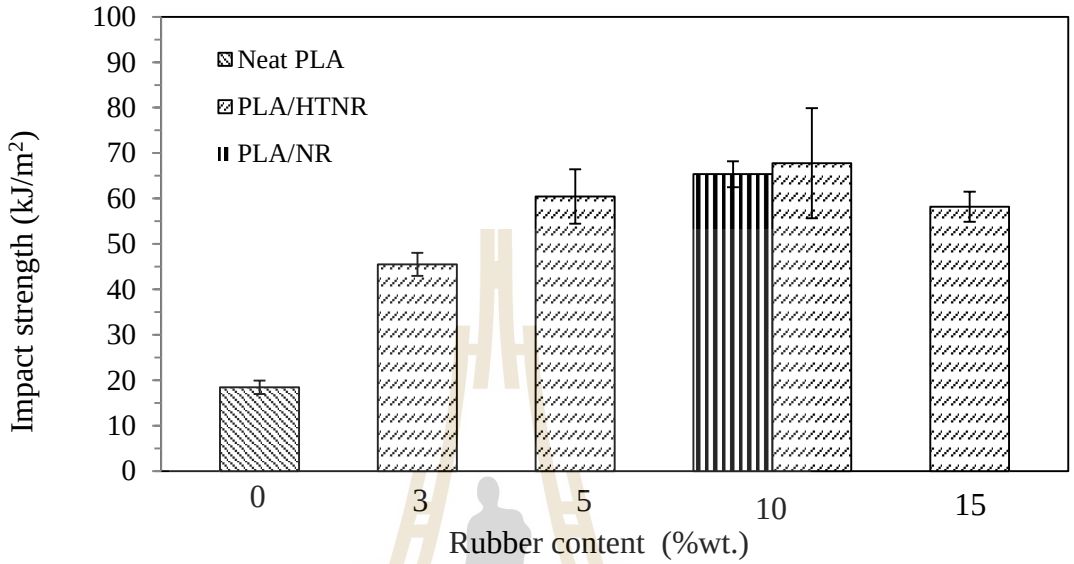

Figure 4.9 Impact strength of neat PLA, PLA/NR, and PLA/HTNR blends with various rubber contents.

4.2.2 Morphological properties of PLA/HTNR

The morphologies of neat PLA and PLA/HTNR blends were investigated using SEM technique. The fractured surfaces from tensile, impact testing and freeze fracture surface specimens were investigated by mean of the relation between mechanical properties and morphologies of the blends. SEM micrographs of tensile fractured surfaces of PLA/HTNR blends are shown in Figure 4.10. The micrographs reveal the longer elongated fibrils when the amount of HTNR increased. These confirmed that the ductile fracture of the blends was occurred and improved by the addition of HTNR.

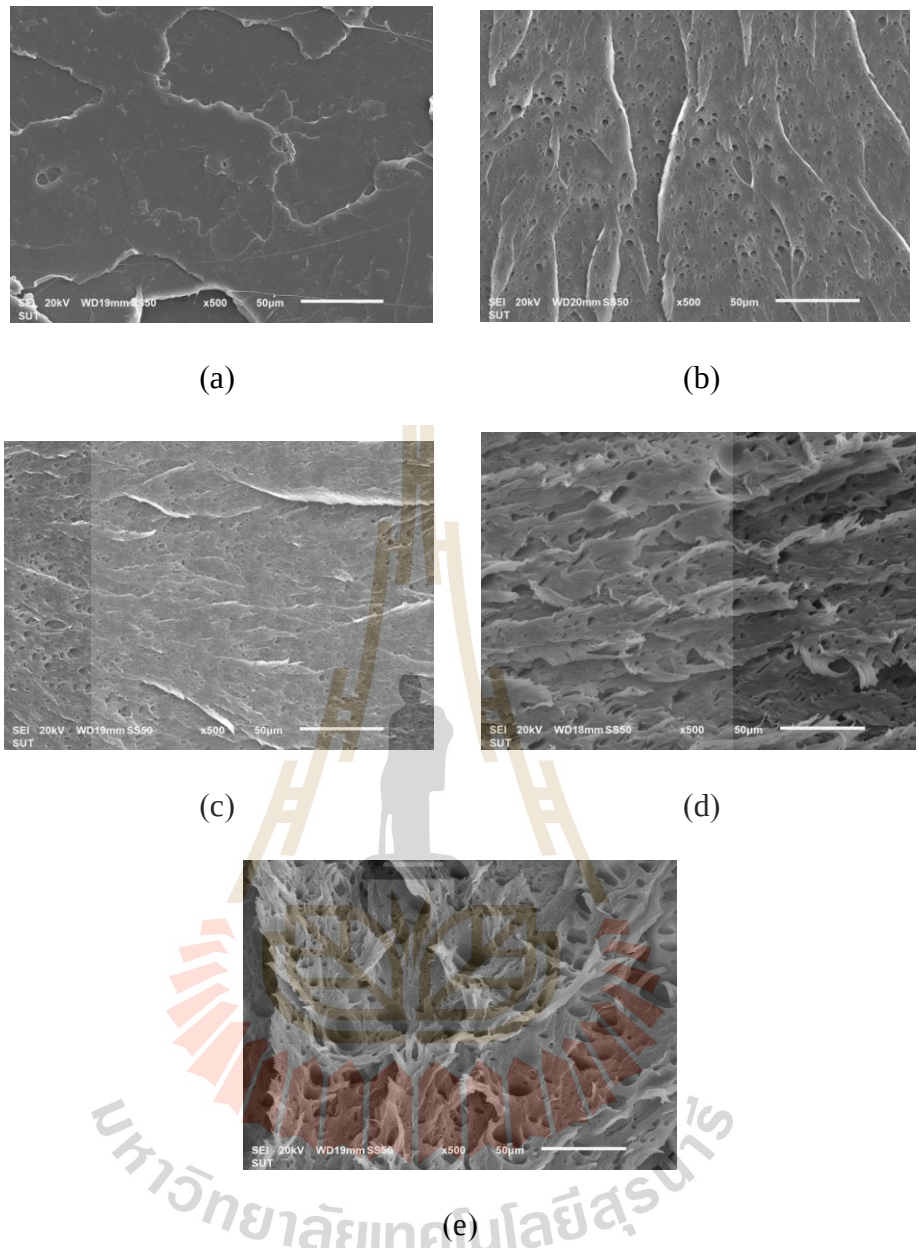

Figure 4.10 SEM micrographs of tensile fractured surface of PLA (a), PLA/HTNR (97/3) (b), PLA/HTNR (95/5) (c), PLA/HTNR (90/10) (d), and PLA/HTNR (85/15) (e) (500X).

SEM micrographs of the impact fracture surfaces of the PLA/HTNR blends are shown in Figure 4.11. It was found that, neat PLA exhibited a typical fractured

surface of a brittle material due to rather a smooth surface and no plastic deformation. The micrographs reveal the fracture surfaces became rougher when the HTNR was added into PLA. These confirmed that the toughness of the blends was occurred and improved by the addition of HTNR. However, at 15 %wt. of HTNR, the HTNR domains in the matrix were quite large. This could be the reason of decreasing of impact strength.

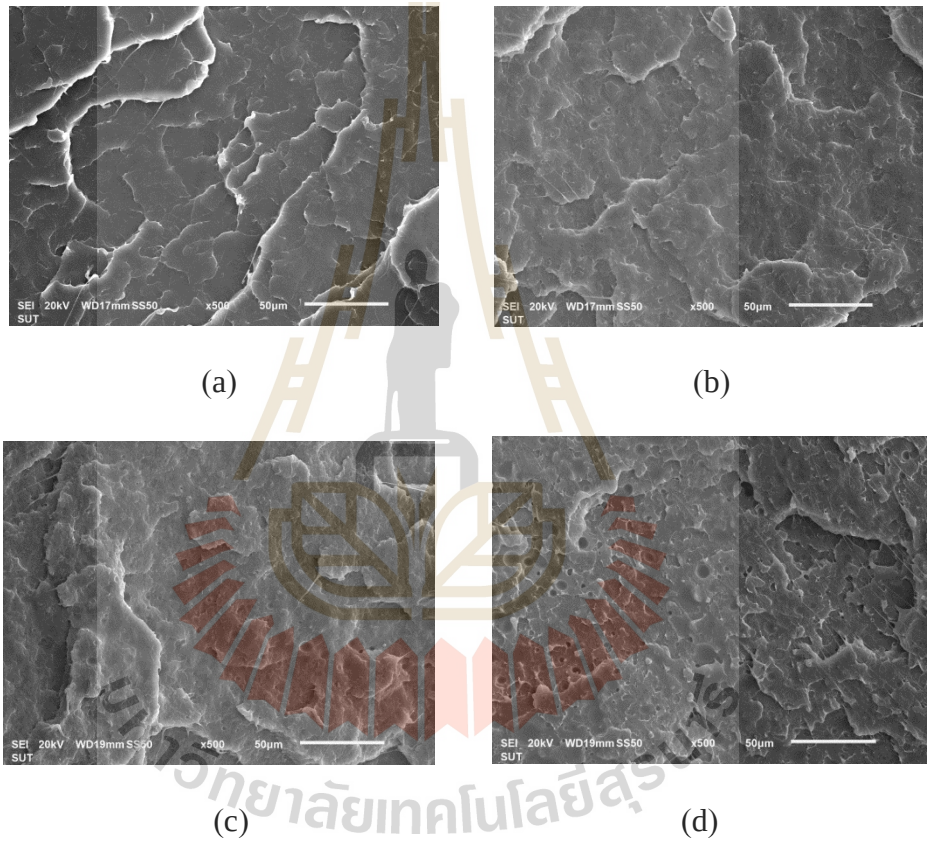

Figure 4.11 SEM micrographs of impact fractured surface of neat PLA (a), PLA/HTNR (97/3) (b), PLA/HTNR (95/5) (c), PLA/HTNR (90/10) (d), PLA/HTNR, and (85/15) (e) (500X).

SEM micrographs of freeze-fractured surfaces of PLA/HTNR blends and the average particle diameter of HTNR particles in the blends are shown in Figure 4.12 and Table 4.4 respectively.

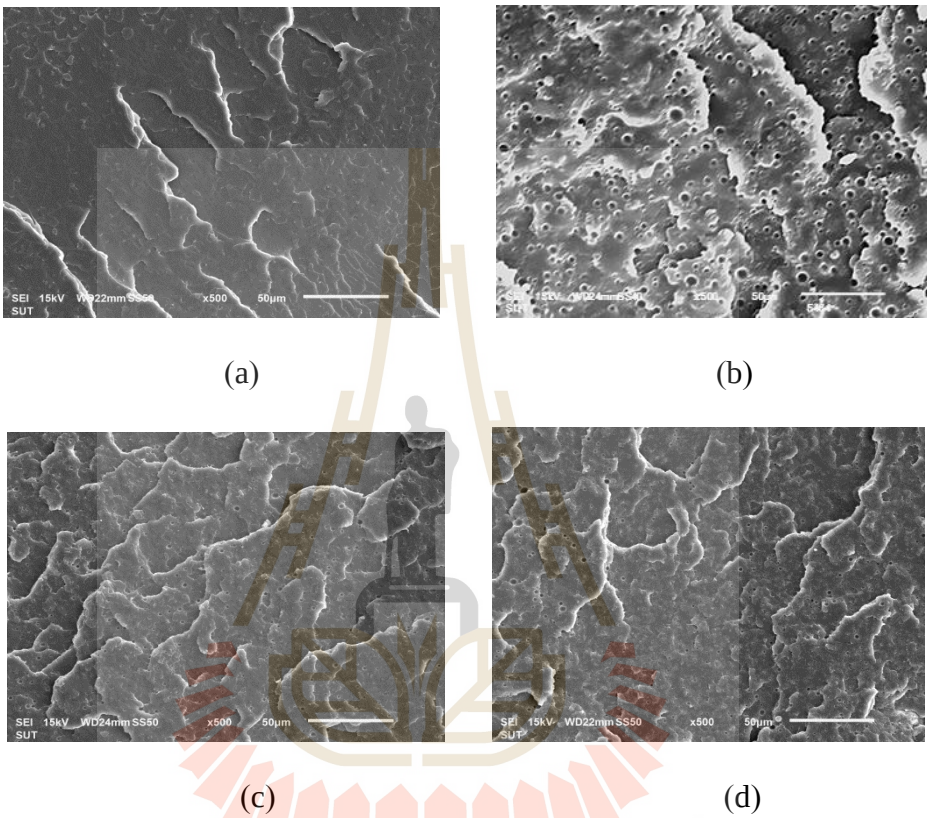

Figure 4.12 SEM micrographs of freeze-fractured surfaces of PLA (a), PLA/NR (90/10) (b), PLA/HTNR (97/3) (c), PLA/HTNR (95/5) (d), PLA/HTNR (90/10) (e), and PLA/HTNR (85/15) (f) (500X).

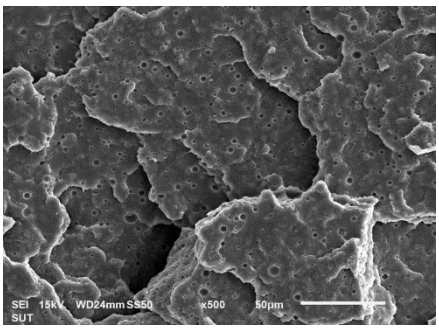

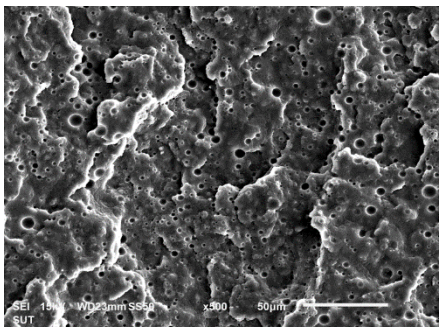

(e) (f)

Figure 4.12 SEM micrographs of freeze-fractured surfaces of PLA (a), PLA/NR (90/10) (b), PLA/HTNR (97/3) (c), PLA/HTNR (95/5) (d), PLA/HTNR (90/10) (e), and PLA/HTNR (85/15) (f) (500X).

The diameter of rubber particle in the blends was measured from SEM micrographs of freeze-fractured surfaces of PLA and its blends (Figure 4.12). The number averaged diameter, d_n was calculated from a minimum of 200 particles according to the following equations (Wu et al,. 2010):

$$d_n = \frac{\sum_i n_i d_i}{\sum_i n_i} \quad (4.1)$$

$$SD = \sqrt{\frac{\sum_i n_i (d_i - d_n)^2}{N}} \quad (4.2)$$

Where d_i is the diameter of particle

n_i is the total number of particles having diameter, d_i

An average HTNR particle sizes in PLA/HTNR (90/10) which showed the highest impact and elongation at break was lower than the average NR particles

sizes in PLA/NR (90/10) as shown in Figure 4.12(b) . The smaller rubber particle size dispersed in the matrix indicates better compatibility between PLA and HTNR.

Table 4.4 Particle diameters of rubber particle in PLA/NR and PLA/HTNR blends.

Samples	Average particle diameter, d_n (μm)	Minimum particle diameter (μm)	Maximum particle diameter (μm)
PLA/NR(90/10)	2.02 ± 0.68	0.45	4.25
PLA/HTNR(97/3)	0.82 ± 0.33	0.20	1.58
PLA/HTNR(95/5)	0.87 ± 0.48	0.33	2.80
PLA/HTNR(90/10)	0.92 ± 0.71	0.21	3.40
PLA/HTNR(85/15)	1.33 ± 0.65	0.30	3.40

The particles size distribution of HTNR in the blends was shown in Figure 4.13. It was observed that the diameter of HTNR dispersed phase was shifted to bigger size with increasing HTNR content. This could be because of coalescence phenomena. The reduction in impact strength of the blend containing 15wt% HTNR was probably due to more coalescence

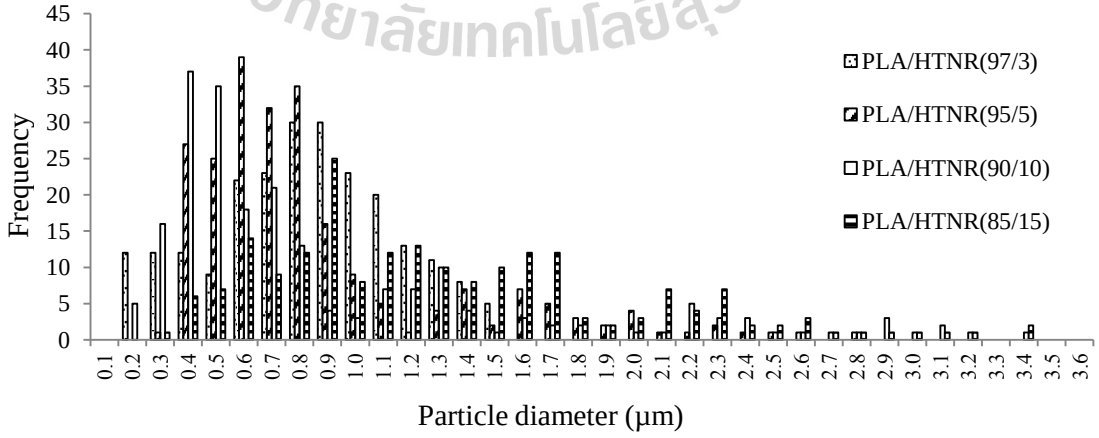

Figure 4.13 Particle size distributions of HTNR particles in PLA/HTNR blends.

From the particle size and particle size distribution, impact strength and tensile properties of PLA/HTNR blends, HTNR particles in PLA/HTNR blends behave as stress concentrators enhancing the fracture energy absorption of brittle PLA and the well distribution of HTNR as small domains in the PLA matrix resulted in an improvement of PLA toughness. The optimal HTNR content to improve the toughness of PLA was found to be 10 wt%, this concentration HTNR droplets provided an optimum balance between coalescence and an enhancement of tensile elongation at break and tensile strength of the blend.

4.2.3 Thermal properties of PLA/HTNR blend

The thermal properties of PLA, PLA/NR(90/10), and PLA/HTNR(90/10) blends were characterized using DSC techniques. The glass transition temperature (T_g), the cold crystallization temperature (T_{cc}) and melting temperature (T_m) of PLA and PLA blends could be observed. In this work. the % of matrix (PL A) crystalline phase (X_c) was estimated using the following equation:

$$\%\text{Crystallinity } (X_c) = 100 \times (\Delta H_m - \Delta H_c)/\Delta H_m^{\circ} \quad (4.2)$$

Where ΔH_m is the measured endothermic enthalpy of melting

ΔH_c = the cold crystallization exothermic enthalpy during the heating scans.

ΔH° = the theoretical melting enthalpy of 100% crystalline PLA was taken to be 93.6 J/g (Mazidi et al., 2018).

DSC curves of the blend obtained from the first and second heating scan are shown in Figure 4.14 and Figure 4.15respectively. The double melting endotherms for neat PLA

were observed at 146.3 and 155.6 ˚C, which associated with the melting of PLA crystals. The lower temperature melting peak (T_{m1}) was relating to melting of less perfect PLA lamellar crystals and the higher temperature melting peak (T_{m2}) was corresponding to melting of more perfect PLA crystals (Zhang et al., 2014; Chen et al., 2014). The Tg of HTNR in PLA/HTNR blend was higher than that of NR in PLA/NR blend, even though the molecular weight of HTNR was lower than that of NR. This might be due to the interaction between HTNR and PLA hindered the movement of HTNR chain in the blend. The T_g of PLA phase in PLA/NR(90/10) and PLA/HTNR(90/10) blends appeared at the same temperature with that of neat PLA. This indicate that the rubber component added into PLA did not have obvious effect on the mobility of PLA chain in the blends. The T_{cc} of PLA phase PLA/NR, and PLA/HTNR (90/10), shifted to higher temperature compared to that of neat PLA. The area of cold crystallization exotherm is quite similar to that of melting endotherm. This suggested that the PLA component in each sample after melt blending is almost in the amorphous state. The crystallinity ($\%X_c$) of the PLA and the blend samples was calculated and listed in Table 4.5. It was found that $\%X_c$ of PLA/NR and, PLA/HTNR blends was lower than neat PLA. This might be because the addition of NR in PLA may hinder the migration and diffusion of PLA molecular chains to the surface of the nucleus in the blends.

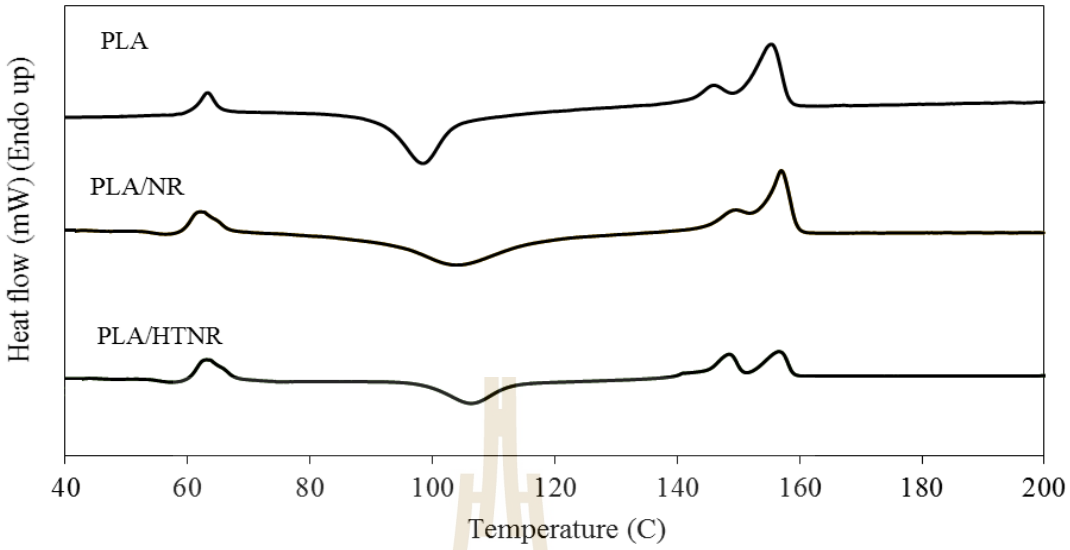

(a) Temperature range 40 – 200 ˚C

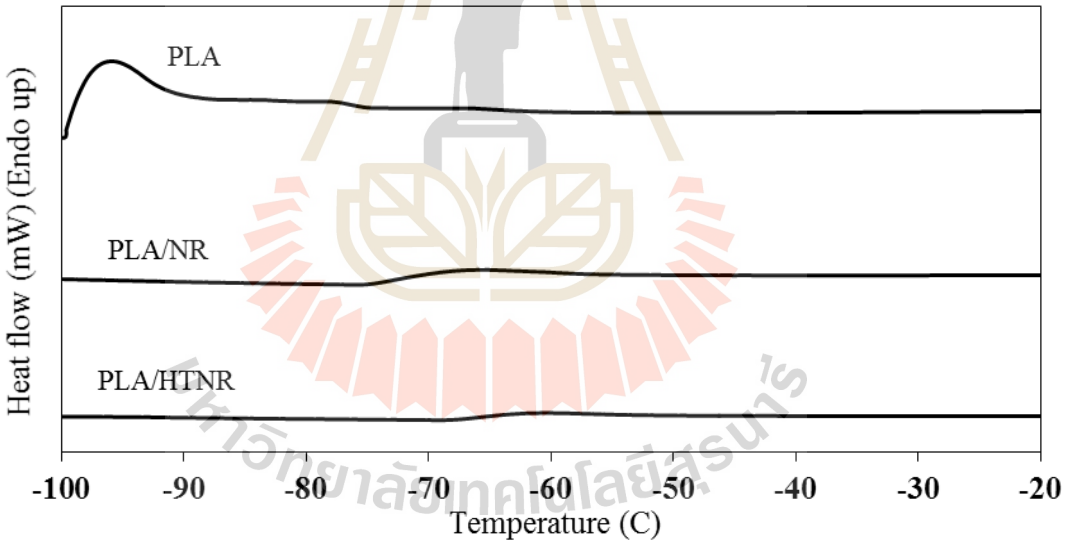

(b) Temperature range -100 – -20 ˚C

Figure 4.14 DSC thermograms of PLA, PLA/NR (90/10) and PLA/HTNR (90/10) blends (the first heating, heating rate 5 °C/min).

Table 4.5 DSC data from the first heating results of PLA, PLA/NR (90/10) and PLA/HTNR(90/10) blends.

sample	rubber phase	PLA phase						
	T_g (˚C)	T_g (˚C)	T_{cc} (˚C)	T_{m1} (˚C)	T_{m2} (˚C)	ΔH_c (J/g)	ΔH_m (J/g)	X_c (%)
Neat PLA	-	63.8	98.5	146.3	155.6	28.64	35.6	7.43
NR	-65.4	-	-	-	-	-	-	-
HTNR	-73.1	-	-	-	-	-	-	-
PLA/NR(90/10)	-69.4	63.8	104.6	150.9	157.5	25.39	28.58	3.40
PLA/HTNR(90/10)	-62.9	63.9	106.5	149.5	157.7	23.43	26.96	3.74

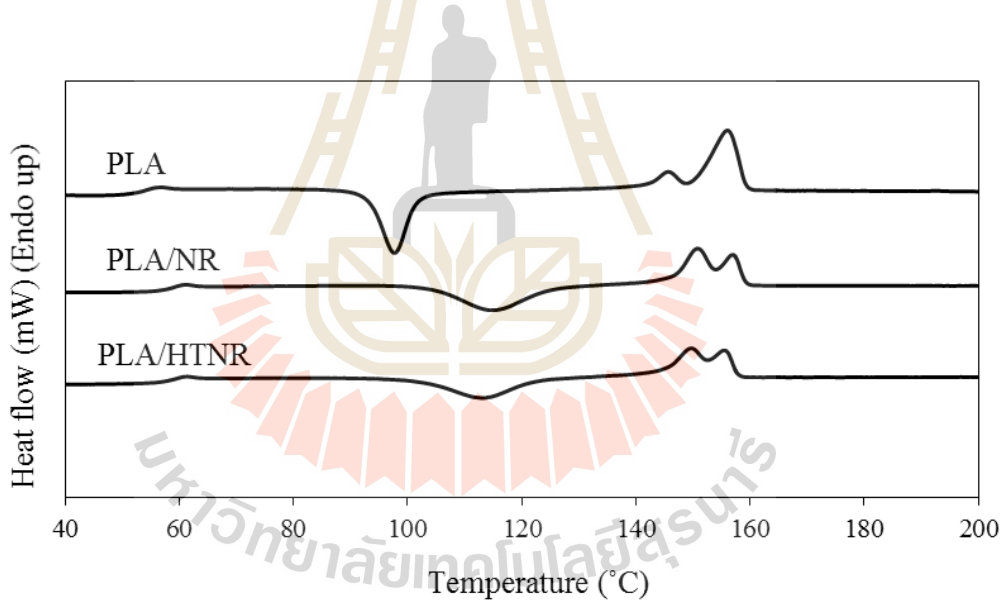

(a) Temperature range 40 – 200 ˚C

Figure 4.15 DSC thermograms of PLA , PLA/NR (90/10) and PLA/HTNR (90/10)) blends (the second heating, heating rate 5 °C/min).

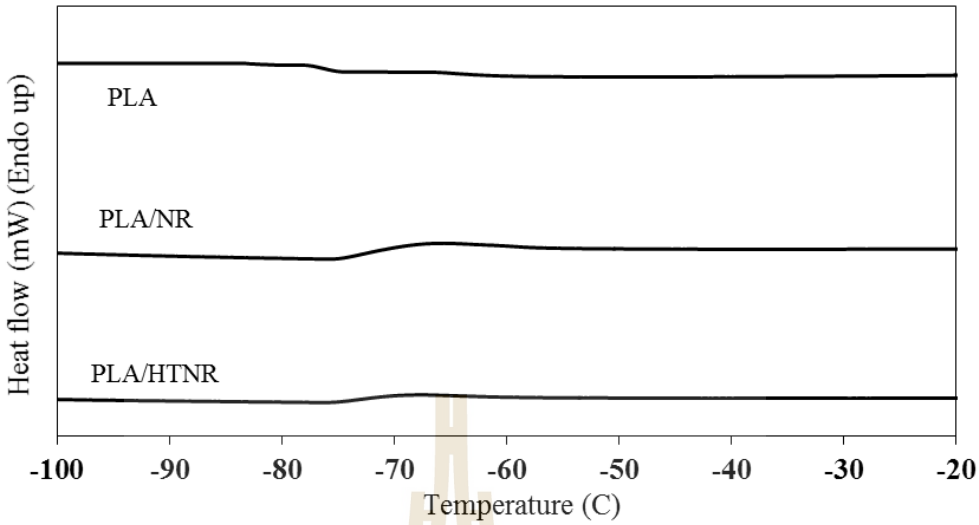

(b) Temperature range -100 – -20 ˚C

Figure 4.15 DSC thermograms of PLA , PLA/NR (90/10) and PLA/HTNR (90/10)) blends (the second heating, heating rate 5 °C/min) (continued).

Table 4.6 DSC data from the second heating results of PLA, PLA/NR(90/10) and PLA/HTNR(90/10) blends.

sample	rubber phase	PLA phase						
	T_g (˚C)	T_g (˚C)	T_{cc} (˚C)	T_{m1} (˚C)	T_{m2} (˚C)	ΔH_c (J/g)	ΔH_m (J/g)	X_c (%)
Neat PLA	-	54	97.5	146.3	155.6	28.64	35.6	7.43
NR	-65.8	-	-	-	-	-	-	-
HTNR	-76.4	-	-	-	-	-	-	-
PLA/NR	-69.4	59.8	118.2	151.2	157.9	23.93	27.08	3.33
PLA/HTNR	-62.9	59.7	116.5	150.5	158.3	22.91	26.36	3.69

The results of the second scan of DSC thermograms, PLA/NR and PLA/HTNR showed an increase of Tg of PLA matrix phase from 54.0°C to 59.8°C. HTNR and NR chains may hinder the movement of PLA chain during second heating. It was different from

expectation that the lower molecular weight HTNR will penetrate to PLA phase and lower Tg of PLA and resulted in an increase of elongation at break of PLA/HTNR blend. Therefore, the highest elongation at break of PLA/HTNR(90/10) blend could be resulted from the better interaction between HTNR and PLA comparing to NR and PLA as discussed earlier. The %Xc of PLA phase in PLA/HTNR(90/10) was higher than that of PLA/NR(90/10) but still lower than that of neat PLA. The Tcc of PLA phase in PLA/NR and PLA/HTNR were higher than that of neat PLA. This was because the addition of NR or HTNR into PLA may interrupted the movement of polymer chains and hinder diffusion of PLA molecular chains to the surface of the nucleus in the blends. This result suggested that NR and HTNR particles impeded the orderly arrangement of the PLA molecular chains. There were two Tm appeared in both PLA/NR and HTNR blends and they are not significantly different from those of PLA.

4.3 Characteristics of pre-PLA

The PLA prepolymers (pre-PLA) were synthesized in two steps from the direct condensation polymerization process. In the first step the lactic acid monomer was dehydrated at 130 ˚C to give an oligomer and then the oligomer was polymerized at 170 ˚C in the second step. After 24 h, another 0.1 vol% catalyst was added to continue condensation reaction and to obtain higher molecular weight of pre-PLA. The appearance of obtained pre-PLA is shown in Figure 4.16. The production yield of pre-PLA are tabulated in Table 4.7.

Figure 4.16 The photograph of pre-PLA product produced using condensation polymerization.

Table 4.7 Production yield of pre-PLA.

pre-PLA	Production yield (%)
PLA1	62.83 ± 5.15
PLA2	67.21 ± 6.37
PLA2	66.78 ± 7.18

4.3.1 Molecular weight of pre-PLA

The number average molecular weight ($\bar{M}_n$), weight average molecular weight ($\bar{M}_w$), and polydispersity index (PDI) of pre-PLA obtained from GPC technique are listed in Table 4.8.

Table 4.8 Molecular weight and polydispersity index of pre-PLA.

Pre-PLA	LA (ml)	1st step		2nd step		Molecular weight		
		$Sn(Oct)_2$ (v/v%)	Reaction time (h)	$Sn(Oct)_2$ (v/v%)	Reaction time (h)	$\bar{M}_n$	$\bar{M}_w$	PDI
PLA1	150	0.2	24	-	-	3,090	4,388	1.42
PLA2	150	0.2	24	0.1	18	6,542	10,982	1.68
PLA3	150	0.2	24	0.1	24	9,696	23,968	2.46

From the data shown in table 4.8, molecular weight and PDI of pre-PLA which produced via condensation polymerization were increased with increasing the amount of initiator and reaction time. The GPC chromatograms of PLA1, PLA2, and PLA3 was shown in Figure 4.17. GPC curve of pre-PLA became broader with an increase of molecular weight of pre-PLA.

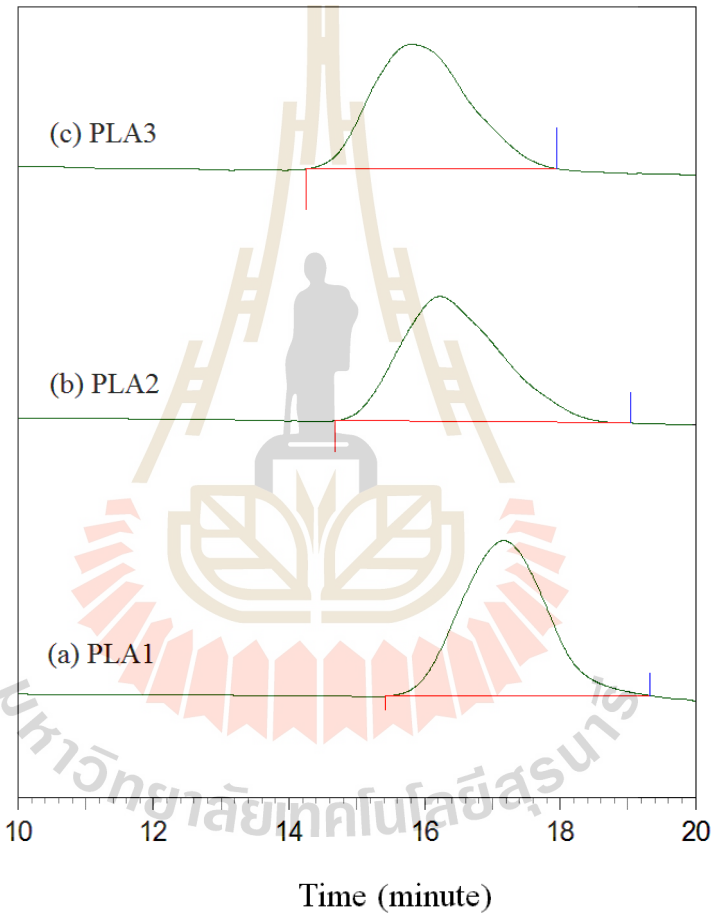

Figure 4.17 GPC chromatograms of PLA1 (a), PLA2 (b), and PLA3 (c).

4.3.2 Chemical structure of pre-PLA

The ^{1}H-NMR spectrum of the pre-PLA is shown in Figure 4.18 (a). The main characteristic peaks of pre-PLA was indicated at 5.2 ppm (H13) and 1.54 ppm (H14) which corresponded to methine proton (-C<u>H</u>(CH_3)-) and methyl proton (-C<u>H</u>$_3$) in repeating unit, respectively. The methyl proton (-C<u>H</u>$_3$) at the chain end was observed at 1.2 ppm (H17). The peak signals due to the methine proton (-CH) adjacent to the OH end group appeared at 4.35 ppm (H16). ^{13}C-NMR spectrum of pre-PLA is illustrated in Figure 4.18 (b). The characteristic peak of pre-PLA was noted at 16.83 ppm (C14) which were signal of methyl carbon, (-<u>C</u>H_3). The chemical shift at 69.20 ppm (C13) was signal of methane carbon adjacent to carbonyl group (-O<u>C</u>H(CO)-) and the peak signal at 169.50 ppm (C15) was corresponding to carbonyl carbon (-<u>C</u>=O).

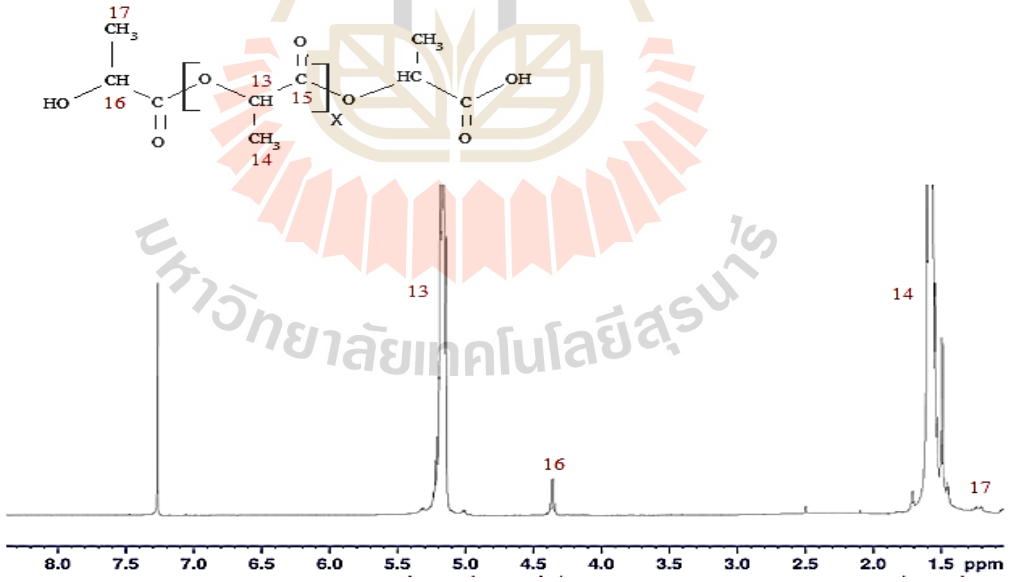

(a) ^{1}H-NMR of PLA1

Figure 4.18 NMR spectra of ^{1}H-NMR of pre-PLA (a) and ^{13}C-NMR of pre-PLA (b).

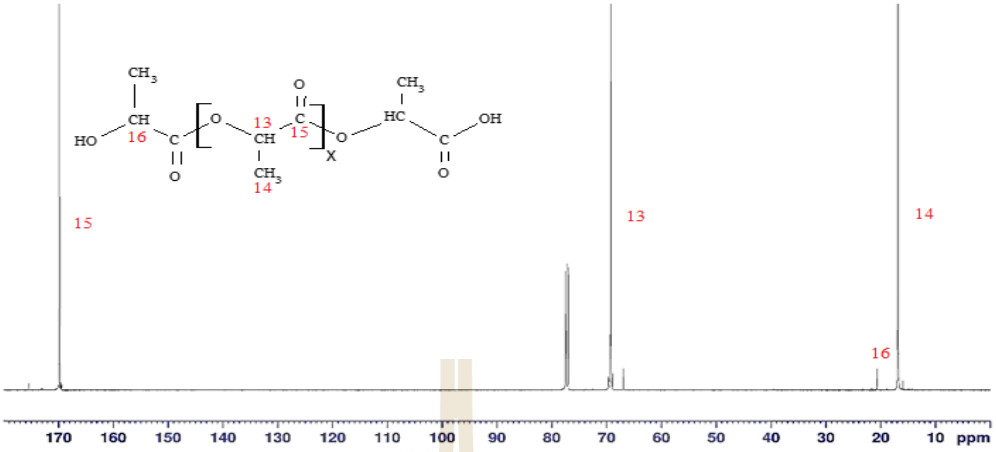

(b) ^{13}C-NMR of PLA1

Figure 4.18 NMR spectra of ^{1}H-NMR of pre-PLA (a) and ^{13}C-NMR of pre-PLA (b). (Continued.)

The FT-IR spectrum of pre-PLA is shown in Figure 4.19. The peaks at 2997 and 2929 cm^{-1} are assigned to the -CH stretching region. The peak at 1,750 cm^{-1} was corresponding to C=O stretching region. The peak at 1,456 cm^{-1} was corresponding to CH_3. The C-O-C asymmetric mode appears at 1,090 cm^{-1}.

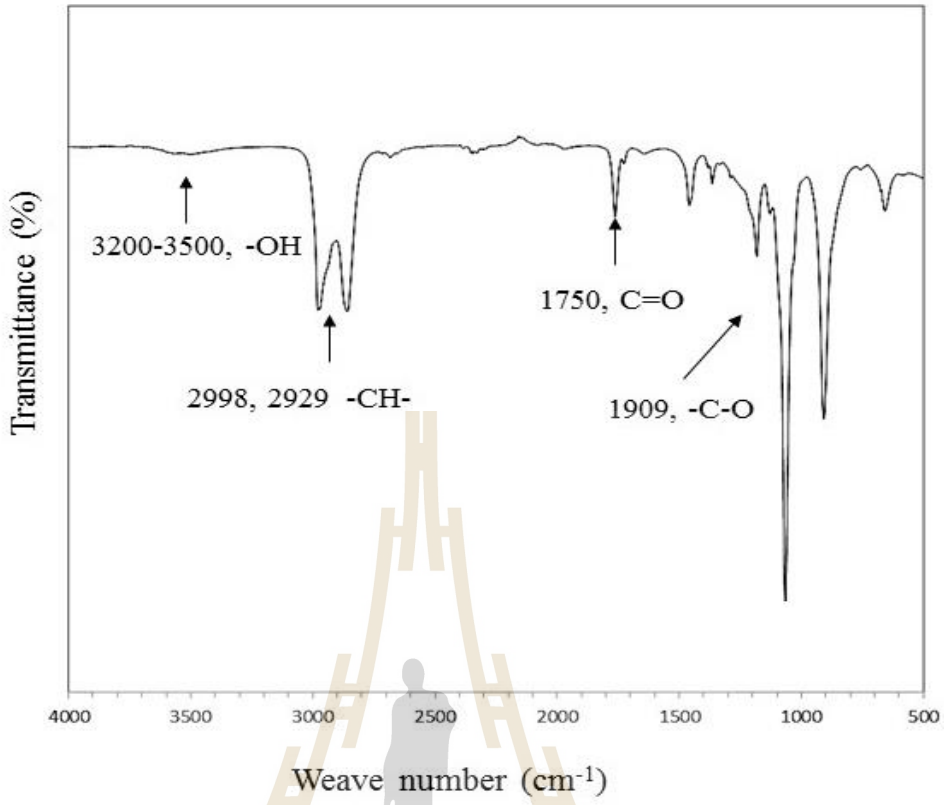

Figure 4.19 FT-IR spectrum of PLA1.

4.4 Characteristics of PLA-NR-PLA triblock copolymers

4.4.1 Molecular weight of PLA-NR-PLA triblock copolymers

PLA-NR-PLA triblock copolymers were synthesized via condensation polymerization of HTNR ($\bar{M}_n$= 28,000 g/mol) and three different molecular weights of pre-PLA that were PLA1 ($\bar{M}_n$= 3,090 g/mol), PLA2 ($\bar{M}_n$= 6,542 g/mol), and PLA3 ($\bar{M}_n$= 9,696 g/mol). The molar ratio of pre-PLA and HTNR was 2:1. The obtained block copolymers exhibited soft but not sticky character, yellow color, and hardly soluble in chloroform. The molecular weight of PLA-NA-PLA triblock copolymers were determined using GPC. Figure 4.20 showed GPC chromatograms of pre-PLA, HTNR, and PLA-NA-PLA triblock copolymers, respectively. It was found that the obtained

block copolymer after purified by dissolving in CH_2Cl_2 and precipitating in an excess distilled ethanol showed a single broader peak. Polydispersity index of PLA-NA-PLA triblock copolymers were increased with an increase of molecular weight of triblock copolymer.

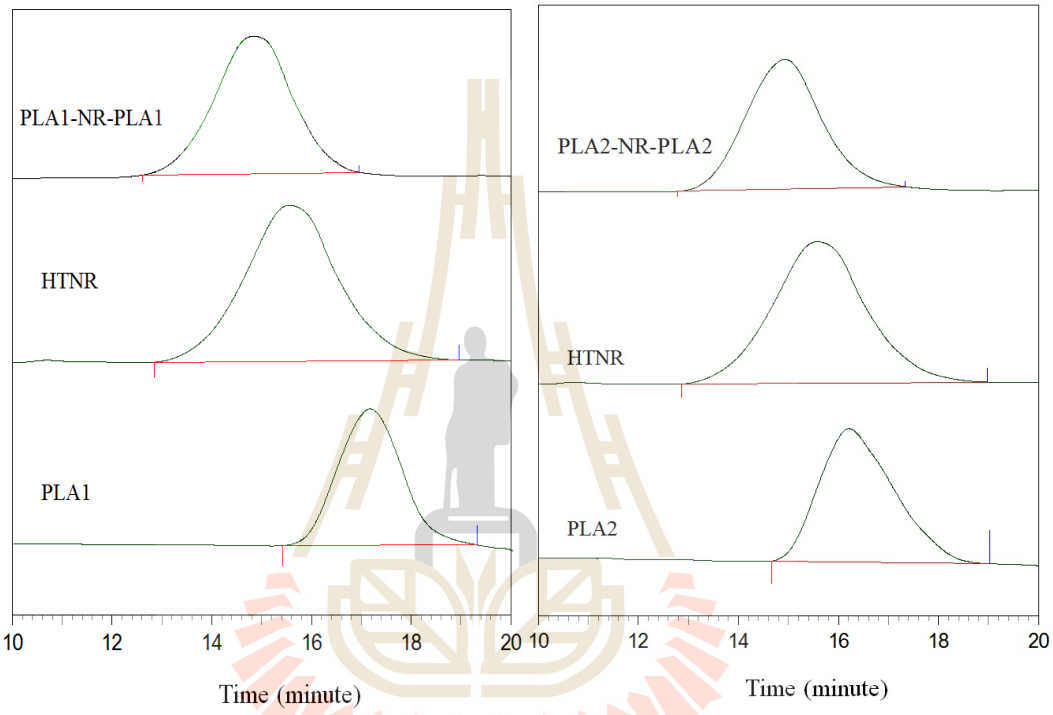

(a) PLA1-NR-PLA1 (b) PLA2-NR-PLA2

Figure 4.20 GPC chromatograms of PLA1-NR-PLA1 (a), PLA2-NR-PLA2 (b), and PLA3-NR-PLA3 (c).

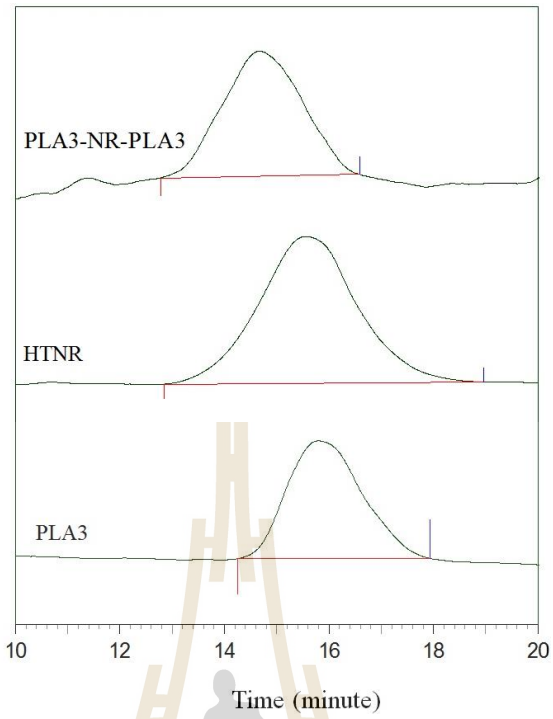

(c) PLA3-NR-PLA3

Figure 4.20 GPC chromatograms of PLA1-NR-PLA1 (a), PLA2-NR-PLA2 (b), and PLA3-NR-PLA3 (c). (Contined)

The molecular weights of the HTNR, pre-PLA and PLA-NR-PLA triblock copolymers are listed in Table 4.9. It was found that $\bar{M}_n$ of triblock copolymer from GPC technique are in good agreement with the prediction from $\bar{M}_n$ of pre-PLA and HTNR with a molar ratio of 2:1 ($\bar{M}_{ncal}$).

Table 4.9 Molecular weight and PDI of HTNR, pre-PLA, and PLA- NR-PLA triblock copolymers.

Samples	Molecular weight			Polydispersity index (PDI)
	$\bar{M}_n$ (g/mol)	$\bar{M}_{ncal}$ (g/mol)	$\bar{M}_w$ (g/mol)	
HTNR	28,003	-	98,030	3.5
PLA1	3,091	-	4,388	1.42
PLA2	6,542	-	10,982	1.68
PLA3	9,696	-	23,968	2.47
PLA1-NR-PLA1	34,681	34,180	62,476	1.8
PLA2-NR-PLA2	41,214	41,087	95,204	2.31
PLA3-NR-PLA3	48,487	47,392	116,097	2.39

4.4.2 Chemical structure of triblock copolymers

The ^{1}H-NMR spectrum of the pre-PLA, HTNR, and PLA1-NR-PLA1 are compared in Figure 4.21. The main characteristic peaks of the PLA end-block were indicated at 5.12 ppm (H13) and 1.54 ppm (H14) which corresponded to methine proton (-C<u>H</u>(CH_3)-) and methyl proton (-C<u>H</u>$_3$), respectively. The characteristic peaks of NR in PLA-NR-PLA were observed at 2.04 ppm (H1, H4) and 1.68 ppm (H5) which belonged to methylene proton (-C<u>H</u>$_2$-) and methyl proton (-C<u>H</u>$_3$) of HTNR. The peaks at 3.2 ppm and 3.4 ppm which belonged to methylene proton (OH-CH_2-) adjacent to hydroxyl groups of HTNR were disappeared as expected. This was because of the condensation reaction between hydroxyl group of HTNR and carboxyl group of pre-PLA leading to ester linkage in block copolymer. The occurrence of two new ester linkages was

confirmed by the observation of the peak at 4.1 ppm (H18) (chumeka *et al.*, 2015) and 3.8 ppm (H19) which corresponding to methylene proton of ester group (-$COOCH_2$-). ^{13}C-NMR spectrum of pre-PLA, HTNR, and PLA1-NR-PLA1 as illustrated in Figure 4.22 showed chemical shift of methine carbon (=$\underline{C}$H-) of HTNR at 125 ppm (C3). The peak at 135 ppm (C2) belonged to saturated carbon connected to methyl group (-$\underline{C}(CH_3)$=). The characteristic peak of pre-PLA in block copolymer was noted at 169.5 ppm (C15) and 16.8 ppm (C14) which were signal of carbonyl carbon (-$\underline{C}$=O), and methyl carbon (-$\underline{C}H_3$), respectively. The chemical shift at 69.2 ppm (C18) and 68 ppm (C19) belonged to ester link between HTNR and pre-PLA. The disappearances of chemical shift of hydroxyl group in pre-PLA at 60 ppm (C12) and 62 ppm (C11) confirmed the condensation reaction between the OH group of the HTNR and the COOH group of the pre-PLA leading to a new ester linkage in PLA-NR-PLA triblock copolymer.

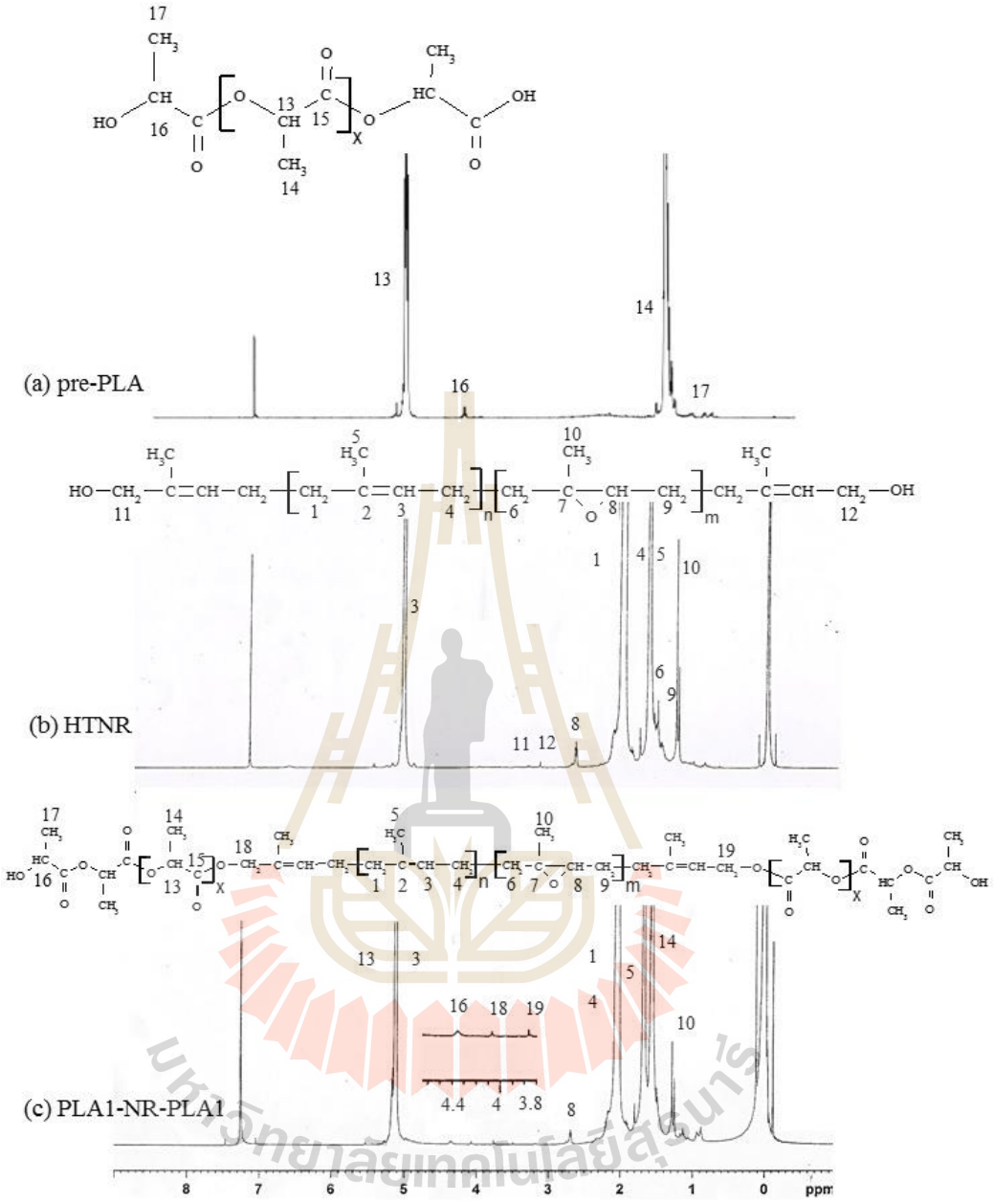

Figure 4.21 ^{1}H-NMR spectra of pre-PLA, HTNR, and PLA1-NR-PLA1.

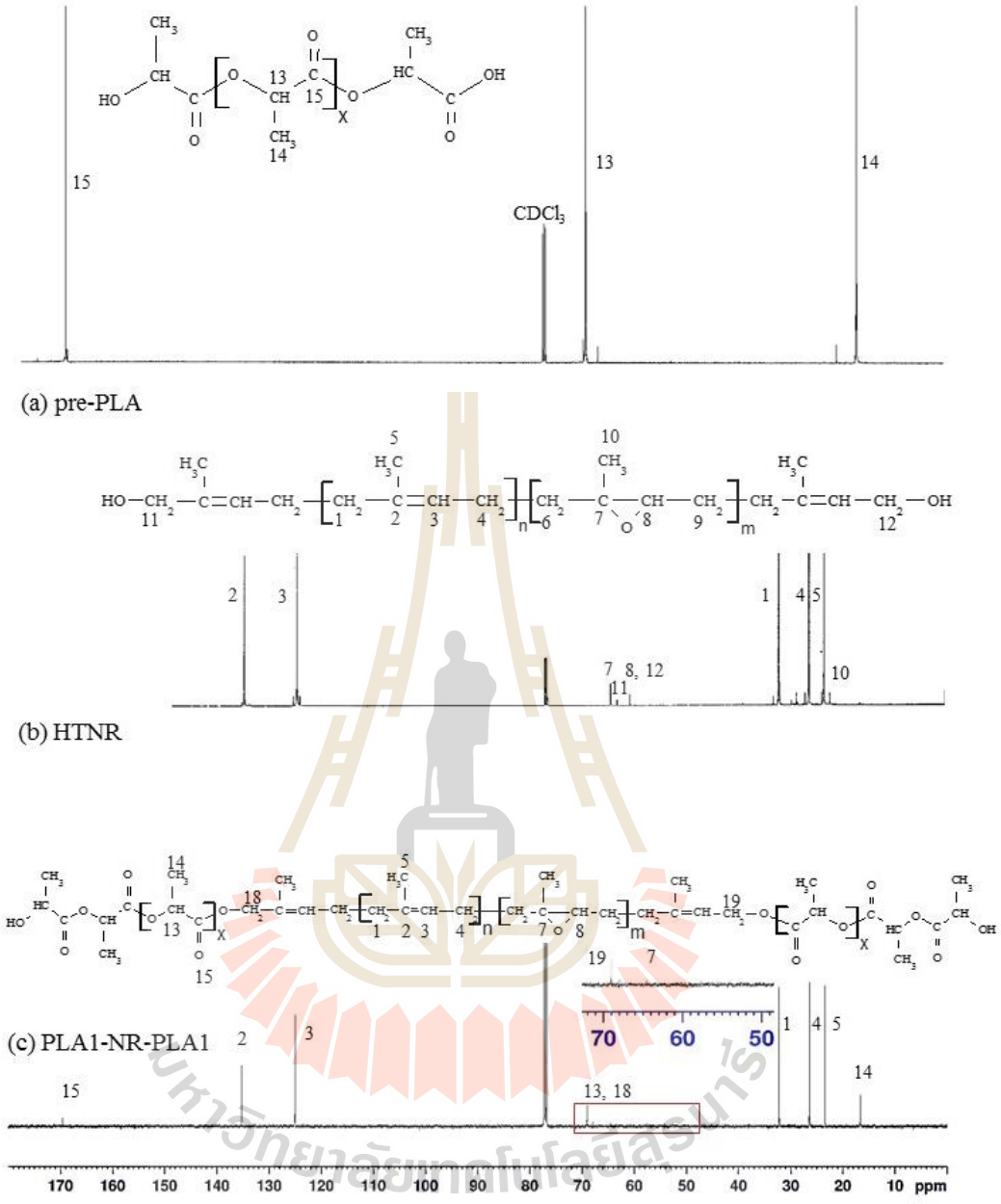

Figure 4.22 ^{13}C-NMR spectra of pre-PLA, HTNR, and PLA1-NR-PLA1.

The FTIR spectra of pre-PLA, HTNR and triblock copolymers are shown in Figure 4.23. The peak at 1750 cm^{-1} was corresponding to -C=O stretching region. The peak at 2998 cm^{-1} was assigned to the -CH stretching region. The region between 1457 cm^{-1} and 1090 cm^{-1} was corresponding to CH_3 band and C-O-C, respectively. FTIR spectrum of HTNR (Figure 4.21 (b)) showed asymmetric =CH stretching at 3030 cm^{-1}. The peak at 2965 cm^{-1} was corresponding to symmetric CH_3 stretching. The peak at 1664 cm^{-1} corresponded to C=C stretching. The peak of -OH group in HTNR was disappeared in FT-IR spectrum of PLA1-NR-PLA1 block copolymer due to ester linkage between OH group of HTNR and COOH group of PLA in PLA1-NR-PLA1 block copolymer.

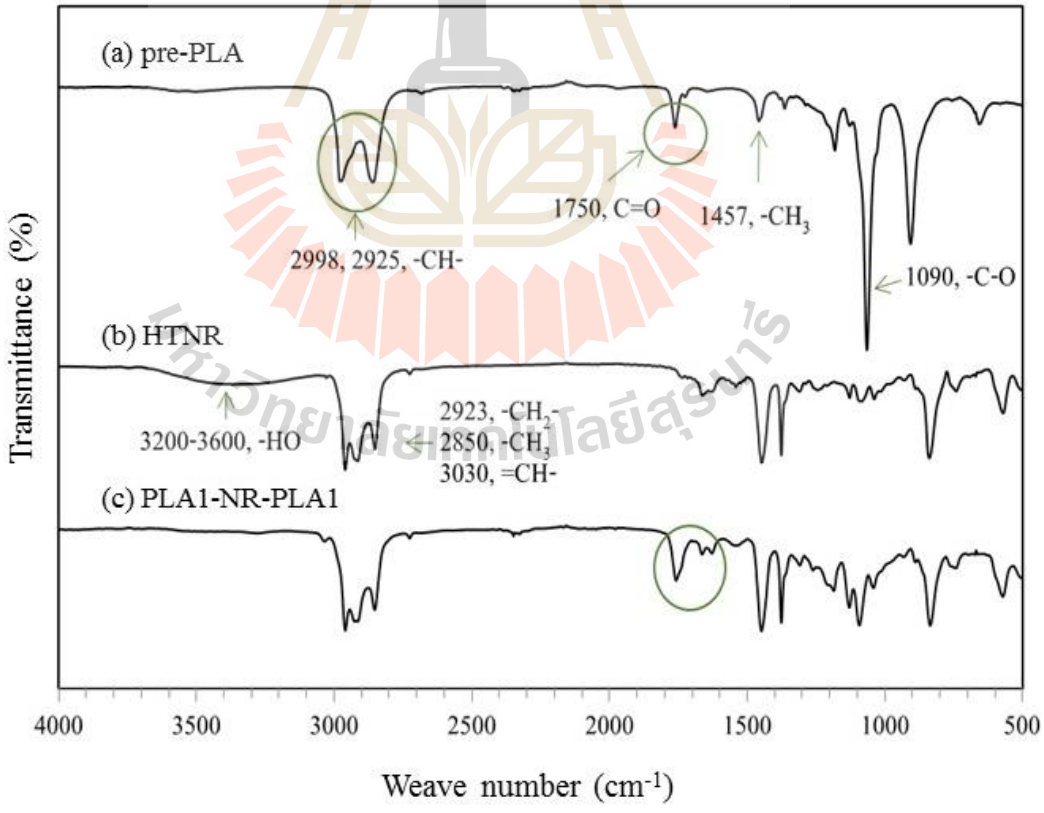

Figure 4.23 FT-IR spectrum of PLA1 (a), HTNR (b), and PLA1-NR-PLA1 (c).

The ^{1}H-NMR spectrum and ^{13}C-NMR spectrum of the PLA1-NR-PLA1, PLA2-NR-PLA2, and PLA3-NR-PLA3 are shown in Figure 4.24 and Figure 4.25, respectively. The spectrum of PLA1-NR-PLA1, PLA2-NR-PLA2, and PLA3-NR-PLA3 are similar in the chemical shifts of the protons and carbons which are in the same ranges, but some peak signals of PLA2-NR-PLA2 and PLA3-NR-PLA3 in ^{13}C-NMR did not clearly appear as PLA1-NR-PLA1 due to higher molecular weight of PLA2-NR-PLA2 and PLA3-NR-PLA3.

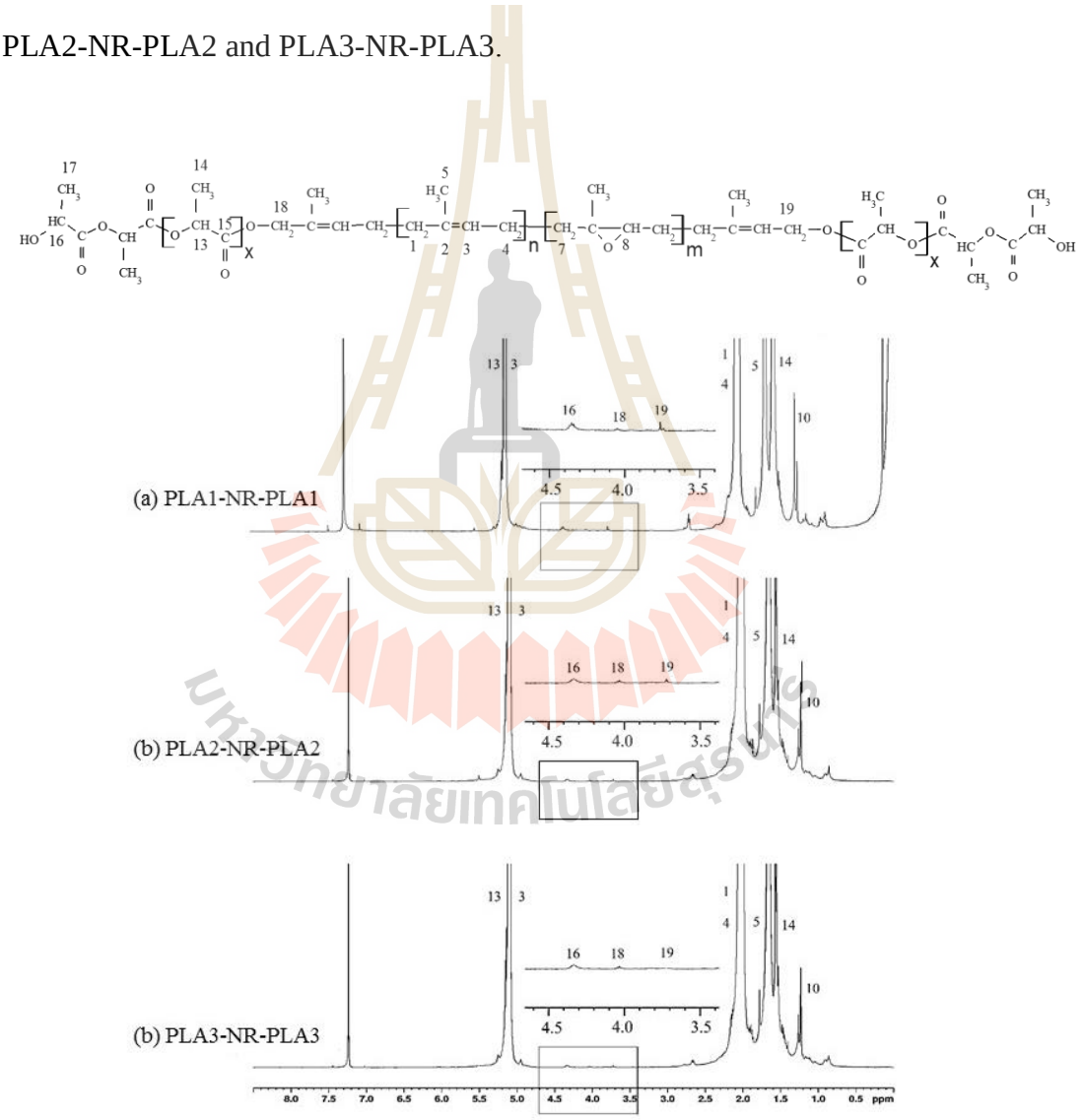

Figure 4.24 ^{1}H-NMR spectra of PLA1-NR-PLA1 (a), PLA2-NR-PLA2 (b), and PLA3-NR-PLA3(c).

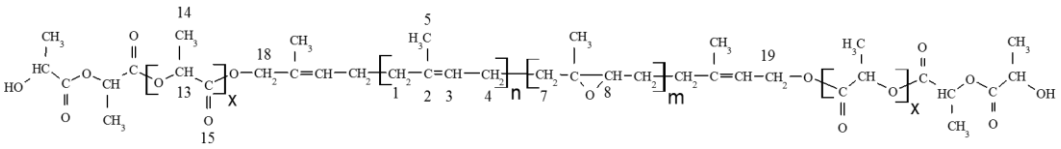

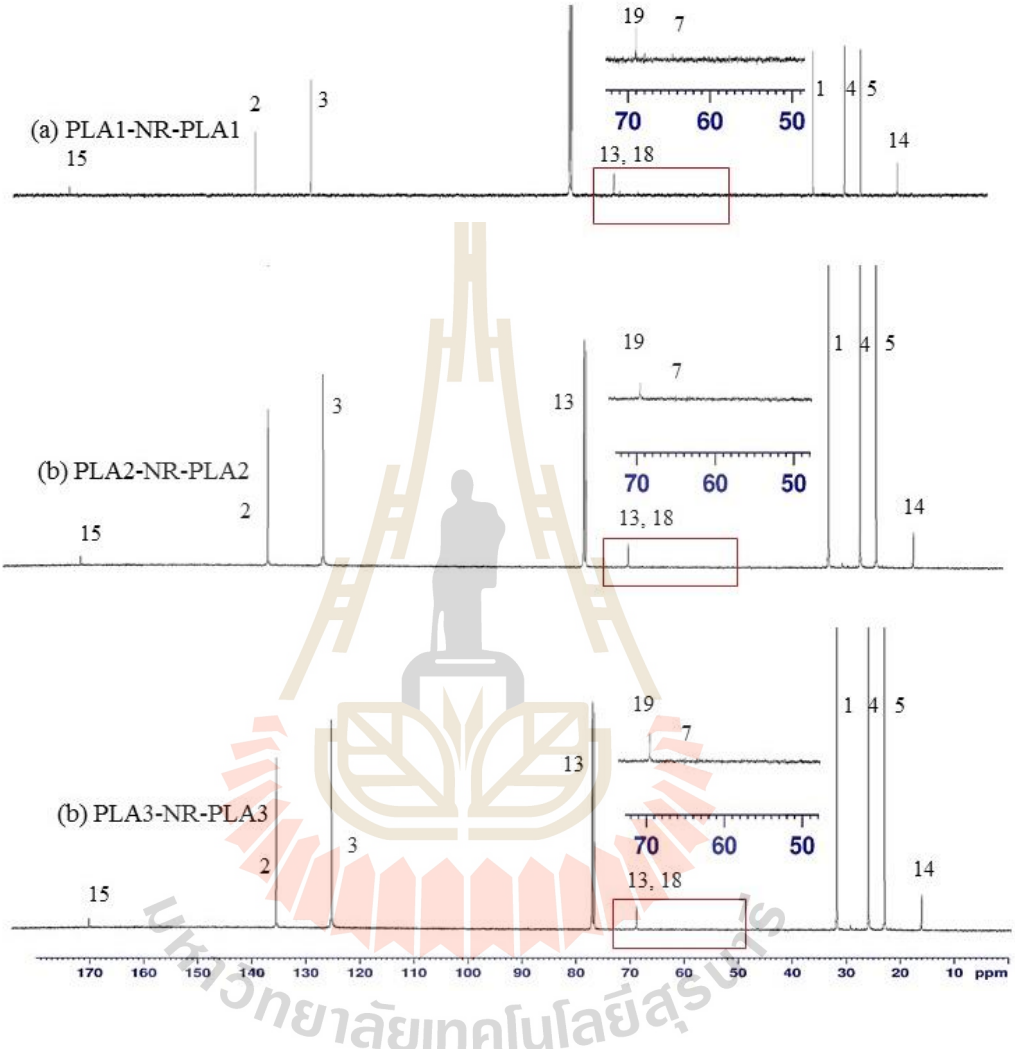

Figure 4.25 ^{13}C-NMR spectra of PLA1-NR-PLA1 (a), PLA2-NR-PLA2 (b), and PLA3-NR-PLA3(c).

4.5 Mechanical and morphological and thermal properties of PLA/PLA-NR-PLA triblock copolymer blends

4.5.1 Mechanical properties of PLA/PLA-NR-PLA blends

PLA-NR-PLA triblock copolymers that were prepared from pre-PLA and HTNR ($\bar{M}_n$ = 28000 g/mol with hydroxyl functionality of 1.77 ± 0.21) were further used to study the efficiency as impact modifier for PLA. The amount of triblock copolymer in the blends was kept at 10 %wt. according to the optimum mechanical properties of PLA/HTNR blends (Section 4.2) was found for PLA/HTNR(90/10). In addition, to study the effect of actual rubber content, the amount of triblock copolymer used for blending with PLA was adjusted to give 10 %wt. rubber content. The blends containing 10 %wt. rubber were denoted by adding R-10 into their names. The obtain results were discussed as following.

4.5.1.1 Tensile properties of PLA/PLA-NR-PLA triblock copolymer blends

The tensile stress-strain curves of neat PLA, PLA/NR, PLA/HTNR, and PLA/PLA-NR-PLA blends are plotted in Figure 4.26. Tensile strength, tensile modulus and elongation at break of all PLA/PLA-NR-PLA blends were increased with an increase of the length of PLA end block. This might be because the higher molecular weight of PLA (3000, 6000, and 9000 g/mol), a hard segment in triblock copolymer provided an increase in tensile strength and tensile modulus. The elongation at break of PLA/PLA-NR-PLA blends was also increased with increasing molecular weight of PLA end block. This was because longer chain length of PLA end block provided more entanglement with PLA matrix. Therefore, PLA-NR-PLA with a higher molecular weight of PLA end block should be more compatible with PLA.

Comparing to PLA/HTNR blend, the elongation at break of PLA/PLA-NR-PLA blends containing 10 %wt. of triblock copolymers was lower than that of PLA/HTNR blend. This could be because the actual rubber content in PLA/PLA1-NR-PLA1, PLA/PLA2-NR-PLA2, and PLA/PLA3-NR-PLA3 blends was 8.07 %wt., 6.79 %wt., and 5.78 %wt. respectively. However, tensile strength and tensile modulus of PLA/PLA-NR-PLA blends was higher than those of PLA/HTNR blend.

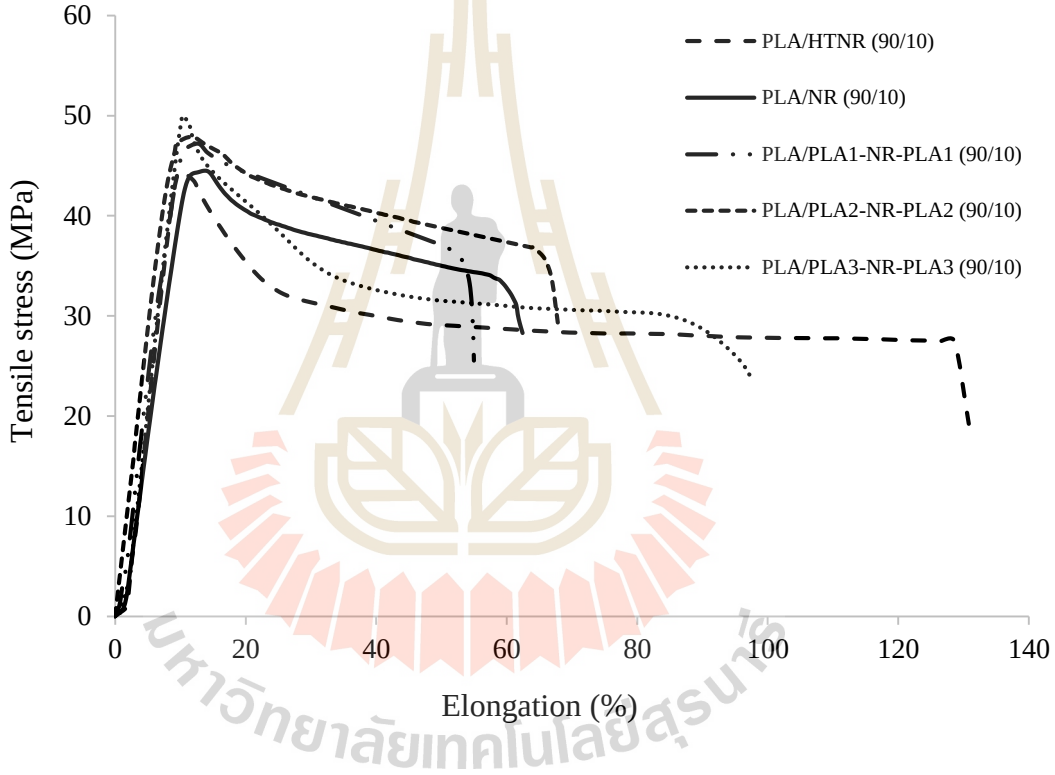

Figure 4.26 Stress-strain curves of PLA/HTNR, and PLA/PLA-NR-PLA blends at 10 %wt. rubber.

The tensile stress-strain curves of PLA/NR, PLA/HTNR, and PLA/PLA-NR-PLA blends that contained 10 %wt. of rubber are plotted in Figure 4.27. When the rubber content in PLA/triblock copolymer blends was adjusted to actual 10 %wt., the

elongation at break of PLA/PLA-NR-PLA blends was significantly increase whereas tensile modulus and tensile strength tended to decrease.

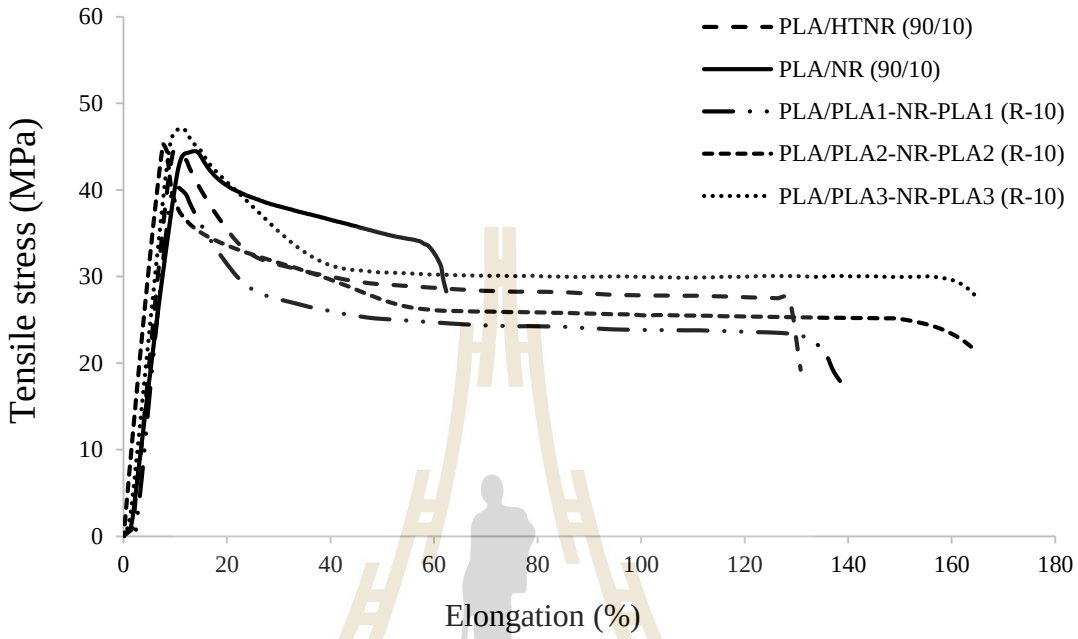

Figure 4.27 Stress-strain curves of PLA/PLA-NR-PLA(R-10), PLA/HTNR (90/10), and PLA/NR (90/10) blends.

The mechanical properties of all blends were also listed in Table 4.10.

Table 4.10 Tensile strength, modulus, elongation at break and impact strength of the blends.

Samples	Impact strength (kJ/m^2)	Tensile strength (MPa)	Modulus (GPa)	Elongation at Break (%)
neat PLA	18.41 ± 1.49	61.47 ± 3.69	0.68 ± 0.03	12.91 ± 1.00
PLA/NR(90/10)	65.35 ± 2.85	42.60 ± 0.64	0.55 ± 0.02	60.54 ± 13.00
PLA/HTNR (90/10)	67.78 ± 12.10	44.46 ± 1.08	0.54 ± 0.02	127.23 ± 6.00
PLA/PLA1-NR-PLA1 (90/10)	48.98 ± 4.22	46.79 ± 2.23	0.58 ± 0.02	50.23 ± 12.25
PLA/PLA1-NR-PLA1 (R-10)	59.91 ± 7.88	40.31 ± 4.03	0.50 ± 0.04	130.43 ± 13.25
PLA/PLA2-NR-PLA2 (90/10)	50.53 ± 6.46	47.30 ± 2.49	0.60 ± 0.03	67.23 ± 8.13
PLA/PLA2-NR-PLA2 (R-10)	64.32 ± 6.75	44.58 ± 4.11	0.53 ± 0.05	147.23 ± 20.06
PLA/PLA3-NR-PLA3 (90/10)	54.31 ± 3.87	49.88 ± 3.42	0.61 ± 0.04	75.90 ± 9.94
PLA/PLA3-NR-PLA3 (R-10)	70.35 ± 5.18	46.88 ± 2.48	0.54 ± 0.02	159.23 ± 16.78

4.5.1.2 Impact properties of PLA/PLA-NR-PLA triblock copolymer blends

Figure 4.28 shows the impact strength of PLA, PLA/NR, PLA/HTNR and PLA/PLA-NR-PLA blends. Impact strength of the blends was higher than that of neat PLA. This was because NR, HTNR, and PLA-NR-PLA phase absorbed and dissipated the crack energy produced and prevented the abrupt breaking of the specimen. For the blend containing 10%wt. of impact modifier, the maximum impact strength was found to be PLA/HTNR> PLA/NR> PLA/PLA3-NR-PLA3> PLA/PLA2-NR-PLA2> PLA/PLA1-NR-PLA1, respectively. The impact strength of 54.31 ± 3.87, 50.53 ± 6.46, and 48.98 ± 4.22 kJ/m^2 was found for PLA/PLA3-NR-PLA3, PLA/PLA2-NR-PLA2, and PLA/PLA1-NR-PLA, respectively. However, an impact strength of

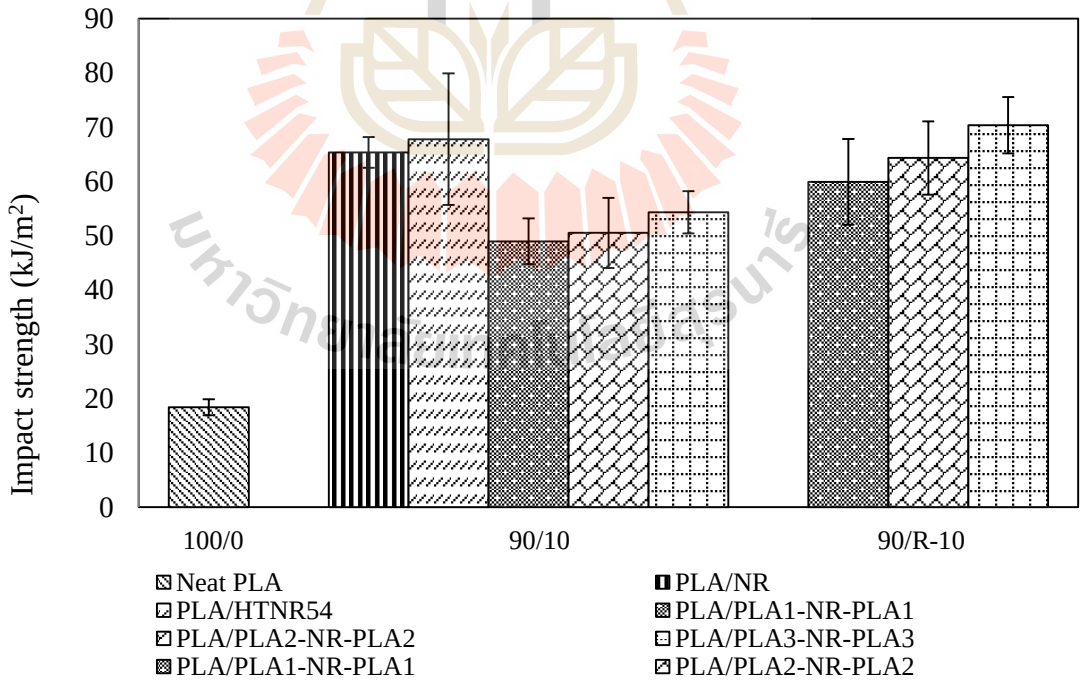

Figure 4.28 Impact strength of PLA, PLA/NR, PLA/HTNR, and PLA/PLA-NR-PLA blends with difference rubber content.

both of PLA/PLA3-NR-PLA3, PLA/PLA2-NR-PLA2, and PLA/PLA1-NR-PLA1 was lower than PLA/NR and PLA/HTNR blend. This was because the actual rubber content in PLA/PLA1-NR-PLA1, PLA/PLA2-NR-PLA2 and PLA/PLA3-NR-PLA3 blends was 8.07 %wt., 6.79 %wt. and 5.78 %wt. respectively. As an actual rubber content was 10 %wt., the impact strength of all PLA/PLA-NR-PLA blends was improved and increased with increasing PLA chain length. However, only PLA/PLA3-NR-PLA3(R-10) seem to show higher impact strength than PLA/HTNR and PLA/NR blend. The longer chain of PLA in PLA3-NR-PLA3 could lead to higher entanglement with PLA matrix.

4.5.2 Morphological properties of PLA/PLA-NR-PLA blend

SEM micrographs of freeze-fractured surfaces of PLA, PLA/HTNR and PLA/PLA-NR-PLA blends are shown in Figure 4.29 and Figure 4.30, respectively.

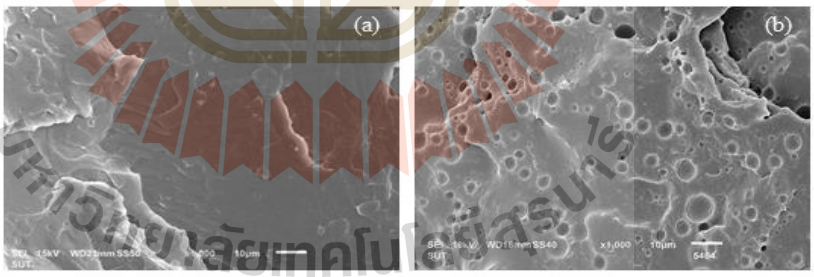

Figure 4.29 SEM micrographs of freeze-fractured surface of PLA (a) (x1000), PLA/NR (b) (1000x), PLA/HTNR (c) (1000x), PLA/PLA1-NR-PLA1 (d-1) (1000x), PLA/PLA1-NR-PLA1 (d-2) (3000x), PLA/PLA2-NR-PLA2 (e-1) (1000x) and PLA/PLA2-NR-PLA2 (e-2) (3000x) PLA/PLA3-NR-PLA3 (f-1) (1000x) and PLA/PLA3-NR-PLA3 (f-2) (3000x).

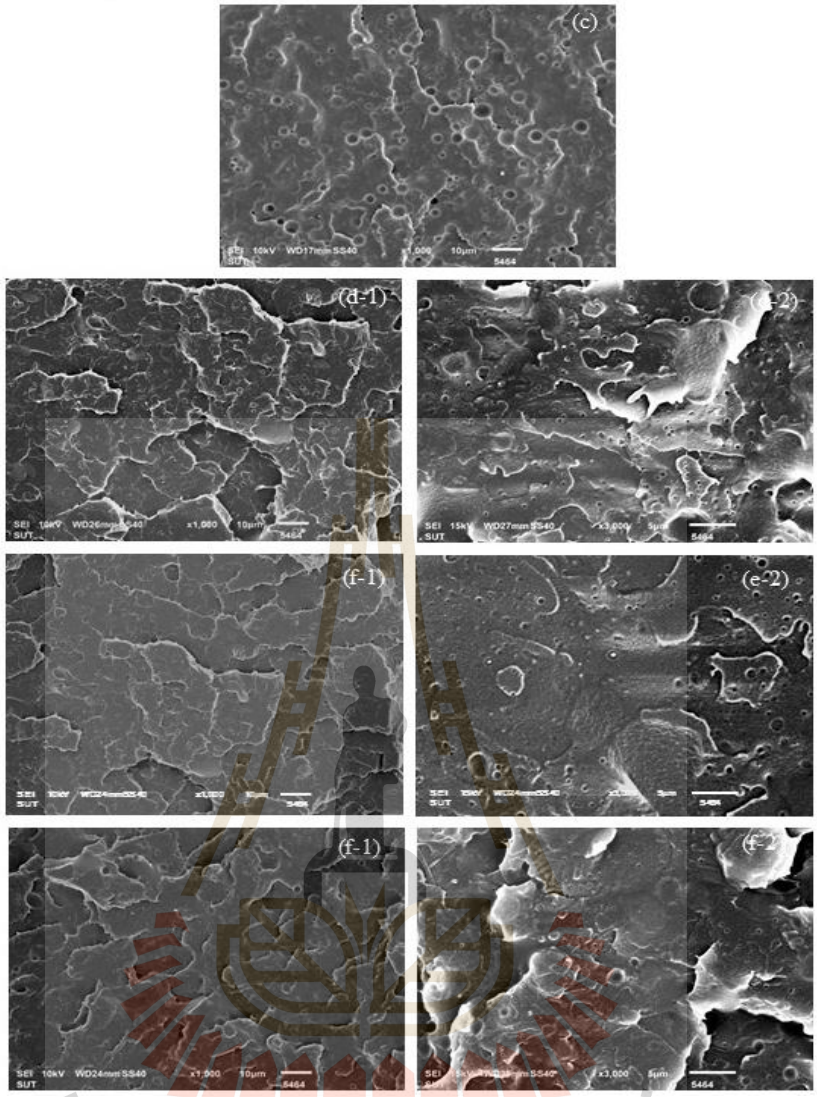

Figure 4.29 SEM micrographs of freeze-fractured surface of PLA (a) (x1000), PLA/NR (b) (1000x), PLA/HTNR (c) (1000x), PLA/PLA1-NR-PLA1 (d-1) (1000x), PLA/PLA1-NR-PLA1 (d-2) (3000x), PLA/PLA2-NR-PLA2 (e-1) (1000x) and PLA/PLA2-NR-PLA2 (e-2) (3000x) PLA/PLA3-NR-PLA3 (f-1) (1000x) and PLA/PLA3-NR-PLA3 (f-2) (3000x). (Continued)

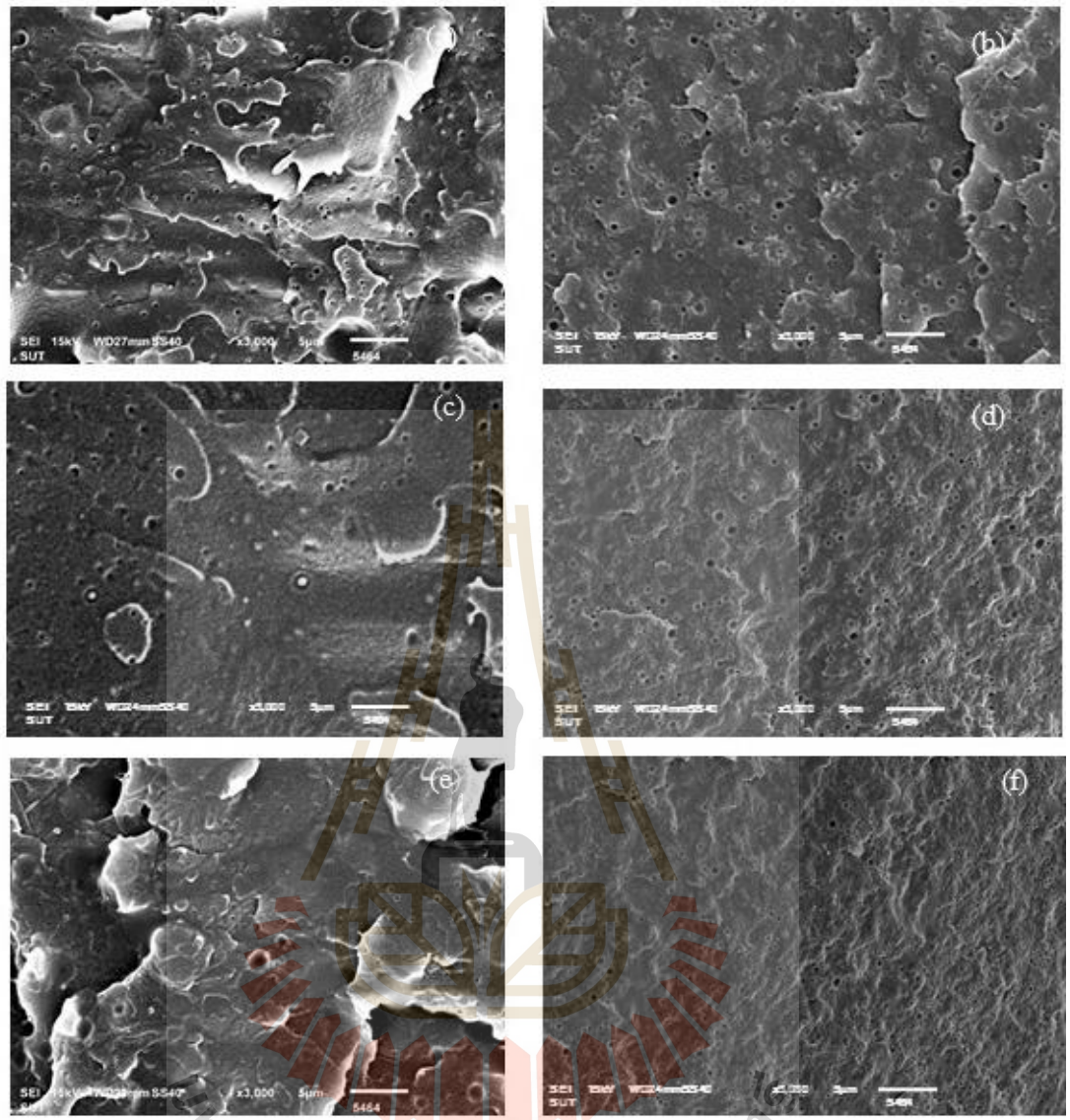

Figure 4.30 SEM micrographs of freeze-fractured surface of PLA/PLA1-NR-PLA1(90/10) (a) ,PLA/PLA1-NR-PLA1 (R-10) (b), PLA/PLA2-NR-PLA2 (90/10) (c) and PLA/PLA2-NR-PLA2 (R-10) (d) PLA/PLA3-NR-PLA3 (90/10) (e) and PLA/PLA3-NR-PLA3 (R-10) (f) (3000x).

The average particle diameter of HTNR particles in the blends are shown in Table 4.11. The blends showed well dispersion of rubbery particles in PLA matrix. For the blend containing 10 %wt. of impact modifier, the size of HTNR, PLA1-NR-

PLA1, PLA2-NR-PLA2 and PLA3-NR-PLA3 particles in the blends was 0.92 µm, 0.34 µm, 0.29 µm and 0.22 µm, respectively. This could be attributed to more compatibility between PLA matrix and triblock copolymer. However, the blend which lowest disperse particle size did not showed the highest impact strength. This might be because the lack of amount of rubber to absorb or dissipate the crack energy produced. As shown in SEM micrographs of PLA/PLA-NR-PLA blends (Figure 4.29). For PLA/triblock copolymer blends with actual rubber content of 10 %wt., rubber particle size in the blend was increased but still lower than HTNR and NR particles in PLA/HTNR and PLA/NR blend, respectively.

Table 4.11 The average diameters of rubber particle in PLA blends.

Samples	Number average particle diameter (µm)	Minimum particle diameter (µm)	Maximum particle diameter (µm)
PLA/NR (90/10)	2.02 ± 0.68	0.45	4.25
PLA/HTNR (90/10)	0.92 ± 0.71	0.3	3.4
PLA/PLA1-NR-PLA1 (90/10)	0.34 ± 0.03	0.11	0.7
PLA/PLA1-NR-PLA1 (R-10)	0.46 ± 0.03	0.1	0.85
PLA/PLA2-NR-PLA2 (90/10)	0.29 ± 0.05	0.11	0.7
PLA/PLA2-NR-PLA2 (R-10)	0.31 ± 0.09	0.2	0.85
PLA/PLA3-NR-PLA3(90/10)	0.25 ± 0.06	0.11	0.31
PLA/PLA3-NR-PLA3(R-10)	0.29 ± 0.06	0.15	0.3

4.5.3 Thermal properties of PLA/PLA-NR-PLA blends

Figure 4.31 and Figure 4.32 shows DSC thermograms of PLA1, PLA2, PLA3, HTNR and triblock copolymers. The thermal transitions and related data are summarized in Table 4.12. DSC thermogram of PLA-NR-PLA triblock copolymer exhibited two values of Tg, the first T_{g1} was at lower temperature and the second one at higher temperature, according to the HTNR and PLA segments, respectively. The Tg of PLA segments from second heating scan was slightly lower than that from first heating scan. The thermal degradation of low molecular weight PLA may occur. T_{g2} of the PLA-NR-PLA increased with an increase of molecular weight of pre-PLA. The molecular weight of PLA1, PLA2, and PLA3 were 3,090, 6,542, and 9,696 g/mol, respectively. PLA-NR-PLA triblock copolymers showed only one T_m in the first heating scan and exhibited crystallization behavior. %Xc of PLA phase in triblock copolymer also increased with an increase of PLA chain length. However, cold crystallization temperature (Tcc) was not found. This might be because NR in middle block of copolymer interrupt the cold crystallization process.

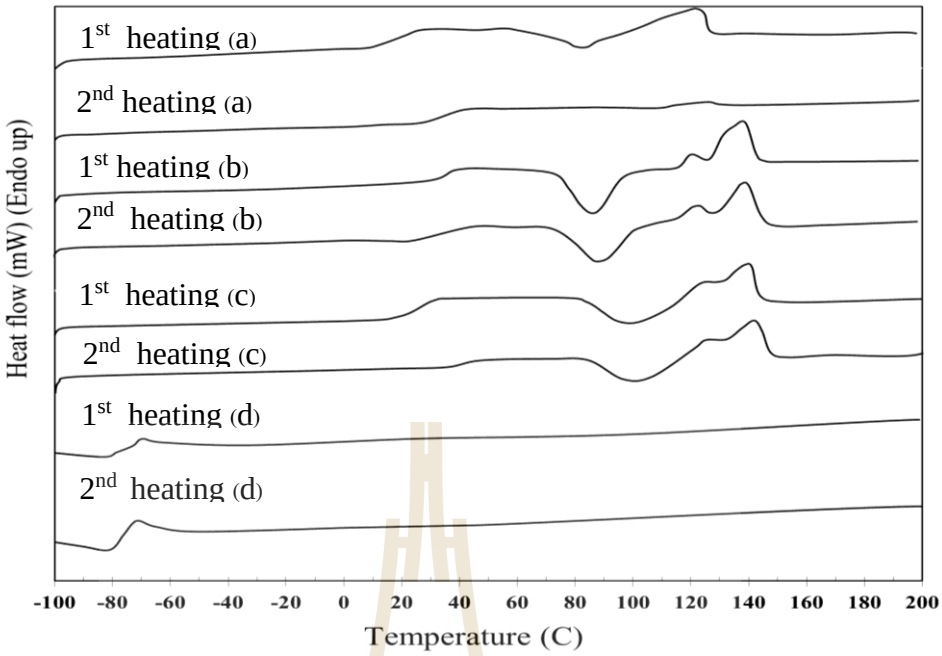

Figure 4.31 DSC thermograms of PLA1(a), PLA2(b), PLA3(c), and HTNR (d) (heating rate 5 °C/min).

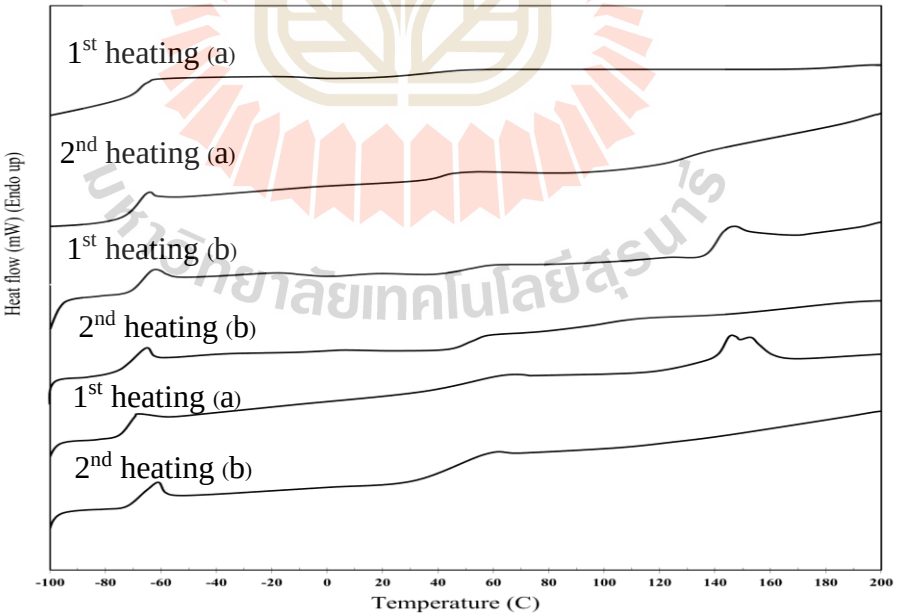

Figure 4.32 DSC thermograms of PLA1-NR-PLA1 (a), PLA1-NR-PLA1 (b), and PLA3-NR-PLA3 (c) (heating rate 5 °C/min).

Table 4.12 DSC data from the first and second heating results of pre-PLA, HTNR and PLA- NR-PLA triblock copolymer.

Sample	Transition Temperature (˚C)						
	1st heating				2nd heating		
	T_{g1} (˚C)	T_{g2} (˚C)	T_m (˚C)	X_c (%)	T_{g1} (˚C)	T_{g2} (˚C)	T_m (˚C)
HTNR	-73.1	-	-	-	76.4	-	-
PLA1	-	32.4	125.0	2.1	-	40.6	-
PLA2	-	36.5	141.0	2.4	-	42.4	143.5
PLA3	-	46.0	147.5	3.8	-	49.7	149.2
PLA1-NR-PLA1	-68.4	44.5	136.9	-	-68.2	42.5	-
PLA2-NR-PLA2	-68.6	52.6	148.2	4.6	-68.6	50	-
PLA3-NR-PLA3	-68.6	54.7	148.7	9.8	-68.8	52.6	-

The DSC thermograms of PLA/PLA-NR-PLA blends containing 10%wt. of PLA-NR-PLA triblock copolymer are shown in Figure 4.33. The thermal transition and related data are summarized in Table 4.13. It was found that, after the addition of triblock copolymer in to PLA, Tg of PLA phase in the blends was steadily decreased as the molecular weight of PLA chain end in triblock copolymer increase. During hot blending, triblock copolymer was well mixing with PLA but while cooling down phase separation of NR segment occurred. However, some triblock copolymer molecules may be trapped inside PLA matrix, especially high molecular weight PLA-NR-PLA triblock copolymer and imparted the flexibility and mobility to the PLA chains. The decrease of the Tg of PLA phase might be one of the reasons that led to increasing impact strength and elongation at break in an order of PLA/PLA3-NR-PLA3> PLA/PLA2-NR-PLA2> PLA/PLA1-NR-PLA1. DSC thermograms from the first heating scan of all blends showed only one Tm which was related to the melting of less perfect PLA

lamellar crystals. The appearance of triblock copolymer may hinder lamellar arrangement. PLA phase did not show any Tm for the second heating scan.

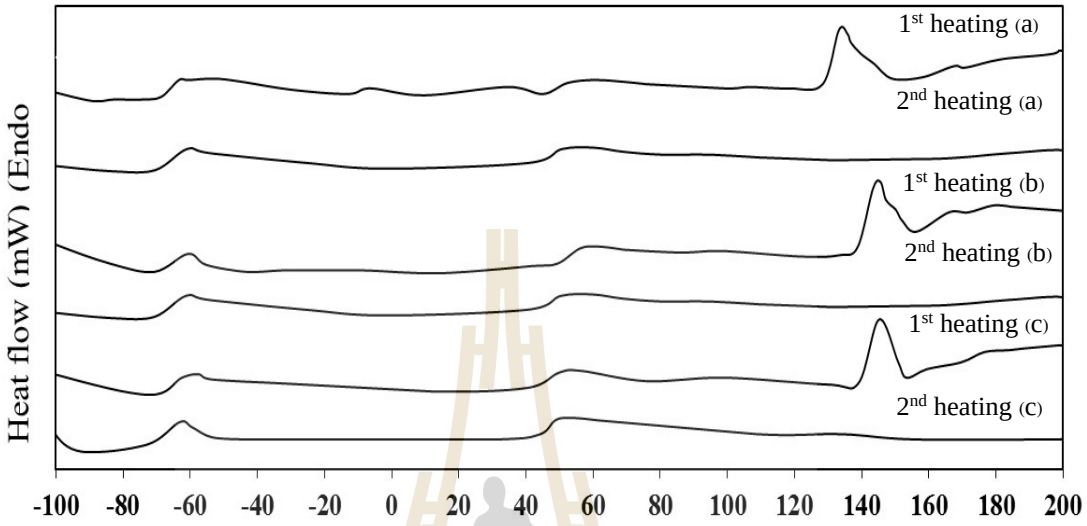

Figure 4.33 DSC thermograms of PLA/PLA1-NR-PLA1 (a), PLA/PLA2-NR-PLA2 (b), and PLA/PLA3-NR-PLA3 (c) (heating rate 5 °C/min).

Table 4.13 DSC data from the first and second heating scan of (a) PLA/PLA1-NR-PLA1 (90/10) (b) PLA/PLA2-NR-PLA2 (90/10) (c) PLA/PLA3-NR-PLA3 (90/10)

Sample	Transition Temperature (˚C)						
	1st heating				2nd heating		
	T_{g1} (˚C)	T_{g2} (˚C)	Tm (˚C)	X_c (%)	T_g1 (˚C)	T_{g2} (˚C)	T_m (˚C)
(a)	-68.4	53.4	136.9	-	-68.2	52.5	-
(b)	-68.6	50.8	148.2	4.6	-68.6	49.0	-
(c)	-68.6	49.9	148.7	9.8	-68.8	47.6	-

4.6 The Effect of PLA-NR-PLA Triblock copolymers on Mechanical and Morphological Properties of PLA/NR Blend

4.6.1 Mechanical properties of PLA/NR/PLA-NR-PLA blends

In the case of PLA toughness improvement using NR, the elongation at break and impact strength of PLA/NR were achieved at some level, whereas the tensile strength of the blends tended to significantly decrease. In order to extent an enhancement of impact strength and elongation at break while maintain or lower the reduction of tensile strength, compatibilizer was added into PLA/NR blend (Mohd Ruf et al., 2018). Therefore, the compatibilizing effect of PLA-NR-PLA triblock copolymer on mechanical and morphological properties of PLA/NR blend containing 10 %wt. of NR which is the optimum content (Chumaka et al., 2014) was studied.

4.6.1.1 Tensile properties of PLA/NR/PLA-NR-PLA blends

Tensile properties of the blends are plotted in Figure 4.34-4.37 and listed in Table 4.16. Tensile modulus and tensile strength of the PLA/NR blend were only slightly increase after the addition of triblock copolymer. The elongation at break of the blends was significantly increase with an increase of PLA-NR-PLA triblock copolymer content. The highest elongation at break was found to be 199.38 ± 14.09, 163.22 ± 20.56, and 136.43 ± 11.35 for PLA/NR/PLA3-NR-PLA3 (90/7/3), PLA/NR/PLA2-NR-PLA2 (90/7/3), and PLA/NR/PLA1-NR-PLA1 (90/7/3), respectively. From the results obtained, triblock copolymers with higher molecular weight PLA chain end seem to be effective compatibilizer. A higher molecular weight of PLA end block may give more misible with PLA matrix.

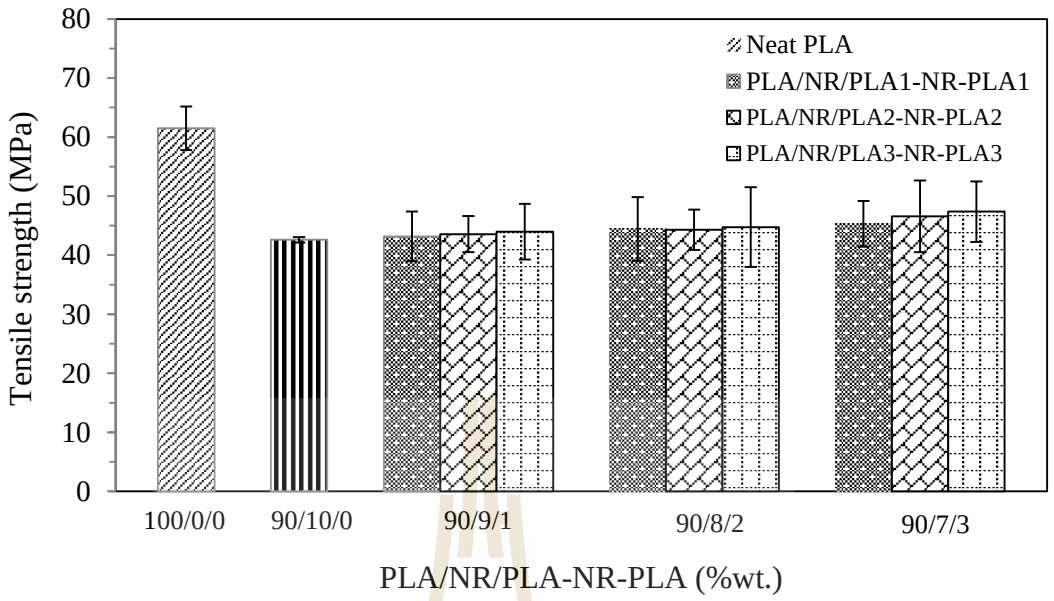

Figure 4.34 Tensile strength of PLA and PLA/NR/PLA-NR-PLA blends with different content of triblock copolymer.

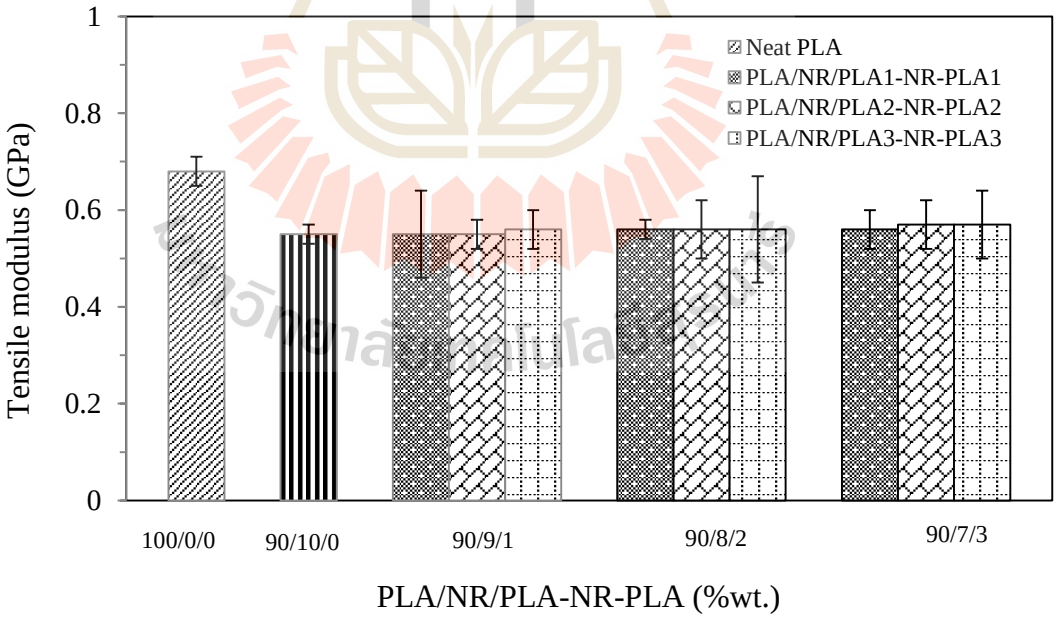

Figure 4.35 Tensile modulus of PLA and PLA/NR/PLA-NR-PLA blends with different content of triblock copolymer.

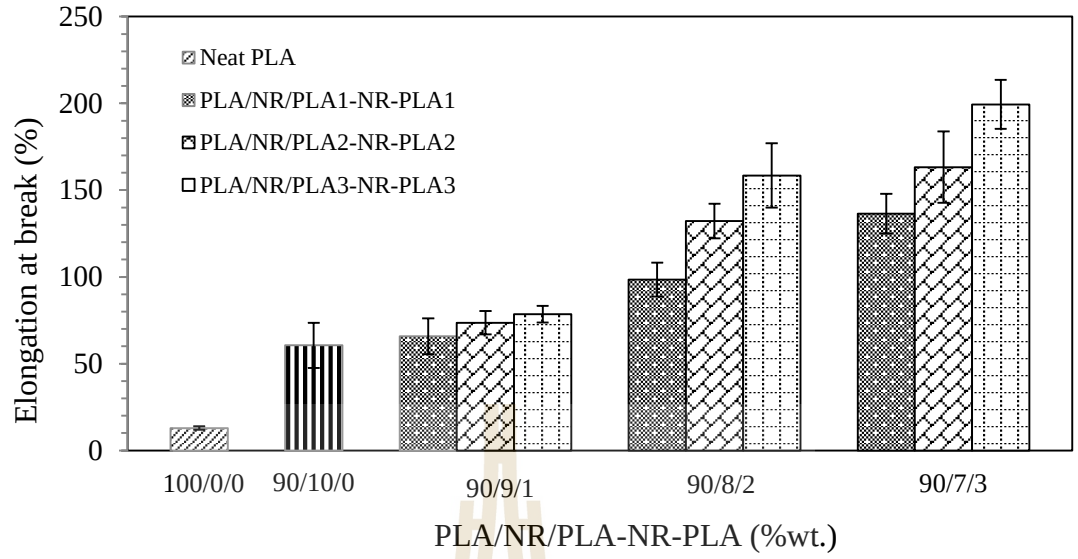

Figure 4.36 Elongation at break of PLA and PLA/NR/PLA-NR-PLA blends with different content of triblock copolymer.

The tensile stress-strain curves of PLA/NR and PLA/NR/PLA-NR-PLA blends with the highest elongation at break are plotted in Figure 4.33.

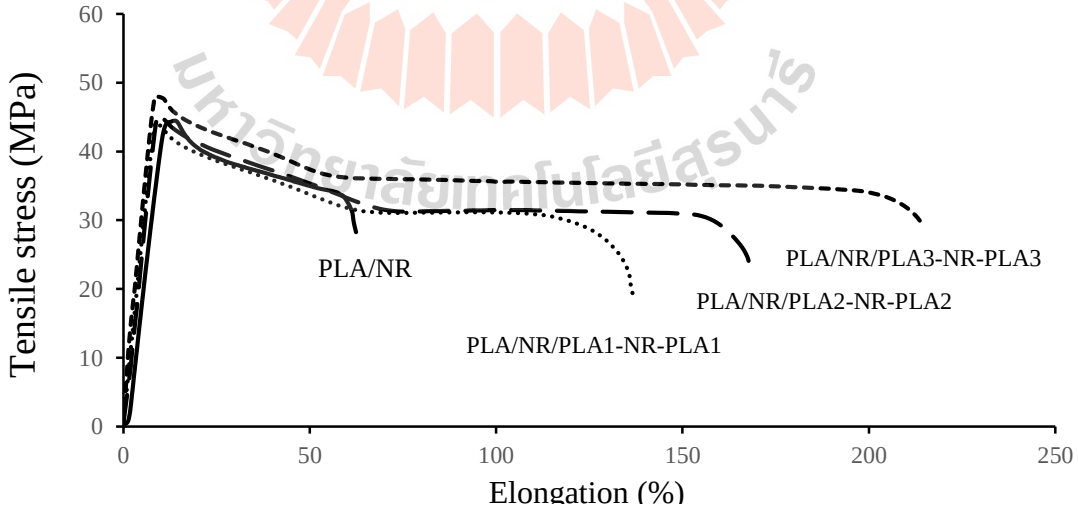

Figure 4.37 Stress-strain curves of PLA/NR (90/10) and PLA/NR/PLA-NR-PLA (90/7/3) blends.

Table 4.14 Tensile strength, modulus, elongation at break and impact strength of the PLA/NR/PLA-NR-PLA blends.

Samples	Impact strength (kJ/m^2)	Tensile strength (MPa)	Modulus (GPa)	Elongation at Break (%)
neat PLA	18.41 ± 1.49	61.47 ± 3.69	0.68 ± 0.03	12.91 ± 1.00
PLA/NR(90/10)	65.35 ± 2.85	42.60 ± 0.64	0.55 ± 0.02	60.54 ± 13.00
PLA/NR/PLA1-NR-PLA1 (90/9/1)	50.64 ± 4.22	43.19 ± 3.44	0.55 ± 0.09	65.79 ± 10.25
PLA/NR/PLA1-NR-PLA1 (90/8/2)	54.82 ± 5.41	44.45 ± 2.87	0.56 ± 0.02	98.43 ± 9.85
PLA/NR/PLA1-NR-PLA1 (90/7/3)	60.91 ± 3.88	45.33 ± 3.72	0.56 ± 0.04	136.43 ± 11.35
PLA/NR/PLA2-NR-PLA2 (90/9/1)	58. 37 ± 3.06	43.56 ± 3.48	0.55 ± 0.03	73.63 ± 6.68
PLA/NR/PLA2-NR-PLA2 (90/8/2)	68.55 ± 3.43	44.30 ± 4.49	0.56 ± 0.06	152.23 ± 9.98
PLA/NR/PLA2-NR-PLA2 (90/7/3)	73.38 ± 6.05	46.58 ± 2.18	0.57 ± 0.05	163.22 ± 20.56
PLA/NR/PLA3-NR-PLA3 (90/9/1)	65.31 ± 4.73	43.98 ± 3.46	0.56 ± 0.04	78.50 ± 4.84
PLA/NR/PLA2-NR-PLA2 (90/8/2)	77.62 ± 6.75	44.74 ± 4.18	0.56 ± 0.11	158.47 ± 18.56
PLA/NR/PLA3-NR-PLA3 (90/7/3)	79.58 ± 5.83	47.38 ± 2.50	0.57 ± 0.07	199.38 ± 14.09

4.6.1.2 Impact properties of PLA/PLA-NR-PLA triblock copolymer blends

Figure 4.38 shows the impact strength of PLA, PLA/NR, and PLA/NR/PLA-NR-PLA blends. It was found that the highest impact strength of 79.58 kJ/m^2 was obtained from the PLA/NR/PLA3-NR-PLA3 (90/7/3) blends. The molecular weight of the PLA-NR-PLA triblock copolymer might affected the impact strength of the blends, and a higher molecular weight of PLA-NR-PLA triblock copolymer tended to increase the impact strength. The higher molecular weight of PLA in triblock copolymer contributed to more compatible between PLA matrix and NR phase. An increase of impact strength was same trend with an increase of elongation at break in PLA/NR/PLA blends.

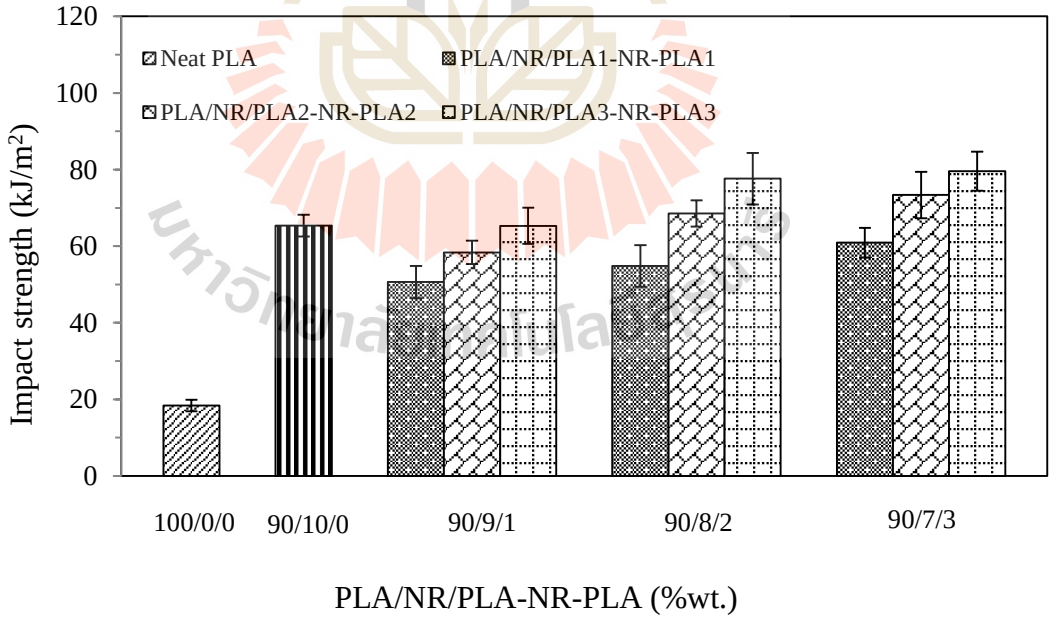

Figure 4.38 Impact strength of PLA/NR/PLA-NR-PLA blends with various rubber contents.

In general a triblock copolymer is used as a non-reactive compatibilizer in the polymer blend. Triblock copolymer contains a segment miscible with one blend component and another segment with the other blend component. The copolymer segments are not necessarily identical with the respective blend components. It is locate at the interface between immiscible blend phases, reducing the interfacial tension between blend components whereas increasing interfacial adhesion at the same time, reducing the resistance to minor phase breakup during melt mixing thus reducing the size of the dispersed phase, and stabilizing the dispersion against coalescence. The finer morphology and the increased interfacial adhesion usually result in improved physical properties. In this research work, only triblock copolymer with long PLA chain end of 6542 and 9693 g/mole acted as an effective compatibilizer for PLA/NR blends. Another evidence that confirmed an improvement of impact strength of PLA/NR blend after the addition of PLA-NR-PLA triblock copolymer was reduction in the diameter of rubber domain in PLA matrix and well dispersion of rubber particles in the blends as discussed in the following section.

4.6.2 Morphological properties of PLA/NR/PLA-NR-PLA blend

The morphologies of PLA/NR/PLA-NR-PLA blends were investigated using SEM. The average diameters of the rubber particles in the blends are listed in Table 4.17. SEM micrographs were exampled from PLA/NR (90/10), PLA/NR/PLA1-NR-PLA1 (90/7/3), PLA/NR/PLA2-NR-PLA2 (90/7/3), and PLA/NR/PLA3-NR-PLA3 (90/7/3), respectively. The SEM micrographs of phase separated are shown in Figure 4.39. The PLA/NR blend exhibits a typical morphology of an immiscible blend which large dispersed rubber particles size of 2.02 ± 0.68 μm, coarse, and wide range of particles diameter. The change in morphology of PLA/NR blends with addition of

PLA-NR-PLA triblock copolymer were observed. The incorporation of the PLA-NR-PLA block copolymer into the PLA/NR blend, the particle size of NR phase in PLA/NR/PLA-NR-PLA blends were significantly decreased and showed more regular and a finer dispersion of particles. This indicate that the added PLA-NR-PLA triblock copolymer acted as an efficient compatibilizing agent. The disperse particle size was

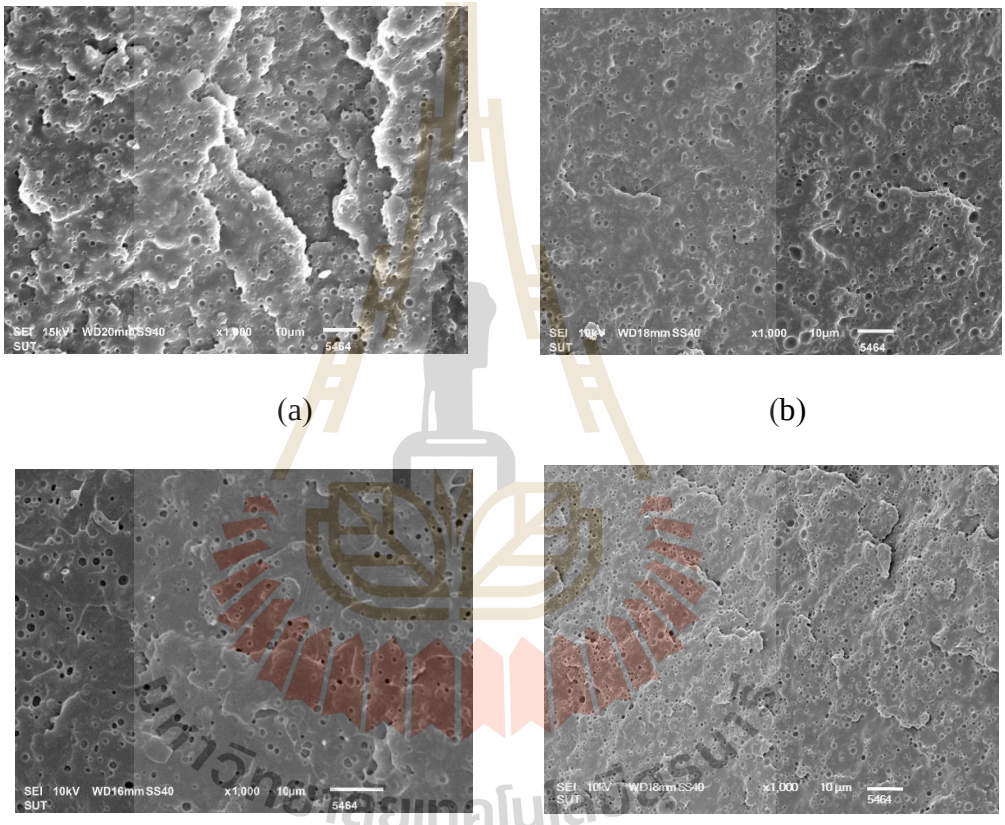

Figure 4.39 SEM micrographs of freeze-fractured surface of PLA/NR (a) (1000x), PLA/NR/PLA1-NR-PLA1(90/7/3) (b) (1000x), PLA/NR/PLA2-NR-PLA2(90/7/3) (c) (1000x), and PLA/NR/PLA3-NR-PLA3(90/7/3) (d) (1000x).

decreased with an increase amounts of PLA-NR-PLA triblock copolymer in the blends. The blend containing 3 %wt. of PLA-NR-PLA triblock copolymer and higher molecular weight of PLA end block showed the lowest disperse particle diameter.

The relationship between the morphology and the impact strength of PLA/NR/PLA-NR-PLA blends was clearly observed, the smaller disperse particle diameter and fine dispersion provided the higher impact strength. In addition, the higher molecular weight of PLA end block (PLA3> PLA2> PLA1) might be prevent the coalescence of rubber phase in the blends and provide the higher impact strength of 79.58 ± 5.83, 73.38 ± 6.05, and 60.91 ± 3.88 kJ/m^2, respectively with the average particle diameter of 1.66 ± 0.39, 1.77 ± 0.26, and 1.87 ± 0.19 μm.

Table 4.15 The average particle diameters of rubber particle in PLA/NR/PLA-NR-PLA blends.

Designation	The blend compositions			Number average particle diameter (µm)	Minimum particle diameter (µm)	Maximum particle diameter (µm)
	PLA (%wt.)	NR (%wt.)	PLA-NR-PLA (%wt.)			
PLA/NR(90/10)	90	10	0	2.02 ± 0.68	0.45	4.25
PLA/NR/PLA1-NR-PLA1(90/9/1)	90	9	1	1.98 ± 0.14	1.18	3.05
PLA/NR/PLA1-NR-PLA1(90/8/2)	90	8	2	1.93 ± 0.26	0.99	2.58
PLA/NR/PLA1-NR-PLA1(90/7/3)	90	7	3	1.87 ± 0.19	1.03	2.45
PLA/NR/PLA2-NR-PLA2(90/9/1)	90	9	1	1.96 ± 0.11	1.00	2.54
PLA/NR/PLA2-NR-PLA2(90/8/2)	90	8	2	1.89 ± 0.19	0.78	2.35
PLA/NR/PLA2-NR-PLA2(90/7/3)	90	7	3	1.77 ± 0.26	0.96	2.25
PLA/NR/PLA3-NR-PLA3(90/9/1)	90	9	1	1.84 ± 0.24	1.13	2.48
PLA/NR/PLA3-NR-PLA3(90/8/2)	90	8	2	1.75 ± 0.35	1.03	2.04
PLA/NR/PLA3-NR-PLA3(90/7/3)	90	7	3	1.66 ± 0.39	0.94	1.98

4.6.3 Thermal properties of PLA/NR/PLA-NR-PLA blends

The DSC thermograms recorded from the first and second heating scan for neat PLA, PLA/NR, and PLA/NT/PLA-NR-PLA blends are shown in Figure 4.40-4.41. The detail results of DSC are summarized in Table 4.16. Generally, after the addition of PLA-NR-PLA triblock copolymer into PLA, Tg of NR phase increased whereas the Tg of PLA phase decreased. This result indicated the improved miscibility of the blends (Zhang, K., Nagarajan, V., Misra, M., Mohanty, A. K., 2014). A significant change of Tg was found for PLA/NR/PLA3-NR-PLA3. The PLA3-NR-PLA3 seemed to show the best compatibilizing efficiency for PLA/NR blend which was in good agreement with the mechanical properties given in Section 4.6. Tcc peak of these blends became very broad and much less intense compared with neat PLA and PLA/NR blend. Additionally, Tcc was increased compared to that of PLA/NR blend and increased to a higher value as a higher molecular weight of PLA end block was presented in triblock copolymer. An increase in Tcc of these blends might be due to the enhanced phase adhesion between NR particles and PLA matrix, which prevents the interfacial slippage. Tm of PLA phase in all blends was not significantly different from PLA whereas crystallinity of PLA phase in all blends was lower than that of PLA.

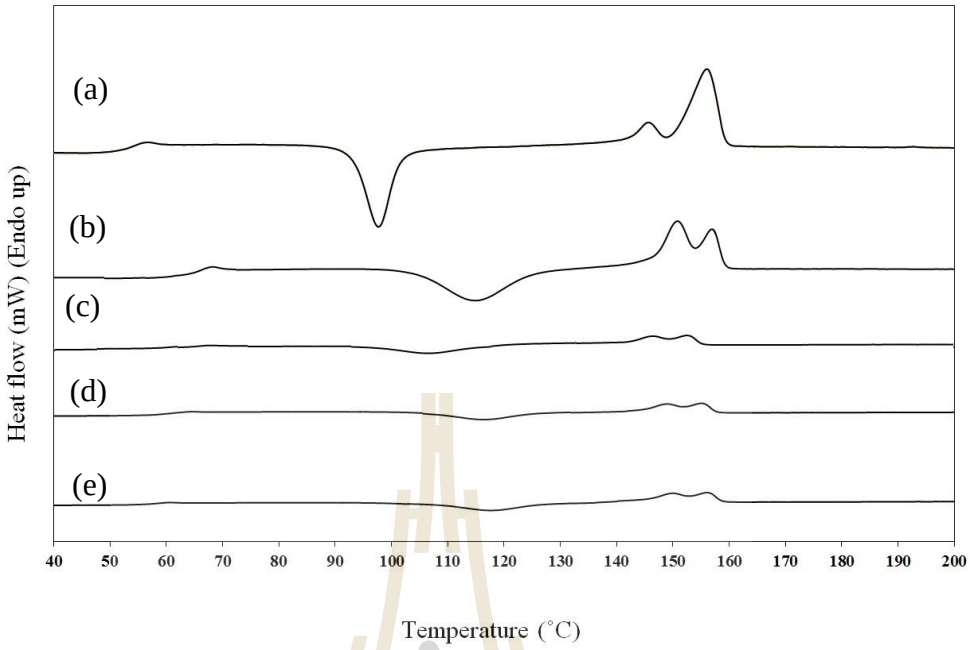

Temperature rang 40 -200 ·C

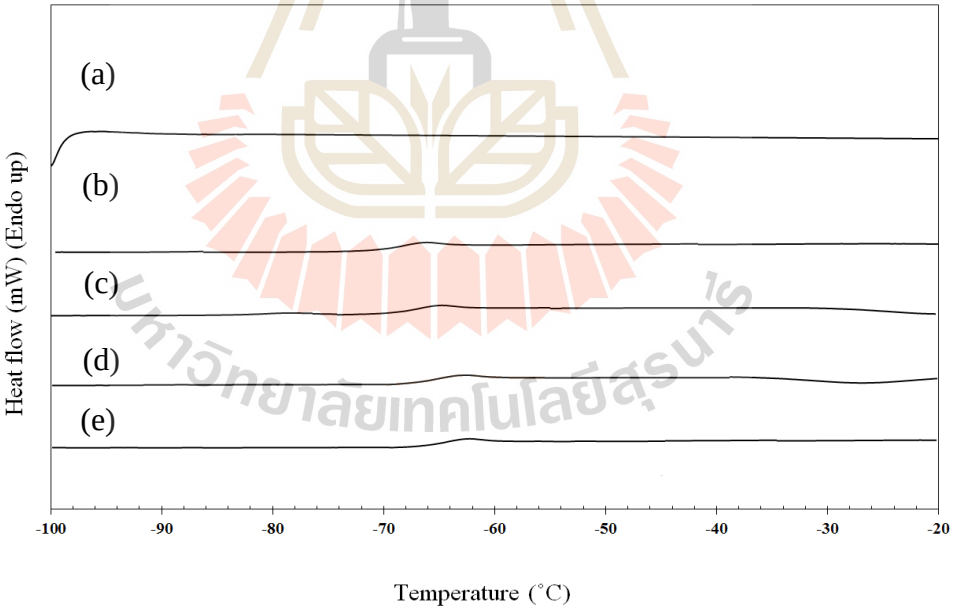

Temperature rang -100 - -20 ·C

Figure 4.40 DSC thermograms of PLA (a), PLA/NR (90/10) (b) and PLA/NR/PLA1-NR-PLA1 (90/10)(c) blends (the first heating, heating rate 5 °C/min).

Table 4.16 DSC data from the first heating scan of (a) neat PLA (b) PLA/NR(90/10) (c) PLA/NR/PLA1-NR-PLA1 (90/7/3) (d). PLA/NR/PLA2-NR-PLA2 (90/7/3) and (e) PLA/NR/PLA3-NR-PLA3 (90/7/3)

Sample	rubber phase	PLA phase						
	T_g (˚C)	T_g (˚C)	T_{cc} (˚C)	T_{m1} (˚C)	T_{m2} (˚C)	ΔH_c (J/g)	ΔH_m (J/g)	X_c (%)
(a)	-	63.8	98.5	146.3	155.6	28.6	35.6	7.4
(b)	-69.4	63.8	104.6	150.9	157.5	25.4	28.6	3.4
(c)	-65.1	57.0	105.5	145.6	155.6	23.8	27.0	3.5
(d)	-64.9	55.8	117.2	151.2	153.9	25.0	29.1	4.4
(e)	-62.7	54.7	119.5	150.5	157.3	26.5	30.9	4.7

Table 4.17 DSC data from the second heating scan of (a) neat PLA (b) PLA/NR(90/10) (c) PLA/NR/PLA1-NR-PLA1 (90/7/3) (d). PLA/NR/PLA2-NR-PLA2 (90/7/3) and (e) PLA/NR/PLA3-NR-PLA3 (90/7/3)

Sample	rubber phase	PLA phase						
	T_g (˚C)	T_g (˚C)	T_{cc} (˚C)	T_{m1} (˚C)	T_{m2} (˚C)	ΔH_c (J/g)	ΔH_m (J/g)	X_c (%)
(a)	-	54	97.5	146.3	155.6	28.64	35.6	7.4
(b)	-69.4	59.8	118.2	151.2	157.9	23.93	27.1	3.3
(c)	-65.1	55.0	117.5	146.3	155.7	23.43	26.6	3.4
(d)	-64.0	53.8	120.2	149.2	153.5	25.01	28.9	4.0
(e)	-61.9	54.2	125.5	153.5	157.4	25.41	29.4	4.2

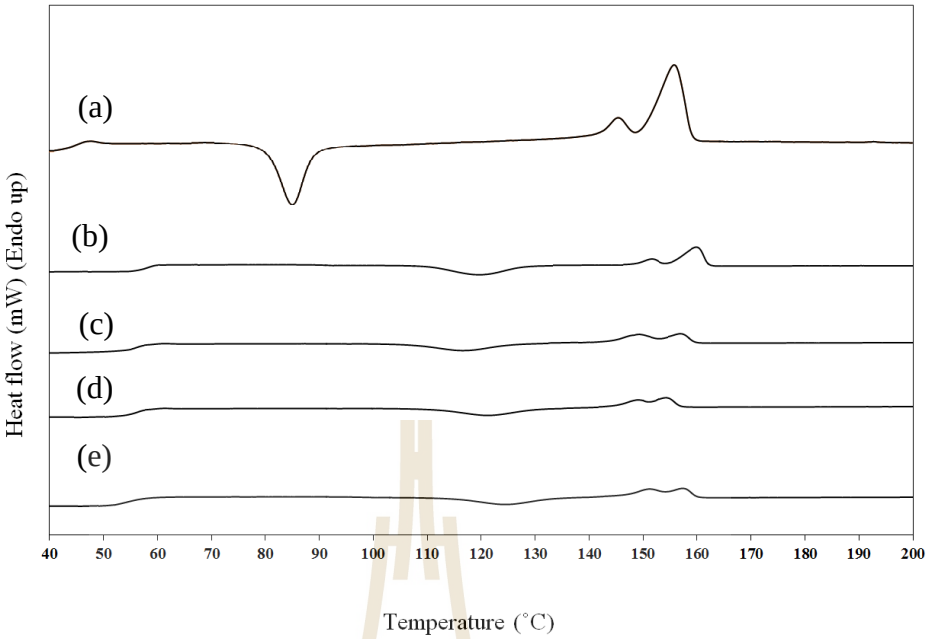

Temperature rang 40 - 200 ·C

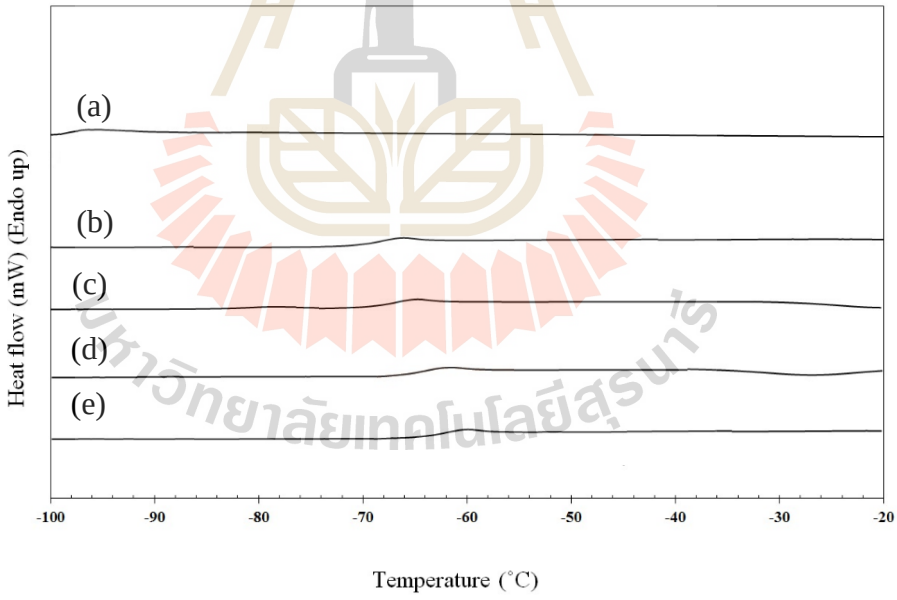

Temperature rang -100 - -20 ˚C

Figure 4.41 DSC thermograms of PLA (a), PLA/NR (90/10) (b) and PLA/NR/PLA1-NR-PLA1 (90/10)(c) blends (the first heating, heating rate 5 °C/min).

CHAPTER V

CONCLUSIONS

5.1 Conclusions

In this research work, hydroxyl terminated natural rubber (HTNR) was prepared by photochemical degradation reaction of masticated natural rubber. The obtained product of HTNR was honey yellow color, viscous, sticky liquid, and soluble in chloroform. Molecular weight of HTNR was evaluated using GPC. $\bar{M}_w$ and $\bar{M}_n$ of HTNR were highly decreased after increasing the reaction time. The HTNR with $\bar{M}_n$ = 28000 g/mole and PDI of 3.12 was selected for further studying. Hydroxyl value and functionality of HTNR estimated according to ASTMD4274-11 were 3.55 ± 0.42 mg KOH/g and 1.77 ± 0.21, respectively. The chemical structure of HTNR with hydroxyl end group was investigated and confirmed by ^{1}H-NMR, ^{13}C-NMR, and FTIR.

Master batch of HTNR and PLA at 50%wt/wt was prepared and used for blending with PLA by melt blending in an internal mixer. The amount of HTNR in the blend was 3, 5, 10, and 15 %wt. From the investigation of mechanical properties of PLA/HTNR blends, it was found that PLA/HTNR blends upon incorporation of 10 %wt. of HTNR showed the highest impact strength of 67.78 ± 12.10 kJ/m^2 that was 3.7 times higher than neat PLA and slightly higher than PLA/NR blend (65.35± 2.85 kJ/m^2). The elongation at break PLA/HTNR (90/10) was increased to 127.23 ± 6.00% which was 10 and 2.1 times higher than PLA and PLA/NR blend respectively. However, tensile strength and tensile modulus were lower than neat PLA whereas they

were slightly higher than those of PLA/NR blend. From morphologies observation of freeze fracture surface of PLA/HTNR (90/10), the average particle diameter of HTNR was 0.92 ± 0.71 μm that was lower than average particle diameter of PLA/NR blends which was 2.02 ± 0.68 μm. From the DSC analysis, the T_g of HTNR phase in PLA/HTNR blend was higher than that of NR phase in PLA/NR blend. The T_{cc} of PLA phase in PLA/NR and PLA/HTNR blends were higher than that of neat PLA. There were two T_m appeared in both PLA/NR and HTNR blends and they are not significantly different from those of PLA.

In order to prepare PLA-NR-PLA triblock copolymers from HTNR and PLA, three types of low molecular weight PLA (pre-PLA) including PLA1, PLA2 and PLA3 were synthesized using condensation polymerization of lactic acid. The chemical structure of pre-PLA was investigated and confirmed by ^{1}H-NMR and FTIR. The yields of synthesis block copolymer PLA1-NR-PLA1, PLA2-NR-PLA2and PLA3-NR-PLA3 were 34.87 ± 0.84, 30.43 ± 0.32 and 29.85 ± 1.87 percent by weight (%wt) respectively. The molecular weight of PLA1, PLA2 and PLA3 obtaining from GPC technique was 3,091, 6,542 and 9,696 g/mol, respectively.

PLA- NR- PLA triblock copolymers were produced via condensation polymerization of HTNR and pre-PLA at 170 ˚C for 24 h. Toluene and $Sn(Oct)_2$ were used as a solvent and an initiator, respectively. The synthetic block copolymers from PLA1, PLA2, and PLA3 were respectively coded as PLA1- NR- PLA1, PLA2- NR- PLA2, and PLA3- NR- PLA3. Chemical structure of triblock copolymers was characterized using ^{1}H- NMR, ^{13}C- NMR and FTIR. The achievement of triblock copolymer was confirmed by the disappearance of OH group in HTNR and a new ester linkage due to condensation reaction of the OH group in HTNR and the COOH group

in pre-PLA. Molecular weight of triblock copolymer was evaluated using GPC technique. PLA1-NR-PLA1, PLA2-NR-PLA2, and PLA3-NR-PLA3 had molecular weight of 34,681, 41,214, and 48,487g/mol, respectively. $\bar{M}_n$ of triblock copolymer from GPC technique are in good agreement with the prediction from $\bar{M}_n$ of pre-PLA and HTNR with a molar ratio of 2:1 ($\bar{M}_{ncal}$). PLA-NR-PLA triblock copolymers were further used to study the efficiency as impact modifier for PLA. The blend was prepared using an internal mixer at 170˚C for 10 min. Compression molding were used for specimen preparation. The amount of triblock copolymer in the blends was kept at 10 %wt. according to the optimum mechanical properties found for PLA/HTNR (90/10) blends and also from other references (Juntuek et al., 2012; Pongtanayut, Thongpin, and Santawitee, 2013). In addition, to study the effect of actual 10 %wt. rubber content in PLA/triblock copolymer blends, the amount of triblock copolymer used for blending with PLA was adjusted to give 10 %wt. rubber content and denoted by R-10 after their names. From the mechanical observation, the blend containing either 10 %wt. triblock copolymer or 10 %wt. rubber content, the impact strength was increased with an increase of molecular weight of PLA end block. The impact strength of PLA/PLA1-NR-PLA1, PLA/PLA2-NR-PLA2, and PLA/PLA3-NR-PLA3 were 48.98 ± 4.22, 50.53 ± 6.46, and 54.31 ± 3.87 kJ/m^2, respectively. The impact strength of PLA/PLA-NR-PLA was higher than PLA about 2.6-3.8 times but still lower than that of PLA/NR and PLA/HTNR blends. However, tensile modulus and tensile strength of PLA/PLA-NR-PLA blend tended to be higher than those of PLA/HTNR blend. From morphologies observation, an average rubber particle diameter in PLA/PLA-NR-PLA blends was smaller than in PLA/HTNR blend. The average particle diameter of PLA1-NR-PLA1, PLA2-NR-PLA2, and PLA3-NR-PLA3 were 0.34 ± 0.03, 0.29 ± 0.05, and

0.25 ± 0.06 μm, respectively. In the case of an actual rubber content was 10 %wt., the impact strength of all PLA/PLA-NR-PLA blends was significantly improved. However, only PLA/PLA3-NR-PLA3(R-10) seemed to show higher impact strength than PLA/HTNR and PLA/NR blends. The tensile strength and tensile modulus were in the same trend. From the current research work, it could be concluded that at the same 10 %wt. rubber content, PLA3-NR-PLA3 is the most efficient toughening agent for PLA. From DSC results of PLA/PLA-NR-PLA blend, it was found that, after the addition of triblock copolymer in to PLA, T_g of PLA phase in the blends was steadily decreased as the molecular weight of PLA chain end in triblock copolymer increased. All blends showed only one T_m which was related to the melting of less perfect PLA lamellar crystals. PLA phase did not show any Tm for the second heating scan. Cold crystallization temperature (T_{cc}) was not found.

The compatibilizing effect of PLA-NR-PLA triblock copolymers for PLA/NR blend was also investigated. It was found that, after the addition of triblock copolymer into PLA/NR blend, impact strength and tensile properties were improved. The magnitude of improvement increased with an increase of the amount of triblock copolymer. The optimum properties was found for PLA/NR/PLA3-NR-PLA3 (90/7/3) with impact strength of 79.58 ± 5.83kJ/m^2, tensile strength of 47.38 ± 2.50 MPa, and elongation at break of 199.38 ± 14.09 %. The morphology of PLA/NR/PLA3-NR-PLA3 (90/7/3) showed the average particle diameter of 1.66 ± 0.39 μm that was lower than particle diameter of NR in PLA/NR blend. From thermal analysis of PLA/NR/PLA-NR-PLA blend, T_g of NR phase generally increased whereas the T_g of PLA phase decreased. A significant change of T_g was found for PLA/NR/PLA3-NR-PLA3. The PLA3-NR-PLA3 seemed to show the best compatibilizing efficiency for

PLA/NR blend, which was in good agreement with the mechanical properties. T_{cc} peak of these blends became very broad and much less intense compared with neat PLA and PLA/NR blend. Additionally, T_{cc} was increased compared to that of PLA/NR blend and increased to a higher value as a higher molecular weight of PLA end block was presented in triblock copolymer. T_m of PLA phase in all blends was not significantly different from PLA whereas crystallinity of PLA phase in all blends was lower than that of PLA.

5.2 Suggestions for further works

5.2.1 Synthesis other types of copolymer from PLA and NR for using as toughening agent or compatibilizer for PLA.

5.2.2 Characterize the interaction between HTNR and PLA using other technique such as AFM or FTIR.

REFFERENCES

Abdullah, I. (1994). Liquid Natural Rubber: Preparation and Application. **Progress in Pacific Polymer Science.** 3: 351-365.

Achmad, F., Yamane, K., Quan, S., and Kokugan, T. (2009). Synthesis of polylactic acid by direct polycondensation under vacuum without catalysts, solvents and initiators. **Chemical Engineering Journal.** 151: 342-350.

Aluthge, D.C., Xu, C., Othman, N., Noroozi, N., Hatzikiriakos, S.G., Mehrkhodavandi, P. (2013). PLA−PHB−PLA Triblock Copolymers: Synthesis by Sequential Addition and Investigation of Mechanical and Rheological Properties. **Macromolecules.** 46: 3965-3974.

Argilant technology. An Introduction to gel permeation chromatography and size exclusion chromatography. Web site: https://www.agilent.com/cs/library/Primers/Public/5990-6969EN%20GPC%20SEC%20Chrom%20Guide.pdf

Astlett Rubber Inc. (2012). Standard Thai Rubber (STR): Specification Scheme. Oakville, Canada. Available from: http://www.astlettrubber.com/pdf/nr/str.pdf. Accessed date:2012.

Auras, R., Harte, B., and Selke, S. (2004). An Overview of Polylactides as Packaging Materials. **Macromolecular Bioscience.** 4: 835-864.

Auras, R., Lim, L.T., Selke, S.E.M., and Tsuji, H. (2010). **Poly(lactic acid): Synthesis, Structures, Properties, Processing, and Applications.** New Jersey : John Wiley & Sons, Inc.

Baker C.S.L., Gelling I.R. (1987) Epoxidized Natural Rubber. In: Whelan A., Lee K.S.

(eds). Developments in Rubber Technology.4. Springer, Dordrecht

Berthé, V., Ferry, L., Bénézet, J. C., and Bergeret, A. (2010). Ageing of different biodegradable polyesters blends mechanical and hygrothermal behavior. **Polymer Degradation and Stability.** 95: 262-269.

Bijarimi, M., Ahmad, S., and RASID, R. (2014). Melt blends of poly(lactic acid)/natural rubber and liquid epoxidised natural rubber. **Journal of Rubber Research.** 17: 57-68.

Bitinis, N., Verdejo, R., Cassagnau, P., and Lopez-Manchado, M.A. (2011). Structure and properties of polylactide/natural rubber blends. **Materials Chemistry and Physics.** 129: 823-831.

Bhowmick, A.K. and Stephens, H.L. (2001). Handbook of elastomers. (2nd ed.). New York: Marcel Dekker.

Bonsignore, P. V. (1995). Production of high molecular weight polylactic acid. **U.S.** Patent 5,470,944.

Braihi, A.J. (2016). Miscibility of polymer blends. miscibility. Babylon University-College of Materials Engineering, Polymer and Petrochemical Industries Department, Babylon, Iraq. Available from: www.uobabylon.edu.iq/eprints/Pubdoc_2_9987_348.docx

Chanchaichujit, J., Saavedra-Rosas, J.F. (2018). Using Simulation Tools to Model Renewable Resources ;The Case of the Thai Rubber Industry. Spring nature, Switzerland, 158p.

Chavalitpanya, K., and Phattanarudee, S. (2013). Poly(Lactic Acid)/Polycaprolactone Blends Compatibilized with Block Copolymer. **Energy Procedia.** 34: 542-548.

Chen, C.C., Chueh, J.Y. Tseng, H., Huang, H.M., and Lee, S.Y.(2003). Preparation and

characterization of biodegradable PLApolymeric blends. **Biomaterials.** 24: 1167-1173.

Chen, L., Qiu, X., Deng, M., Hong, Z., Luo, R., Chen, X., Jing, X. (2006). Poly(L-lactide)/starch blends compatibilized with poly(L-lactide)-g-starch copolymer **Carbohydrate Polymers.** 65: 75-80.

Choi, N-S., Kim, C-H., Cho, K.Y., and Park, J-K. (2002). Morphology and hydrolysis of PCL/PLLA blends compatibilized with P(LLA-co-CL) or P(LLA-b-CL). **Journal of Applied Polymer Science.** 86:1892-98.

Chuasuwan, C. (2018). Natural rubber processing. Thailand Industry Outlook 2018-20. Bangkok: Krungsri Research. Available from : https://www.krungsri.com/bank/getmedia/5fc8fc4b-5f60-48ad-a306-5533ed9df767/IO_Rubber_2018_EN.aspx. Accessed date: March , 2018.

Chumeka, W., Pasetto, P., Pilard, J.F., Tanrattanakul, V. (2014) Bio-based triblock copolymers from natural rubber and poly (lactic acid): Synthesis and application in polymer blending. **Polymer.** 55: 4478-4487.

Chumeka, W., Pasetto, P., Pilard, J.F., and Tanrattanakul, V. (2015). Bio-Based Diblock Copolymers Prepared from Poly(lactic acid) and Natural Rubber. **Journal of Applied Polymer Science.** 132: 41426- 41436.

Chumeka, W., Tanrattanakul, V., Plilard, J. F., and Pasetto. P. (2013). Effect of Poly(Vinyl Acetate) on Mechanical Properties and Characteristics of Poly(Lactic Acid)/Natural Rubber Blends. **Journal of Polymers and the Environment.** 21:450-460.

Collyer, A.A. (1994). **Rubber toughened engineering plastics.** London, UK: Chapman & Hall.

Dahlan, H. M., Khairul Zaman, M. D., and Ibrahim, A. (2000). Liquid natural rubber (LNR) as a compatibilizer in NR/LLDPE blends. **Journal of Applied Polymer Science,** 78(10): 1776-1782.

Datta, R., Tsai, SP., Bonsignore, P., Moon, SH., and Frank, J. R. (1995). Technological and economic potential of poly(lactic acid) and lactic acid derivatives. **FEMS Microbiology Reviews.** 16: 221-231.

Deng, Y., and Thomas, N. L. (2015). Blending poly (butylene succinate) with poly(lactic acid): Ductility and phase inversion effects. **European Polymer Journal.** 71: 534-546.

Eastwood, E., Viswanathan, S., O'Brien, C.P., Kumar, D., Dadmun, M.D. (2005). Methods to improve the properties of polymer mixtures: optimizing intermolecular interactions and compatibilization. Polymer. 46: 3957-3970.

Endo, S., Takizawa, R., Okuda, K., Takada, H., Chiba, K., Kanehiro, H., Ogi, H., Yamashita, R., Date, T. (2005). Concentration of polychlorinated biphenyls (PCBs) in beached resin pellets: variability among individual particles and regional differences. **Marine Pollution Bulletin.** 50: 1103-1114.

Endres, H.J., and Siebert-Raths, A. (2011). **Engineering Biopolymers.** Ohio: Hanser Publications.

Eyiler, E., Chu, I. W., and Walters, K. B. (2014). Toughening of poly(lactic acid) with the renewable bioplastic poly(trimethylene malonate). **Journal of Applied Polymer Science**. 131, 40888.

Fang, H., Jiang, F., Wu, Q., Ding, Y., and Wang, Z. (2014) Supertough Polylactide Materials Prepared through In Situ Reactive Blending with PEG-Based Diacrylate Monomer. **ACS Applied Materials & Interfaces.** 6 (16): 13552-13563.

Folkes, M.J. and Hope, P.S. (1993). **Polymer blends and alloys.** Glasgow: Blakie Academic & Professional, an imprint of Chapman & Hall.

Garlotta, D. (2001). A Literature Review of Poly (Lactic Acid). **Journal of Polymers and the Environment.** 9: 63-84.

Gironi, F., and Piemonte, V. (2011). Bioplastics and Petroleum-based Plastics: Strengths and Weaknesses. **Energy Sources, Part A.** 33:1949-1959.

Grijpma, D.W., Zondervan, G.J., and Pennings, A. J. (1991). High molecular weight copolymers of l-lactide and ε-caprolactone as biodegradable elastomeric implant materials. **Polymer Bulletin.** 25: 327-333.

Grijpma, D.W., Van Hofslot, R.D.A., Supèr, H., Nijenhuis, A.J., and Pennings, A.J. (2004). Rubber toughening of poly(lactide) by blending and block copolymerization. **Polymer Engineering & Science.** 34: 1674-1684.

Gui, Z., Xu, Y., Cheng, S., Gao, Y., and Lu, C. (2013). Preparation and characterization of polylactide/poly(polyethylene glycol-co-citric acid) blends. **Polymer Bulletin.** 2013, 70, 325–342.

Hadjichristidis, N., Pispas, S., and Floudas, C.A. (2003). **Block copolymer: synthetic strategies, physical properties, and applications.** New Jersey, USA: john Wiley & Sons, Inc., Publication.

Herculano, R.D., Tzu, L.C., Silva, C.P., Brunello, C.A., Queiroz, A.A.A., Kinoshita, A., and Graeff, C.F.O. (2011). Nitric Oxide Release Using Natural Rubber Latex as Matrix. **Materials Research.** 14(3): 355-359.

Hillmyer, M.A. and Schmidt, S.C. (1999). Synthesis and Characterization of Model Polyisoprene-Polylactide Diblock Copolymers. **Macromolecules.** 32: 4794-4801.

Hillmyer, M.A. and Wang, Y. (2001). Polyethylene-poly(L-lactide) diblock copolymers: Synthesis and compatibilization of poly(L-lactide)/polyethylene blends. **Journal of Polymer Science Part A: Polymer Chemistry.** 39: 2755-2766.

Horák, Z., Fortelný, I., Kolařík, J., Hlavatá, D., Sikora, A. (2005). Polymer Blends. In: **Encyclopedia in Polymer Science and Technology.** New York, USA: John Wiley & Sons, Inc.

Jaratrotkamjorn, R., Khaokong, C., and Tanrattanakul, V. (2012). Toughness enhancement of poly(lactic acid) by melt blending with natural rubber. **Journal of Applied Polymer Science.** 124: 5027-5036.

Jăso, V., Cvetinov, M., Rakic´, S., and Petrović, Z. S. (2014). Bio-Plastics and Elastomers from Polylactic Acid/Thermoplastic Polyurethane Blends. Journal of Applied Polymer Science. 131: 41104-41112.

Jedliński, Z., Kurcok, P., and Lenz, R. W. (1995). Synthesis of Potentially Biodegradable Polymers. **Journal of Macromolecular Science, Part A: Pure and Applied Chemistry.** 32: 797-810.

Jiao, L., Huang, CL., Zeng, JB. Wang, YZ., and Wang, YL. (2012). Miscibility, crystallization and mechanical properties of biodegradable blends of poly(l-lactic acid) and poly(butylene succinate-b-ethylene succinate) multiblock copolymer. **Thermochimica Acta.** 539: 16-22.

Juntuek, P., Ruksakulpiwat, C., Chumsamrong, P., and Ruksakulpiwat, Y. (2012). Effect of glycidyl methacrylate-grafted natural rubber on physical properties of polylactic acid and natural rubber blends. **Journal of Applied Polymer Science.** 125: 745–754.

Kaplan, D.L. (1998). **Biopolymers from renewable resources.** Springer-Verlag Berlin Heidelberg: Germany. 374-379.

Kfoury, G., Raquez, J.M., Hassouna, F., Odent, J., Toniazzo, V., Ruch, D., and Dubois, D. (2013). Recent advances in high performance poly(lactide): from "green" plasticization to super-tough materials via (reactive) compounding. **Polymer chemistry.** 1: 1-46.

Kovuttikulrangsie, S. and Sakdapipanich, J.T. (2005). The molecular weight (MW) and molecular weight distribution (MWD)of NR from different age and clone Hevea trees. **Songklanakarin Journal of Science and Technology.** 27(2): 337-342.

Kricheldorf, H.R., and Serra, A. (1985). Influence of various metal salts on the optical purity of poly(L-lactide). **Polymer Bulletin.** 14: 497-502.

Kricheldorf, H.R. and Sumbél, M. (1989). Polylactones-18. Polymerization of l, l-lactide with Sn(II) and Sn(IV) halogenides. **European Polymer Journal.** 25: 585-591.

Kroschwitz, I. and Jacqueline, I. (1990). Concise encyclopedia of polymer science and engineering. New York: John Wiley and Sons, Inc.

Kulkarni, R. K., Moore, E. G., Hegyeli A. F., and Leonard, F. (1971). Biodegradable poly(lactic acid) polymers. **Journal of Biomedical Materials Research.** 5: 169-181.

Kunz-Douglass, S., Beaumont, P.W.R., Ashby, M.F. (1980). A model for the toughness of epoxy-rubber particulate composites. **Journal of Materials Science.** 15: 1109-1123.

Langer, R. and Tirrell, D.A. (2004). Designing materials for biology and medicine.

Nature. 428: 487-492.

Ma, P., Cai, X., Zhang, Y., Wang, S., Dong, W., Chen, M., and Lemstra, P. J. (2014). In-situ compatibilization of poly(lactic acid) and poly(butylene adipate-co-terephthalate) blends by using dicumyl peroxide as a free-radical initiator. **Polymer Degradation and Stability.** 102, 145-151.

Maglio, G., Malinconico, M., Migliozzi, A., and Groeninckx, G. (2004). Immiscible Poly(L-lactide)/Poly(ε-caprolactone) Blends: Influence of the Addition of a Poly(L-lactide)-Poly(oxyethylene) Block Copolymer on Thermal Behavior and Morphology. **Macromolecular Chemistry and Physics.** 205: 946-950.

Mahapatro, A., and Singh, D.K. (2011). Biodegradable nanoparticles are excellent vehicle for site directed in-vivo delivery of drugs and vaccines. **Journal of Nanobiotechnology.** 9: 55.

Masutani, K., and Kimura, Y. (2014). Chapter 1: PLA Synthesis. From the Monomer to the Polymer. **Poly(lactic acid) Science and Technology: Processing, Properties, Additives and Applications.** 1-36. RSC Publishing.

Mazidi, M.M., Edalat, A., Berahman, R., and Hosseini, F.S. (2018). Highly-Toughened Polylactide- (PLA-) Based Ternary Blends with Significantly Enhanced Glass Transition and Melt Strength: Tailoring the Interfacial Interactions, Phase Morphology, and Performance. **Macromolecules**. 51: 4298-4314.

Merz, E.H., Claver, G.C., and Baer, M. (1956). Studies on heterogeneous polymeric systems. **Journal of Polymer Science.** 22: 325-341.

Mohd Ruf, M.F.H., Ahmad, S., Chen, R.S., Shahdan, S. Zailan, F.D. (2018). Liquid natural rubber toughened poly(lactic acid) blend: effect of compatibilizer types and loading and loading on thermos-mechanical properties.

Nature Works LLC (2007). Technology Focus Report: Toughened PLA. Available from: https://www.natureworksllc.com/~/media/Files/NatureWorks/Technical-Documents/White-Papers/Toughened-PLA-Technology-Focus-pdf.pdf. Accessed date: March 1, 2017. Mar 1, 2007.

Nature Works LLC. Ingeo biopolymer4043D Technical Data Sheet. Minneapolis, USA: Nature Works LLC. Available from: https://www.natureworksllc.com/~/media/Files/NatureWorks/Technical-Documents/Technical-Data-Sheets/TechnicalDataSheet_4043D_3D-monofilament_pdf.pdf?la=en.

Nor, H.M. and Ebdon, J.R. (1998). Telechelic liquid natural rubber: a review. **Progress in Polymer Science.** 23: 143-177.

Nakason, C., Kaesaman, A., Supasanthitikul, P. (2004). The grafting of maleic anhydride onto natural rubber. **Polymer Testing** 23: 35-41.

Omay, D.,and Guvenilir, Y. (2013). Synthesis and characterization of poly(d,l-lactic acid) via enzymatic ring opening polymerization by using free and immobilized lipase. **Biocatalysis and Biotransformation.** 31(3): 132-140.

Pan P., Kai W., Zhu B., Dong T., Inoue Y. (2007). Polymorphous crystallization and multiple melting behavior of poly(L-lactide): Molecular weight dependence. Macromolecules. 40: 6898-6905.

Peponi, P., Marcos-Fernández, A., and Kenny, J.M. (2012). Nanostructured morphology of a random P(DLLA-co-CL) copolymer. **Nanoscale Research Letters.** 7: 103.

Phetphaisit, C.W., Pray-in, Y., and Punyodom, W. (2013). Mechanical properties and morphology of poly(lactic acid)/modified natural rubber blends. **NU Science Journal.** 9(2): 18-28.

Pongtanayut, K., Thongpin, C., Santawitee, O. (2013). The Effect of Rubber on Morphology, Thermal Properties and Mechanical properties of PLA/NR and PLA/ENR blends. **Energy Procedia.** 34: 888-897.

Qi, F., Tang, M., Chen, X., Chen, M., Guo, G., and Zhang, Z. (2015). Morphological structure, thermal and mechanical properties of tough poly (lactic acid) upon stereocomplexes. **European Polymer Journal.** 71: 314-324.

Raghoebar, G. M. et al. (2006). Resorbable screws for fixation of autologous bone grafts. **Clinical Oral Implants Research.** 17: 288-293.

Rasal, R.M., Amol V. Janorkar, A.V., and Hirta, D.E. (2010). Poly(lactic acid) modifications. **Progress in Polymer Science.** 35: 338-356.

Ravindran, T., Gopinathan-Nayar, M.R., and Josheph, D. (1998). Production of hydroxyl terminated liquid natural rubber-mechanism of photochemical depolymerisation and hydroxylation. **Journal of Applied Polymer science.** 35: 1227-1239.

Robeson, L. (2007). Polymer Blends A Comprehensive Review. Hanser, NH, 459p.

Robeson, L. (2014). Historical Perspective of Advances in the Science and Technology of Polymer Blends. **Polymers.** 6: 1251-1265.

Rolere, S., Liengprayoon, S., Vaysse, L., Sainte-Beuve, J., and Bonfils, F. (2015). Investigating natural rubber composition with Fourier Transform Infrared (FT-IR) spectroscopy: A rapid and non-destructive method to determine both protein and lipid contents simultaneously. **Polymer Testing.** 43: 83-93.

Sachlos, E. and Czernuszka, J.T. (2003). Making tissue engineering scaffolds work. Review: the application of solid freeform fabrication technology to the production of tissue engineering scaffolds. **European Cells and Materials.** 5: 29-40.

Saetung, A., Rungvichaniwat, A., Campistron, I., Klinpituksa, P., Laguerre, A., Phinyocheep, P., and Pilard, J.F. (2010). Controlled degradation of natural rubber and modification of the obtained telechelic oligoisoprenes: preliminary study of their potentiality as polyurethane foam precursors. J. Appl. Polym. Sci., 117:1279-1289.

Saramolee, P., Lopattananon, N., & Sahakaro, K. (2014). Preparation and some properties of modified natural rubber bearing grafted poly(methyl methacrylate) and epoxide groups. **European Polymer Journal.** 56: 1-10.

Sawamoto, M., and Higashimura, T. (1991). Livine cationic polymerization of vinyl monomer: New initiators and functional polymer synthesis, **Makromolekulare Chemie. Macromolecular Symposia.** 47: 67.

Seppälä, J., Hiljanen-Vainio, M., and Karjalainen, T. (1998). Biodegradable lactone copolymers. I. Characterization and mechanical behavior of ε-caprolactone and lactide copolymers. **Journal of Applied Polymer Science.** 59: 1281-1288.

Shashidhara, G. M., and Pradeepa, K. G. (2013). Preparation and characterization of polyamide 6/liquid natural rubber blends. **Journal of Applied Polymer Science.** 131(2). doi:10.1002/app.39750

Shen, L., Haufe, J., and Patel, M. K. (2009). Product overview and market projection of emerging bio-based plastics PRO-BIP 2009. Group Science, Technology and Society (STS), Copernicus Institute for Sustainable Development and Innovation, Utrecht University.

Shi, X., Li, Q., and Zheng, A. (2014). Effects of heat treatment on the damping of EVM/PLA blends modified with polyols. **Polymer Testing.** 35: 87-91.

Singh, R. P., Pandey, J. K., Rutot, D., Degée, Ph., and Dubois, Ph. (2003). Biodegradation

of poly(ε-caprolactone)/starch blends and composites in composting and culture environments: the effect of compatibilization on the inherent biodegradability of the host polymer. **Carbohydrate Research.** 338: 1759-1769.

Sipos, L., Zsuga, M., and Kelen, T. (1992). Living ring-opening polymerization of l,l-lactide initiated with potassium t-butoxide and its 18-crown-6 complex. **Polymer Bulletin.** 27: 495-502.

Songprateepkul, S., Rakmae, S., Deeprasertkul, C., Suppakarn, N., and Chumsamrong, P. (2011). The preparation of Poly(lactic acid) via chain linked hydroxy-terminated lactic acid prepolymer. **Advanced Materials Research.** 410: 337-340.

Thailand Board of Investment (2016). Thailand: The World's Leader in Natural Rubber Production. Thailand Investment Review. Bangkok: BOI. Available from: www.boi.go.th/upload/content/TIR_AUGUST_PROOF_10_44271.pdf Accessed date: August 30, 2017.

Thomas, S., Grohens, Y., and Jyotishkumar, P. (2015). Characterization of Polymer Blends: Miscibility, Morphology, and Interfaces. 1st ed. Wiley-VCH Verlag GmbH & Co. KGaA. 966p.

Tokiwa, Y., Calabia, B.P., Ugwu, C.U., and Aiba, S. (2009) Biodegradability of plastics. **International Journal of Molecular Science.** 10: 3722-3742.

Urayama, H., Moon, S.I., and Kimura, Y. (2003). Microstructure and Thermal Properties of Polylactides with Different L- and D-Unit Sequences: Importance of the Helical Nature of the L-Sequenced Segments. **Macromolecular Materials and Engineering.** 288(2): 137-143.

Utara, S., and Boochathum, P. (2011). Effect of Molecular weight of natural rubber on

the Compatibility and Crystallization Behavior of LLDPE/NR Blends. **Polymer-Plastics Technology and Engineering.** 50(10): 1019-1026.

Utracki, L.A. (2002). **Polymer Blends Handbook volume 1.** Dordrecht: Kluwer Academic Publishers.

Vaidya, A.N., Pandey, R.A., Mudliar, S., Kumar, M.S., Chakrabarti, T., and Devotta, S. (2005). Production and Recovery of Lactic Acid for Polylactide-An Overview. **Critical Reviews in Environmental Science and Technology.** 35: 429-467.

Vink, E.T.H., Rábago, K.R., Glassner, D.A., and Gruber, P.R. (2003). Applications of life cycle assessment to NatureWorks™ polylactide (PLA) production. **Polymer Degradation and Stability.** 80: 403-419.

Westall, B. (1968). The molecular weight distribution of natural rubber latex. **Polymer.** 9: 243-248.

Whiteman, N. (2000). "2000 Polymer, Laminations and coating conferences". Chicago. IL. 631-635.

Wootthikanokkhan, J., Kasemwananimit, P., Sombatsompop, N., Kositchaiyong, A., Isarankura na Ayutthaya, S., and Kaabbuathong, N. (2012). Preparation of Modified Starch-Grafted Poly(lactic acid) and a Study on Compatibilizing Efficacy of the Copolymers in Poly(lactic acid)/Thermoplastic Starch Blends. **Journal of Applied Polymer Science.** 126: E388-E395.

Wu, D., Zhang, Y., Yuan, L., and Zhang, M. (2010). Viscoelastic interfacial properties of compatibilized poly(ε-caprolactone)/polylactide blend. **Journal of Polymer Science Part B: Polymer Physics.** 48: 756-765.

Xiao, L., Wang, B., Yang, G., and Gauthier, M. (2012). Poly(Lactic Acid)-Based

Biomaterials: Synthesis, Modification and Applications. **Biomedical Science, Engineering and Technology.** New York: InTech publisher.

Xu, C., Yuan, D., Fu, L., and Chen, Y. (2014). Physical blend of PLA/NR with co-continuous phase structure: Preparation, rheology property, mechanical properties and morphology. Polymer Testing. 37: 94-101.

Xu, Y., Loi, J., Delgado, P., Topolkaraev, V., McEneany, R. J., Macosko, C. W., and Hillmyer, M. A. (2015). Reactive Compatibilization of Polylactide/Polypropylene Blends. **Industrial & Engineering Chemistry Research.** 54 (23): 6108-6114.

Yang, Y., Xiong, Z., Zhang, L., Tang, Z., Zhang, R., and Zhu, J. (2016). Isosorbide dioctoate as a "green" plasticizer for poly(lactic acid). **Materials and Design**. 91: 262-268.

Yu, H.Y., Yang, X.Y., Lu, F.F., Chen, G.Y., and Yao, J.M. (2016). Fabrication of multifunctional cellulose nanocrystals/poly(lactic acid)nanocomposites with silver nanoparticles by spraying method. **Carbohydrate Polymers.** 140: 209-219.

Yuan, D., Chen, K., Xu, C., Chen, Z., and Chen, Y. (2014). Crosslinked bicontinuous biobased PLA/NR blends via dynamic vulcanization using different curing systems. **Carbohydrate Polymers.** 113: 438-445.

Yuan, D., Xu, C., Chen, Z., and Chen, Y. (2014). Crosslinked bicontinuous biobased polylactide/natural rubber materials: Super toughness, "net-like"-structure of NR phase and excellent interfacial adhesion. **Polymer Testing.** 38: 73-80.

Zhang, W., Li, Y., Chen, X., Wang, X., Xu, X., and Liang, Q. (2005). Synthesis and characterization of the paclitaxel/MPEG-PLA block copolymer conjugate. **Biomaterials.** 26: 2121-2128.

Zhang, C., Man, C., Pan, Y., Wang, W., Jiang, L., and Dan. Y. (2011). Toughening of polylactide with natural rubber grafted with poly(butyl acrylate). **Polymer International.** 60: 1548-1555.

Zhang, K., Nagarajan, V., Misra, M., and Mohanty, A. K. (2014). Supertoughened Renewable PLA Reactive Multiphase Blends System: Phase Morphology and Performance. **ACS Applied Materials & Interfaces.** 6 (15), 12436-12448.

Zhao, Q., Ding, Y., Yang, B., Ning, N., and Fu, Q. (2013). Highly efficient toughening effect of ultrafine full-vulcanized powdered rubber on poly(lactic acid) (PLA). **Polymer Testing.** 32: 299-305.

Zhu, A., Zhang, M., Wu, J., and Shen. J. (2002). Covalent immobilization of chitosan/ heparin complex with a photosensitive hetero-bifunctional crosslinking reagent on PLA surface. **Biomaterials.** 23: 4657-4665.

APPENDIX A

DETERMINATION OF HYDROXYL NUMBERS AND FUNCTIONALITY

A1. Determination of Hydroxyl Numbers and functionality

Hydroxyl number and functionality of HTNR54 was estimated according to ASTM D4274-11by using test method C. The hydroxyl group is esterified with a solution of phthalic anhydride in pyridine under reflux conditions at 115°C. The excess reagent is titrated with standard sodium hydroxide solution.

A1.1 Reagents preparation

A1.1.1 Pyridine reagent

Firstly, pyridine 1300 ml was distilled from phthalic anhydride 78 g, discarding the fraction boiling below 114 to 115°C. Sample was stored in brown glass bottles and shaked vigorously until dissolved. After that, Phthalic anhydride 27-29 g was dissolved in 700 ml of distilled Pyridene. The reagent must stand overnight before use.

A1.1.2 Phenolphthalein indicator solution

Phenolphthalein indicator solution was prepared from 1 g of phenolphthalein in 100 mL of pyridine.

A1.1.3 Potassium acid phthalate

Potassium acid phthalate reagent grade was purchased from Sigma-Aldrich, USA.

A1.1.4 Sodium hydroxide (NaOH), standard solution

Sodium hydroxide (NaOH), standard solution was prepared by dissolving 4 g of NaOH in 1 L of distilled water. To find the actual normality of NaOH, 4 g of potassium acid phthalate was dried at 100°C for 2 h. Place in a glass-stoppered

container and cool in a desiccator. Weigh 1 g of the dried potassium acid phthalate ($KHC_8H_4O_4$) and transfer it to a 250 ml flask. Distilled water of 100ml was added into the flask. Swirl the flask gently until the sample is dissolved. Add phenolphthalein indicator and titrate to a pink end point with the 0.1 N NaOH solution using a 50 mL buret. Calculate the normality of the NaOH as follows:

$$\text{Normality} = W/ (V \times 0.2042) \quad \text{(A.1)}$$

Where W = weight of $KHC_8H_4O_4$ in g

V = volume of NaOH required for titration of the KHC8H4O4 in ml.

Table A1 Weight of $KHC_8H_4O_4$, volume of NaOH for titration and normality of NaOH

Samples	$KHC_8H_4O_4$ (g)	Volume of NaOH (ml)	Normallity (N)
1	1.0179	38.75	0.1094
2	1.0328	39.35	0.1093
3	1.0080	38.3	0.1096
Average	-	-	0.1094 ± 0.0002

A1.2 Procedure

A1.2.1 Blank titration

Accurately pipetted 25 ml of the phthalic anhydride-pyridine reagent into each flask. Next, swirled the flask to effect solution of the sample. After that, put the air condensers in place, and placeed the flasks in an oil bath, maintained at 115 ± 2°C, for 1 h. Keep sufficient oil in the bath to cover approximately one half of the flask. After the heating period, removed the assembly from the bath and cooled to

room temperature. Washed down the condenser with 50 mL of distilled pyridine, and removed the condenser. Added 0.5 mL of phenolphthalein indicator solution and titrated with 0.1094 N NaOH solution to a pink end point that persists for at least 15 s.

Table A2 Weight of Phthalic anhydride reagent and volume of NaOH for blank titration.

Samples	Phthalic anhydride reagent (g)	Volume of NaOH (ml)
1	1.0528	112.10
2	1.0528	112.50
3	1.0528	112.20
Average	-	112.27 ± 0.21

A1.2.1 Samples titration

The amount of sample was calculated as follows, and weigh to the nearest 0.1 mg. No material must be allowed to touch the neck of the flask:

Sample size = 561/estimated hydroxyl number (A.2)

Since the calculated weight was near the maximum permitted by the test method, adhered closely to the indicated weight. Samples were tested in the same manner.

Table A2 Weight of HTNR54 and volume of NaOH for samples titration.

Samples	Weight of HTNR54 (g)	Volume of NaOH (ml)
1	9.6469	106.00
2	9.2576	107.01
3	8.4910	107.90
Average	-	106.97 ± 0.95

The hydroxyl number, mg KOH/g, and functionality of sample was calculated as follows:

$$\text{Hydroxyl number} = [(B - A)N \times 56.1]/W \quad \text{(A.3)}$$

where: A = NaOH required for titration of the sample, ml,

B = NaOH required for titration of the blank, ml,

N = normality of the NaOH, and

W = sample used, g.

The functionality of HTNR was calculated from hydroxyl number using the following formula:

$$F = (\overline{M}_n \times \text{Hydroxyl number})/56100 \quad \text{(A.4)}$$

Where: $\overline{M}_n$ = number average molecular weight (g/mol) of sample

F = functionality, the number of OH group/mol and

56100 = equivalent weight of KOH, in milligrams.

Table A3 Hydroxyl number and functionality of HTNR54

Samples	Hydroxyl number	functionality
1	3.99	1.99
2	3.49	1.74
3	3.16	1.58
Average	3.55 ± 0.42	1.77 ± 0.21

APPENDIX B

PUBLICATIONS

List of publications

Sawitri Srisuwan, Yupaporn Ruksakulpiwat, and Pranee Chumsamrong. (2015). Physical Properties of Poly(lactic acid)/Hydroxyl Terminated Natural Rubber Blends. Macromolecular Symposia. 354: 118-124.

Sawitri Srisuwan, Yupaporn Ruksakulpiwat, and Pranee Chumsamrong. (2016). The Preparation of Poly(lactic acid)-block-Natural Rubber-block-Poly(lactic acid) from Hydroxyl Terminated Natural Rubber and Poly(lactic acid) Prepolymer. Proceedings of the 6th International Polymer Conference of Thailand; June 30-July 1, 2016; Bangkok, Thailand, p. 206-211.

Sawitri Srisuwan, Yupaporn Ruksakulpiwat, and Pranee Chumsamrong. (2018). Synthesis of Natural Rubber Based Toughening Agents for Poly(lactic acid). Suranaree Journal of Science and Technology. 25(4): 419-430.

BIOGRAPHY

Miss Sawitri Srisuwan was born on May 25, 1986 in Bangkok, Thailand. She attended her Bachelor's degree in Polymer Engineering, School of Polymer Engineering, Institute of Engineering, Suranaree University of Technology, Nakhon Ratchasima in 2008. After that, she continued her study in School of Polymer Engineering at Suranaree University of Technology (SUT) and earned her Master's Degree in Polymer Engineering in 2012. During her graduate study, she got a research assistant scholarship from Suranaree University of Technology and she got a research assistant scholarship from the Center of Excellence for Petroleum, Petrochemical and Advanced Materials, Chulalongkorn University, Thailand. Her research was about "woven sisal fiber reinforced epoxy composites". In 2012, she started her Ph.D. studying in Polymer Engineering, Institute of Engineering, Suranaree University of Technology, Nakhon Ratchasima. Her Ph.D. study was entitled "Synthesis of natural rubber based thoughening agents for poly(lactic acid)" which was under the supervision of Assist. Prof. Dr. Pranee Chumsamrong and Assoc. Prof. Dr. Yupaporn Ruksakulpiwat. Her Ph.D. study was supported by Suranaree University of Technology and the Center of Excellence for Petroleum, Petrochemical and Advanced Materials, Chulalongkorn University, Thailand. In the period of her study, several parts of her work were presented at The 45th International Symposium on Macromolecules (MACRO 2014) in Chiang Mai, Thailand, International Polymer Conference 2016 (PCT 2016) in Bankok, Thailand, and published in Suranaree Journal of Science and Technology, respectively.